Distribution Agreement

In presenting this dissertation as a partial fulfillment of the requirements for an advanced degree from Emory University, I hereby grant to Emory University and its agents the non-exclusive license to archive, make accessible, and display my dissertation in whole or in part in all forms of media, now or hereafter known, including display on the world wide web. I understand that I may select some access restrictions as part of the online submission of this dissertation. I retain all ownership rights to the copyright of the dissertation. I also retain the right to use in future works (such as articles or books) all or part of this dissertation.

Signature:

_____ _____

Kanika Faye Pulliam Date

Interplay Between Nuclear Import and Cell Cycle Control

By

Kanika Faye Pulliam
Doctor of Philosophy

Graduate Division of Biological and Biomedical Sciences
Genetics and Molecular Biology

_____
Anita H. Corbett, Ph.D.
Advisor

_____
Jeremy Boss, Ph.D.
Committee Member

_____
Judith Fridovich-Keil, Ph.D.
Committee Member

_____
David Pallas, Ph.D.
Committee Member

_____
Junmin Peng Ph.D.
Committee Member

Accepted:

_____
Lisa A. Tedesco, Ph.D.
Dean of the Graduate School

_____
Date

Interplay Between Nuclear Import and Cell Cycle Control

By

Kanika Faye Pulliam
B.S., Spelman College, 2001

Advisor: Anita H. Corbett, Ph.D.

An abstract of
A dissertation submitted to the Faculty of the Graduate School of Emory University
in partial fulfillment of the requirements for the degree of
Doctor of Philosophy
in Graduate Division of Biological and Biomedical Sciences
Genetics and Molecular Biology
2009

Abstract

Interplay Between Nuclear Import and Cell Cycle Control
By Kanika Faye Pulliam

The bi-directional transport of proteins across the nuclear envelope via nuclear pore complexes is a highly regulated process that involves many different factors. The classical nuclear import pathway is the most studied mechanism for the transport of proteins into the nucleus. During classical nuclear import, proteins are shuttled into the nucleus by an internal targeting sequence termed the classical nuclear localization signal (cNLS) via interactions with nuclear import receptors. The cNLS receptor, importin α recognizes the cNLS-containing protein or cargo in the cytoplasm as the initial step in the transport process. In an effort to investigate how the classical nuclear transport mechanism affects a fundamental process in biology, we examined the interplay between nuclear transport and progression through the cell cycle in budding yeast, *Saccharomyces cerevisiae*. In eukaryotes, a subset of proteins are transported across the nuclear envelope in a cell cycle dependent manner. Previous studies support a link between nuclear transport and the cell cycle but these studies did not demonstrate a direct role of the nuclear transport machinery in cell cycle regulation. We first demonstrated that the cNLS cargo binding affinity for importin α dictates the rate of import of a cNLS cargo into the nucleus, suggesting that cargo binding to the receptor regulates the import process. We next hypothesized that temporally regulated interactions between specific cNLS cargoes and importin α are required for progression through the cell cycle. Results of our study exploiting importin α mutants with defects in cargo binding and release showed that a defect in cNLS cargo recognition causes a profound delay in progression through the G_1/S transition of the cell cycle. In conclusion, cNLS cargo recognition by the classical nuclear import receptor, importin α is required for efficient transition through the G_1/S stage of the cell cycle. This is the first study to demonstrate a direct role of importin α in regulation of the G_1/S phase of the cell cycle. In conclusion, this work defines the rate-limiting step in the classical nuclear import process and then reveals that the G_1/S stage of the cell cycle is strongly dependent on classical protein import.

Interplay Between Nuclear Import and Cell Cycle Control

By

Kanika Faye Pulliam
B.S., Spelman College, 2001

Advisor: Anita H. Corbett, Ph.D.

A dissertation submitted to the Faculty of the Graduate School of Emory University
in partial fulfillment of the requirements for the degree of
Doctor of Philosophy
in Graduate Division of Biological and Biomedical Sciences
Genetics and Molecular Biology
2009

Acknowledgments

I would like to acknowledge my advisor Anita H. Corbett, Ph.D, and the various members of the Corbett Lab in which, I have interacted. Over the years, they have provided a continual source of knowledge, guidance, enthusiasm, and support in my doctoral training. In particular Dr. Corbett, has been a source of wisdom. She has taught me some lessons which I will carry with me in my personal and professional pursuits.

I also thank my committee members for their expert knowledge and guidance. They have been steady in their commitment and yielded great assistance in the development of my dissertation studies.

I would also like to acknowledge the financial and professional support from the National Institute of Health Minority Supplement, the Facilitating Academic Careers in Science and Engineering Program, the Genetics and Molecular Biology Program, and the Graduate Division of Biological and Biomedical Sciences at Emory University.

Last but not least, I would like to thank my husband John Pulliam, Ph.D., for his continual love, encouragement, and support during the preparation of this dissertation. He believed in me when I did not believe in myself. I would also like to thank my daughter, Maya for her unconditional love, kisses, and hugs.

Table of Contents

List of Figures and Tables

Figure **Page**

Tables Page

General List of Abbreviations

cNLS	classical nuclear localization signal
CEN	centromeric
CDK	cyclin-dependent kinase
DAPI	4', 6-diamidino-2-phenylindole dihydrochloride
DIC	differential interference contrast
FACS	fluorescent activated cell sorting
5-FOA	5-fluoroorotic acid
GFP	green fluorescent protein
GST	glutathione S-transferase
IBB	importin β binding
NES	nuclear export signal
NPC	nuclear pore complex
Nup	nucleoporin
Srp1	suppressor of RNA Polymerase I

CHAPTER 1. GENERAL INTRODUCTION

A daughter cell is generated from a series of actions identified as the cell cycle. Activation or repression of genes, located within the nucleus of a cell, plays a key role in progression through the cell cycle [1, 2]. When the expression of a gene is regulated in response to an intra- or extracellular signal during different stages of the cell cycle, information in the form of specific proteins enters the nucleus. Different transport factors are responsible for shuttling these cargo proteins into the nucleus [3]. The transport factors recognize proteins by the identification of an internal targeting signal located within the cargo protein. Interactions between nuclear-bound proteins that regulate the cell cycle and these carriers play a major role in cell cycle progression.

This dissertation will focus on a role of nuclear transport in regulating the eukaryotic cell cycle. Our studies reveal a critical role for the classical nuclear import machinery in key cell cycle transitions.

1.1 The Nucleus and Cell Compartmentalization

The nucleus of the eukaryotic cell is responsible for separating the genetic material from the cytoplasmic compartments of the cell [4]. During gene expression, mRNA molecules are generated from the DNA located in the nucleus and are further processed into mature mRNA [1]. Then the processed mRNA molecules are transported to the cytoplasm where they are translated into functional proteins. Transcription factors are responsible for regulating gene expression and some are maintained in the cytoplasm separated from the DNA in the nucleus, to prevent premature expression of genes [1, 2]. The compartmentalization of these macromolecules controls genetic stability by regulating access of transcriptional regulators to the nucleus and preventing protein

translation of unprocessed mRNA in the cytoplasm that would lead to nonfunctional proteins [3].

A major feature of the nucleus is the nuclear envelope which is a double membrane structure that physically separates the contents of the nucleus from the cell cytoplasm. The nuclear envelope is impermeable to most macromolecules, allowing for regulated control of entry. Macromolecules must be selectively transported through nuclear pores to cross the nuclear membrane [3-5].

1.2 The Nuclear Pore Complex and Nuclear Pore Proteins

The transport of macromolecules into and out of the nucleus is mediated by nuclear pore complexes (NPCs), dynamic proteinaceous structures perforating the nuclear envelope [6-10]. The movement of small molecules through nuclear pores occurs by passive diffusion but molecules larger than ~40 kDa require energy-dependent transport with the assistance of soluble receptors [11, 12]. The NPC consists of three regions: the nuclear basket, the central core, and the cytoplasmic filaments (Figure 1) [13-16]. The composition of the NPC is similar from yeast to humans, although the size is different. The calculated mass of NPCs is ~40 MDa in the yeast *Saccharomyces cerevisiae* and ~60 MDa in vertebrates [17-20].

Individual components of the NPC have been identified by biochemical and genetic studies [18, 21]. The NPC consists of approximately 30 nucleoporin (Nup) proteins [9, 13, 20]. There are three subgroups of Nups (Figure 1) [9, 22, 23]. Structural Nups make up the architecture of the NPC. Pore membrane proteins (Poms) anchor the

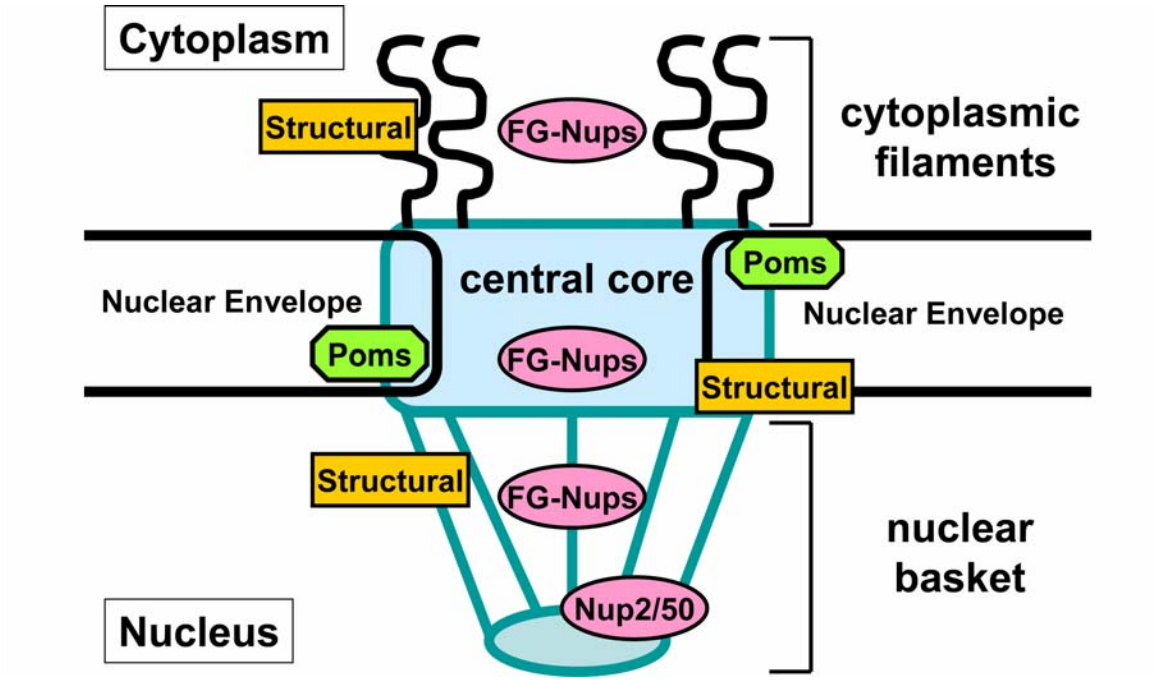

Figure 1. Structure of the Nuclear Pore Complex.
The nuclear pore complex (NPC) consists of three regions: the cytoplasmic filaments, the central core, and the nuclear basket. There are three subgroups of nucleoporins (Nups). Structural Nups make up the architecture of the NPC. Pore membrane Nups (Poms) anchor the NPC in the nuclear envelope. Nups that contain phenylalanine-glycine (FG) repeat motifs line the inside of the NPC. FG-Nups are involved in the physical translocation of macromolecules into and out of the nucleus.

NPC into the nuclear envelope. Lastly, Nups containing phenylalanine-glycine (FG) repeat motifs line the inside of the NPC [24-27]. FG-Nups are involved in the physical translocation of macromolecules into and out of the nucleus [13, 28, 29].

Although dogma dictates that the composition of all NPCs is identical, there are small variations in protein composition that affect transport activity [9, 30-32]. The composition and transport activity of the NPC can depend on the tissue type in multicellular organisms [6, 33], developmental stage [34, 35], and stage of the cell cycle [36]. Proteins that are not considered Nups also associate with the NPC at distinct locations in the nuclear envelope [37]. For example, proteins that associate with the nuclear basket of the NPC may be involved in the quality control of mRNA molecules transported from the nucleus to the cytoplasm by mRNA retention [37, 38].

1.3 Recognition of Nuclear Targeting Signals

The molecular pathway a protein will take to reach its destination is distinguished by the type of nuclear targeting amino acid sequence (signal) located within that protein cargo. The type of targeting signal determines if a protein should be transported into the nucleus or remain in the cytoplasm. Although the destination may be the same for different proteins, the nuclear targeting signal can come in different flavors.

The best characterized signal is the classical nuclear localization signal (cNLS) that functions in targeting proteins or cargoes from the cytoplasm into the nucleus [39]. There are two types of cNLS sequences, composed of either one (monopartite) or two basic clusters of amino acids separated by a linker region (bipartite) [40].

The prototypical monopartite cNLS was first identified by generation of amino acid substitutions in the sequence of the simian virus 40 (SV40) large-T antigen [41, 42].

Mutations in the predicted cNLS sequence led to mislocalization of the SV40 large T antigen protein to the cytoplasm. The cNLS sequence was confirmed by fusion of the wild type cNLS sequence (PKKKRKV) of SV40 to the N-terminus of the mutant SV40 protein and other cytoplasmic proteins coupled with subsequent localization studies. The fusion proteins were localized to the nucleus [41, 42]. This study along with many other subsequent studies revealed a monopartite cNLS contains a consensus sequence of lysine (K) followed by two basic amino acid residues [lysine or arginine (R)] in a loose consensus sequence, K(K/R)X(K/R) [43].

In addition to the prototypical monopartite cNLS sequence, a small downstream cluster of basic amino acid residues is also required for efficient nuclear targeting of a subset of proteins [44-46]. A nuclear targeting signal containing two clusters of basic amino acid residues is termed a bipartite cNLS. A prototypical bipartite cNLS was first discovered in the *Xenopus laevis* nucleoplasmin protein as the sequence, AVKRPAATKKAGQAKKKKLD [44]. Evidence of a bipartite sequence was revealed when the nucleoplasmin predicted monopartite cNLS sequence fused to pyruvate kinase did not localize the fusion protein to the nucleus [44].

The cNLS is not the only nuclear targeting signal. Proteomic analysis in the budding yeast *S. cerevisiae* genome revealed approximately 60% of the proteins that accumulate in the nucleus, contain a predicted cNLS [47]. This analysis suggests the other 40% of proteins located in the nucleus are transported to the nucleus via a different pathway.

Recently, a new class of NLS motif was identified termed the proline tyrosine NLS (PY-NLS). This motif was identified in the splicing factor hnRNP A1 through

structural and complementary biochemical analyses [48]. The PY-NLS is defined by three rules: (1) PY-NLSs are large (>30 residues) and structurally disordered, (2) possess basic amino acid sequences, and have a (3) central hydrophobic or basic motif followed by a C-terminal R/H/K$X_{(2-5)}$PY consensus sequence [48]. Because PY-NLS sequences are defined by both structure and sequence, PY-NLSs could not be identified by conventional sequence analysis methods. The PY-NLS is conserved in *S. cerevisiae* and *in vivo* analysis indicates the PY-NLS is a functional nuclear targeting sequence [49]. Therefore, other nuclear targeting sequences such as the new PY-NLS should be identified to better understand the complex process of nuclear transport.

The other well characterized targeting signal is the classical nuclear export signal (cNES), which directs proteins from the nucleus to the cytoplasm. The classical NES sequence was first discovered in HIV Rev (LQLPPLERLTL) and the protein kinase A inhibitor (PKI; LALKLAGLDI) as a leucine-rich motif [50, 51].

1.4 Identification of Transport Factors

Identifying targeting signals in cargo molecules was the first step toward understanding nuclear transport mechanisms. To understand the mechanism of nuclear transport, it was necessary to identify the cellular machinery that recognizes these targeting signals.

An *in vitro* assay in digitonin-permeabilized vertebrate cells was used to analyze nuclear import of a reporter protein containing the monopartite SV40 cNLS sequence [52]. Digitonin solubilizes the plasma membrane and membrane-bound insoluble proteins of the cell while the nuclear envelope remains intact. Thus the contents of the nucleus remain unchanged and the cytoplasm is depleted of soluble proteins that are not

embedded within the cellular membranes [52]. Through experimentation, cytoplasmic soluble factors were shown to be required for the nuclear import of a SV40 cNLS fusion protein [52]. The same group later identified the receptor proteins exploiting the import activity of proteins containing cNLS sequences [53].

The cytoplasmic factors that are involved in nuclear accumulation of cNLS-containing proteins were identified by use of the permeabilized *in vitro* assay and also through studies in different organisms [54-58]. From groundbreaking work, two cytoplasmic fractions were discovered. Fraction A was determined to be involved in targeting cNLS proteins to the nuclear envelope. Fraction B was determined to play a role in translocation of cNLS proteins through the nuclear pore to the nucleus [54]. The cytoplasmic factors in fraction A were cloned and identified as importin/karyopherin α [57] and importin/karyopherin β [56] heterodimeric receptor involved in cNLS cargo recognition and targeting to the nuclear pore. The small GTPase, Ran, [55] and the nuclear transport factor 2 (NTF2), [58] were identified as factors in fraction B required to mediate ongoing translocation through the nuclear pore into the nucleus. In summary, the cell requires soluble transport receptors for nuclear localization of cNLS cargoes.

1.5 Nuclear Transport Receptors

Further investigation of the transport factors revealed importin β plays two roles in nuclear transport. Although importin β facilitates cNLS cargo targeting to the nuclear pore, importin β also functions in cargo release by interaction with RanGTP. Characterization of importin β and Ran led to the discovery of more nuclear transport receptors that are involved in the bi-directional transport of proteins and interact with Ran. These receptors show homology to importin β, revealing an importin β superfamily of nuclear transport receptors. Although the members of the importin β superfamily possess weak overall sequence homology, they all contain an N-terminal Ran binding domain [59]. The superfamily includes fourteen members in *S. cerevisiae* and approximately twenty-two in mammalian cells [3, 59-63].

Importin β members are composed of HEAT repeats consisting of ~40 tandem amino acid motifs that fold into a pair of α-helices stacking together in parallel to form a superhelical structure. HEAT repeats are involved in protein-protein interactions [59, 64]. The importin β superhelical structure is very flexible allowing for versatility in binding different cargoes [65]. This flexibility makes it difficult to identify predicted signal sequences within cargoes that bind a specific importin β member. In addition, some cargoes are recognized and transported by multiple importin β members via different routes [66-69].

Members of the importin β superfamily are not only involved in the import of cargoes to the nucleus but they also function in the export of NES-containing cargoes and ribonucleoproteins to the cytoplasm. These members are named exportins. For example,

the importin β superfamily member, exportin 1 (Crm1), mediates export of leucine-rich cNES cargoes to the cytoplasm [70, 71].

A small subset of nuclear transport receptors have been documented to function in both import and export of signal-containing cargoes. The importin β receptors, yeast Msn5 (Kap142) and mammalian importin 13, both import and export various cargoes through the NPC [72, 73]. These receptors can modulate their binding characteristics for various proteins. This mechanism suggests some transport receptors must recognize many structurally different NLS cargoes because there are more cargoes than nuclear transport receptors [74]. This is a clear example of the versatility in conformation many transport receptors must possess to recognize different cargoes [65].

Although many nuclear transport receptors bind their cargoes directly, a subset of receptors requires an adapter to mediate interaction between the transport receptor and their cargo. For example, the classical importin β receptor (Kap95/Kapβ1) directly binds some cargoes and also uses the adapter, importin α, to indirectly bind cNLS cargoes and transport them into the nucleus [75-77]. *S. cerevisiae* encodes only one importin α (Srp1). In contrast, there are six isoforms of importin α encoded in the human genome. These isoforms are divided into three phylogenetic groups (α1, α2, and α3) based on sequence similarity [78]. Importin α1 is found in all eukaryotes. Importins α2 and α3 are only found in multicellular animals [78]. The presence of six isoforms of importin α suggests a more complex role for adapter-dependent nuclear import of cNLS cargoes in higher eukaryotes.

1.6 Ran-GTPase Cycle

The small GTPase, Ran, regulates interactions between the nuclear transport receptors and the NLS cargoes. Ran cycles between RanGDP and RanGTP states. The GDP- or GTP-bound state of Ran depends on the regulatory proteins, RCC1 and RanGAP. The nuclear guanine nucleotide-exchange factor RCC1 (RanGEF) catalyzes the conversion of RanGDP to RanGTP in the nucleus [79-81]. The cytoplasmic guanine nucleotide-activating factor, RanGAP, facilitates GTP hydrolysis in the cytoplasm [80, 82-84]. Therefore, increased RanGTP is located in the nucleus and more RanGDP is located in the cytoplasm (Figure 2) [85-87].

RanGTP binds to importin β superfamily receptors to modulate the directionality of transport. Import complexes form in the cytoplasm in the absence of RanGTP while export complexes that form in the nucleus require RanGTP binding to the complex [55, 88-91].

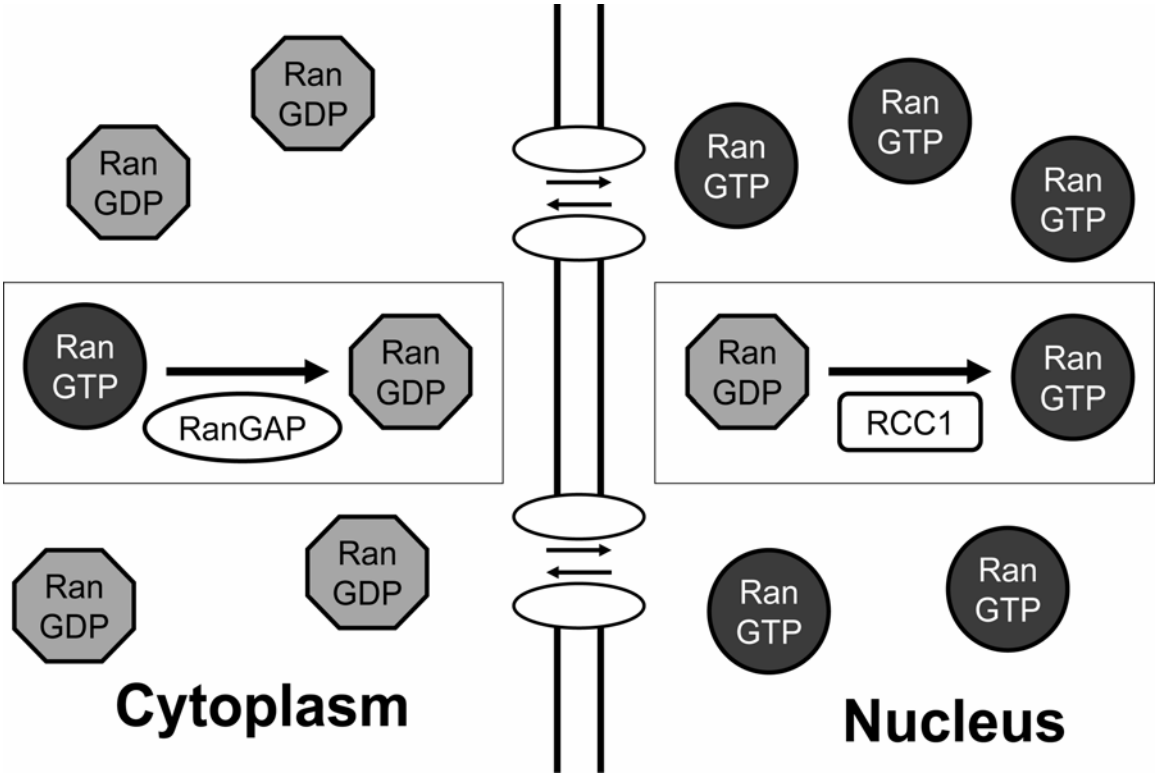

Figure 2. Ran GTPase System.
RanGTP is concentrated in the nucleus while RanGDP is concentrated in the cytoplasm. The nucleotide-bound state of Ran depends on the nuclear guanine nucleotide-exchange factor, RCC1 (RanGEF), which catalyzes the conversion of RanGDP to RanGTP in the nucleus and the cytoplasmic guanine nucleotide-activating factor, RanGAP, which facilitates GTP hydrolysis in the cytoplasm.

1.7 A Model of Classical Nuclear Import

Classical nuclear import is the most well characterized nuclear transport pathway. The classical nuclear import machinery transports ~100-1,000 cargoes per minute per NPC [92]. The classical nuclear import cycle consists of four key steps: (1) assembly; (2) translocation; (3) delivery; and (4) recycling (Figure 3).

During the first step, a trimeric import complex is assembled in the cytoplasm when a cNLS-containing cargo destined for the nucleus is recognized by the heterodimeric receptor consisting of the adapter importin α and the nuclear pore targeting subunit, importin β [75, 93-96]. Second, the trimeric complex is translocated through the NPC to the nucleus by interaction of importin β with FG-Nup proteins [97, 98]. Third, the interaction of RanGTP with importin β triggers the disassembly of the trimeric import complex and delivery of the cNLS cargo into the nucleus [99, 100]. Fourth, after disassembly of the cNLS cargo:carrier complex, the receptors must be recycled back to the cytoplasm for another round of nuclear import. Importin β is transported back to the cytoplasm in complex with RanGTP [101, 102]. Importin α is transported by the export factor, CAS/Cse1, in complex with RanGTP [103-105]. This trimeric export complex is dissociated in the cytoplasm upon hydrolysis of RanGTP to RanGDP and a conformational change in Cse1 [106, 107].

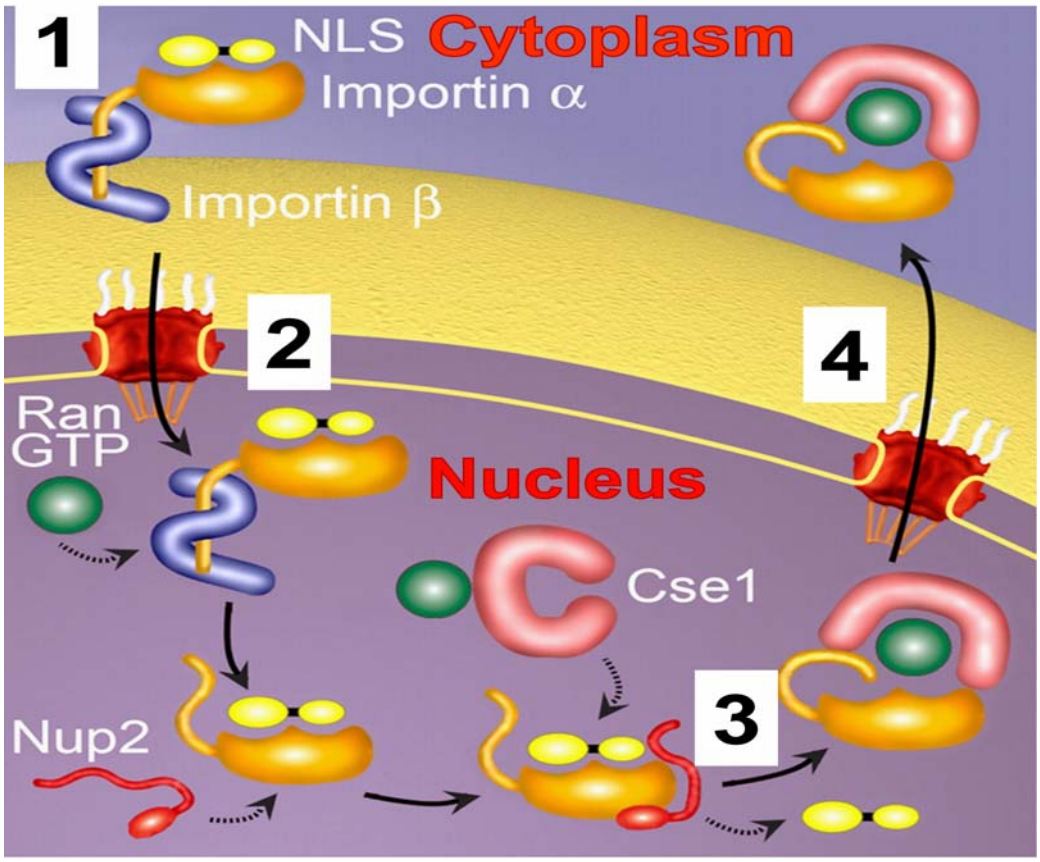

Figure 3. Model of Classical Nuclear Import.
Classical nuclear transport contains four key steps: (1) Assembly of the importin α/β/cNLS cargo import complex in the cytoplasm; (2) Translocation of the import complex through the nuclear pore complex to the nucleus; (3) Delivery of the cNLS cargo into the nucleus; and (4) Recycling of the import receptors back to the cytoplasm for another round of nuclear import.

1.8 Classical Nuclear Transport Factors

Delivery of cNLS cargoes into the nucleus requires coordinated function of receptors (importin α and importin β), the nuclear pore, RanGTP and other factors that facilitate delivery of the cargo into the nucleus including the importin α export receptor, Cse1, and the nucleoporin, Nup2. Knowledge of the function and interaction of these factors with each provides insight into understanding classical nuclear transport of cNLS cargoes to the nucleus.

1.8a The Classical Adapter Receptor: Importin α

In 1994, the first subunit of the heterodimeric import complex, importin α (karyopherin α, Kap60), was identified in *Xenopus* cytosol as a 60 kDa protein [57]. Cloning and sequencing of the importin α gene [57] led to identification of importin α in other organisms [53, 76, 108-112]. Structural and biochemical studies of importin α revealed three functional domains (Figure 4A) [93, 94, 96, 113, 114]. The central domain is composed of tandem armadillo (ARM) repeats that consists of repeating tryptophan and asparagine amino acid residues. ARM repeats contain solvent-accessible surfaces that create extended binding sites for large proteins. The ARM repeats in importin α are involved in cNLS cargo recognition [64, 115]. The cNLS cargo binding domain contains two binding pockets, a major binding pocket consisting of ARM repeats 2-4 and a minor binding pocket region consisting of ARM repeats 6-8. Monopartite cNLS cargoes only bind the major binding pocket while bipartite cNLS cargoes interact with both the major and minor binding pockets [93, 94, 96].

The N-terminal domain of importin α has two important functional roles. First,

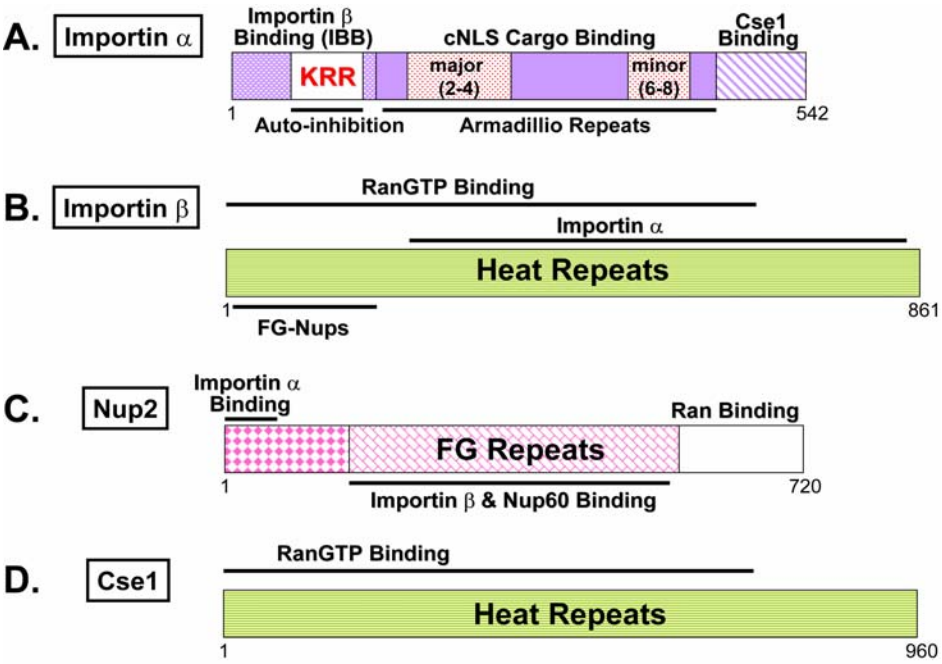

Figure 4. Domain structures of Importin α, Importin β, Nup2, and Cse1.
(A) Importin α contains three functional domains: an N-terminal importin β binding domain (IBB), a central cNLS cargo binding domain, and a C-terminal Cse1 binding domain. The cNLS cargo binding domain contains major and minor cNLS binding pockets. Monopartite cNLS cargoes bind the major binding pocket while bipartite cNLS cargoes interact with both the major and minor binding pockets. (B) Importin β consists of an N-terminal RanGTP binding domain that facilitates release of NLS cargo into the nucleus, an N-terminal FG-Nup binding domain that facilitates translocation of the import complex through the NPC, and a C-terminal importin α binding domain. (C) Nup2 contains an N-terminal importin α binding domain that facilitates release of cNLS cargo, an internal importin β and Nup60 binding domain, and a C-terminal RanGTP binding domain to aid in dissociation of the import complex. (D) Cse1 contains an N-terminal RanGTP binding domain that facilitates re-export of importin α.

the N-terminus contains the importin β binding (IBB) domain, the location where the carrier importin β interacts with importin α in the cytoplasm [116, 117].

Second, located within the IBB domain is a cluster of basic amino acids (KRR) that resembles a cNLS sequence (Figure 4A). This KRR sequence functions in auto-inhibition by competing with cNLS cargoes for binding to the central cNLS cargo binding domain of importin α [105, 118, 119]. There is no binding competition between the cNLS cargo and the IBB domain for the cargo binding domain when the IBB domain of importin α is bound by importin β in the cytoplasm [118]. Therefore, importin α has a high affinity for cNLS cargoes in the cytoplasm while bound to importin β (Figure 5). When importin α enters the nucleus, RanGTP binding to importin β triggers release of importin α and the cNLS cargo. Thus the auto-inhibition motif can compete with the cNLS cargo for binding to the cargo binding domain. In this free state, importin α has a low affinity for the cNLS cargo (Figure 5). This change in the affinity of importin α for the cNLS cargo helps facilitate release of cNLS cargoes into the nucleus. This mechanism has been confirmed in experiments demonstrating that importin α lacking the IBB domain has increased binding affinity for cNLS cargoes [22, 23, 43].

A portion of the N-terminal IBB domain together with the C-terminal domain of importin α creates a binding site for the export receptor Cse1/CAS (Figure 4A) [105, 114, 120]. This interaction is critical because it ensures importin α is not exported with cargo bound in a "futile transport cycle." The importin α:Cse1 interaction is required to recycle importin α back to the cytoplasm after cNLS cargo is released into the nucleus [88, 103-105, 121].

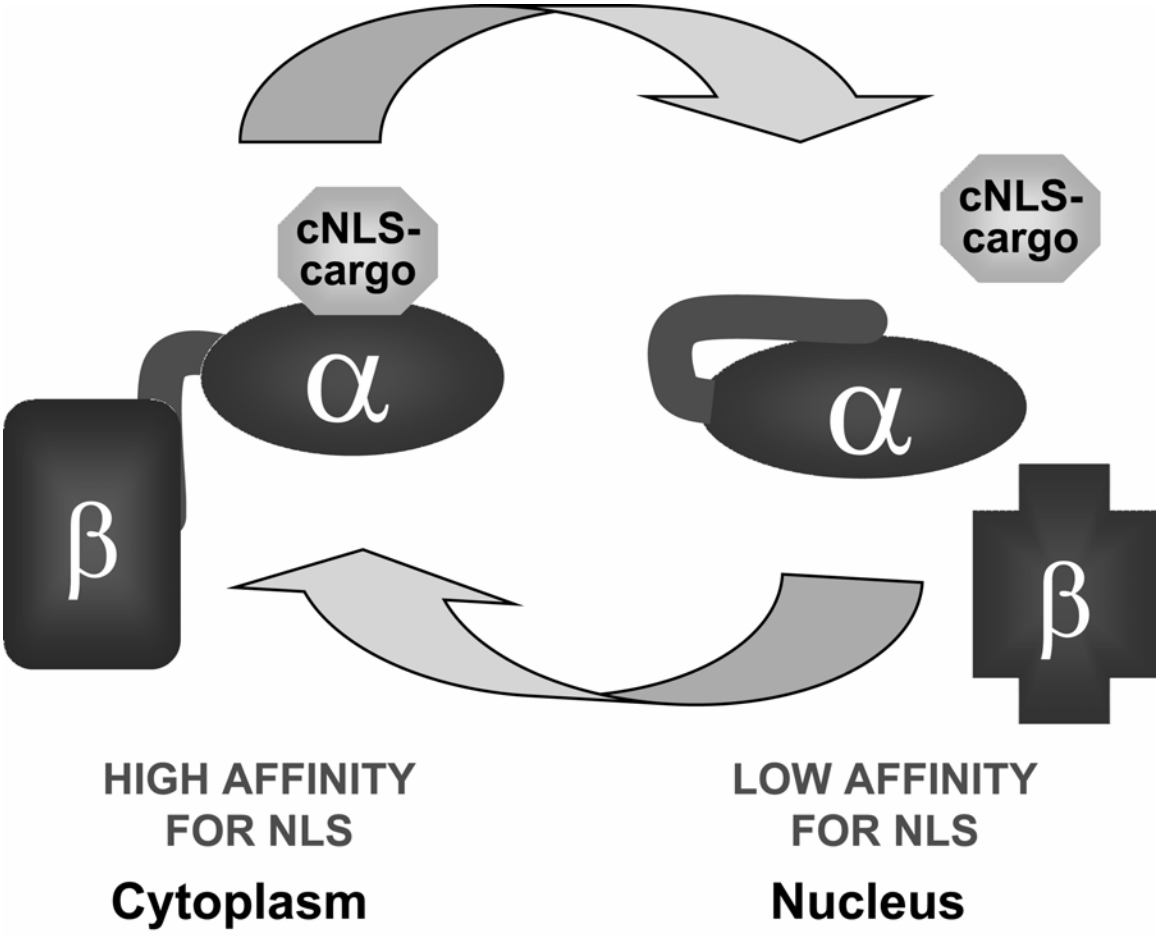

Figure 5. Binding Affinity of Importin α for cNLS cargo.
When the IBB domain of importin α is bound by importin β in the cytoplasm, importin α has a high binding affinity for the cNLS cargo because there is no competition between the auto-inhibitory motif and cNLS cargo for the cNLS binding pocket. Once the trimeric complex is translocated through the NPC into the nucleus, the loss of interaction between the importin α/β heterodimer triggered by RanGTP binding to importin β releases the IBB domain of importin α allowing the auto-inhibitory motif within the IBB domain to compete for binding to the cNLS cargo binding pocket and dissociate the cNLS cargo from importin α. This mechanism results in release of the cNLS cargo into the nucleus.

1.8b The Classical Carrier Receptor: Importin β

Classical importin β (karyopherin β1, Kap95) is the carrier receptor that indirectly binds cNLS cargoes through the adapter, importin α [75, 122]. Importin β contains 19 HEAT repeats consisting of two α helices that function as a docking site for other proteins [64, 115]. Domain analysis of importin β revealed three functional regions (Figure 4B) [123-125]. The N-terminus contains a RanGTP binding domain that facilitates release of cNLS cargo into the nucleus [99]. An additional region within the N-terminus in cooperation with the C-terminus is involved in binding FG-Nups located within the NPC. FG-Nups aid in translocation of the import complex through the NPC to the nucleus [22, 97, 98, 126]. The interaction of importin β with FG-Nups is weak and transient to allow rapid transport of cNLS cargo-carriers [97, 127]. The mechanism of how the FG-Nups facilitate cNLS cargo:carrier movement through the NPC is unknown. Lastly, the C-terminal region of importin β binds importin α in the cytoplasm [75].

1.8c FG-Nucleoporins: Nup2/Nup50

S. cerevisiae Nup2 and the mouse homolog, Nup50, are FG-Nups located on the interior nuclear face of the NPC (Figure 1) [128-130]. Nup2 contains an N-terminal importin α binding domain that cooperates with the C-terminal region, an internal FG repeat importin β and Nup60 binding domain, and a C-terminal Ran binding domain (Figure 4C) [22, 23, 129, 131]. Nup60 is involved in tethering Nup2 to the NPC [132, 133]. Nup2/Nup50 functions in the disassembly of the import complex and then assembly of the importin α export complex [22, 23, 129, 131].

1.8d Classical Export Receptor: CAS/Cse1

CAS/Cse1 is the importin α export receptor in the importin β superfamily that contains 19 HEAT repeats and a RanGTP binding domain like the classical importin β carrier receptor (Figure 4D) [74, 105]. Cse1 in complex with RanGTP mediates export of importin α back to the cytoplasm for subsequent rounds of cNLS cargo import [103, 104]. Cse1 will not interact with importin α unless the cNLS cargo has been released and delivered into the nucleus [104, 114, 125]. Structural studies show that Cse1 coils around RanGTP and importin α [105]. This interaction allows Cse1 to stabilize RanGTP and also allows the auto-inhibition motif in the IBB domain of importin α to bind the cNLS cargo binding domain, preventing cNLS cargo binding [105]. This mechanism helps ensure the proper delivery of the cNLS cargo to the nucleus and the export of cNLS cargo-free importin α to the cytoplasm. The importin α export complex is disassembled in the cytoplasm upon hydrolysis of RanGTP to RanGDP by RanGAP, leading to a conformational change in Cse1 to allow the interaction of the IBB domain of importin α with importin β [104-106].

1.9 Regulation of cNLS Cargo Delivery into the Nucleus

As was discussed previously, there are various factors and mechanisms orchestrating the efficient delivery of cNLS cargoes into the nucleus. Many critical cellular functions are dependent on cNLS cargo transport into the nucleus. There are two major steps in regulating nuclear import of cNLS cargoes. The first is cNLS cargo recognition by importin α in the cytoplasm. The second is the release of the cNLS cargo into the nucleus.

1.9a Recognition of cNLS Cargo in the Cytoplasm

There are many amino acid variations within the nuclear targeting sequence of a functional cNLS. Thermodynamic studies analyzed the relative importance for cNLS cargo binding to *S. cerevisiae* importin α *in vitro* [43]. In this study, a variant monopartite K(K/R)X(K/R) was engineered with or without a second basic cluster amino acids (KR) to represent a bipartite cNLS. Quantitative analysis was performed with either importin α lacking the IBB domain to represent cNLS cargo binding in the cytoplasm or with full-length importin α to represent the efficiency of cargo release into the nucleus since the auto-inhibition motif is located within the IBB domain. This study demonstrated a lysine residue followed by two basic residues is required to bind importin α for monopartite cNLS cargo import into the nucleus [43].

Structural analyses of the interaction between the cNLS cargo and isoforms of importin α have revealed highly conserved critical residues within the binding groove of importin α that mediate cNLS cargo recognition [93, 94, 96, 134]. *In vitro* and *in vivo* characterization of various conserved residues in the cNLS binding region of importin α revealed the functional importance of the major, minor, and linker binding region of importin α in recognition of monopartite and bipartite cNLS cargoes [135]. Functional studies show drastic changes in either of these pockets yield a non-functional protein. *In vivo* functional analyses of these regions revealed a conditional allele of importin α in the minor binding region termed *srp1-E402Q*. As mentioned previously, the minor binding pocket region of importin α is involved in binding bipartite cNLS cargoes [96]. The srp1-E402Q mutant can be utilized as a functional tool to identify bipartite cNLS cargoes

recognized by importin α [135]. Thus, the mechanism of import into the nucleus via importin α can be determined for a subset of bipartite cNLS cargoes.

1.9b Release of cNLS Cargo

The release of cNLS cargoes into the nucleus is much more complex than cNLS cargo recognition in the cytoplasm. The interaction between importin α and importin β must be disrupted before the cNLS cargo is released into the nucleus. Following entry into the nucleus, RanGTP binding triggers a conformational change in importin β leading to the irreversible dissociation of the IBB domain of importin α from importin β [99, 100]. Dissociation of the importin α:importin β interaction leads to release of the cNLS cargo into the nucleus. Interestingly, RanGTP and the IBB domain of importin α bind to overlapping regions of importin β [75, 99, 100].

Although the importin β:importin α interaction is disrupted upon RanGTP binding to importin β, the cNLS cargo interaction with importin α must also be disrupted for cargo release into the nucleus and subsequent export of importin α to the cytoplasm by Cse1. As discussed earlier, dissociation of the cNLS cargo occurs when the auto-inhibition motif within the IBB domain of importin α competes with the cNLS cargo for binding to the cNLS cargo binding pocket [118, 119, 136]. Because nuclear transport occurs at a fast rate of ~100-1000 NLS cargoes per second per NPC, the dissociation of cNLS cargoes from importin α through the auto-inhibition function may not be sufficient to release cargoes with high affinities for importin α [92, 137]. Energetic studies by Hodel *et al*. suggest cNLS cargoes possessing a high binding affinity for importin α may not be efficiently released into the nucleus [43].

The function of the FG-Nup, Nup2/Nup50, is activated once the importin α/β:cNLS cargo trimeric complex is docked at the NPC by interaction with importin β. Nup2/Nup50 is able to compete with cNLS cargoes for binding to two sites on importin α [23]. One higher binding affinity site is used to anchor Nup2/Nup50 to importin α and the other weaker binding affinity site overlaps with the major and minor cNLS cargo binding pocket of importin α to aid in release of the cNLS cargo into the nucleus [22, 23].

Further *in vitro* and *in vivo* characterization of importin α examined the importance of the auto-inhibitory function [118, 136]. A change in one of the amino acids within the auto-inhibition motif create a non-functional the importin α protein that causes cells to die. Studies in *S. cerevisiae* identified a conditional allele in importin α, s*rp1-55* (KRR→^{54}KAR^{56}) [136]. The *srp1-55* mutant shows a defect in the auto-inhibition function and a defect in release of the cNLS cargo into the nucleus [136]. Thus, the Srp1-55 mutant can be used as a tool to identify cNLS cargoes affected by defects in cNLS cargo release into the nucleus [136].

1.10 Regulation of Nuclear Transport

There are three general mechanisms for regulating cNLS cargo nuclear import [138-140]. (1) Intramolecular masking involves the prevention of cNLS cargo recognition by importin α by a conformational change in the cNLS cargo [140-143]. (2) Intermolecular masking is blocking the nuclear targeting sequence of the cNLS cargo from importin α recognition by interaction of the cNLS cargo with another molecule or protein [140, 144, 145]. (3) Modulation of cNLS cargo binding affinity to importin α by

phosphorylation within or adjacent to the cNLS cargo nuclear targeting sequence [140, 146, 147].

In addition to the regulation of nuclear import by cNLS cargo recognition and release by importin α, the nuclear envelope acts as a physical barrier for the regulation of nuclear transport. As mentioned above, macromolecules can only gain access to the nucleus by passage through the NPCs, which are embedded in the nuclear envelope [3, 4]. In higher eukaryotes (Figure 6), the nuclear envelope breaks down at late mitosis leading to free distribution of macromolecules between the nucleus and cytoplasm [148, 149]. In contrast, the nuclear envelope does not breakdown in budding yeast and some other fungi [150]. Thus, macromolecules that enter the nucleus in yeast and fungi depend on the nuclear transport machinery throughout the cell cycle.

1.11 General Overview of the Eukaryotic Cell cycle

The duplication of genetic material to produce a new cell or organism entails many events that comprise the cell cycle. The eukaryotic cell cycle is divided into four phases: cell growth, DNA replication, transfer of genetic material to daughter cells, and cell division (Figure 6). These phases are separated into two stages: interphase and mitosis. Interphase consists of approximately 95% of the cell cycle while mitosis only consists of about 5%. Interphase is subdivided into Gap1 (G_1), Synthesis (S), and Gap2 (G_2) [151]. The G_1 phase separates mitosis and S phase initiation. During the G_1 phase the cells grow and prepare for DNA replication. During S phase (DNA replication), the packaged DNA containing many chromosomes is duplicated to form sister chromatids. The sister chromatids are held together by centromeres. The centromeres are also

duplicated. During G_2 phase, the cell continues to grow and protein synthesis occurs to prepare for mitosis [151].

Mitosis follows interphase. Mitosis (M phase) is the phase where the duplicated contents of the nucleus separate as the daughter cells separate (cytokinesis). Mitosis is subdivided into six key steps [152, 153]. First, early prophase is identified by the movement of kinetochores to the opposite poles of the cell, along with the breakdown of the nuclear envelope. Kinetochores function in sister chromatid movement. Second, during late prophase, the sister chromatids are condensed and the microtubule spindles, which are involved in cellular structure and movement, begin to elongate from the spindle pole bodies. Third, the sister chromatids align near the equator of the cell during metaphase. Fourth, anaphase is identified by the separation of the two sister

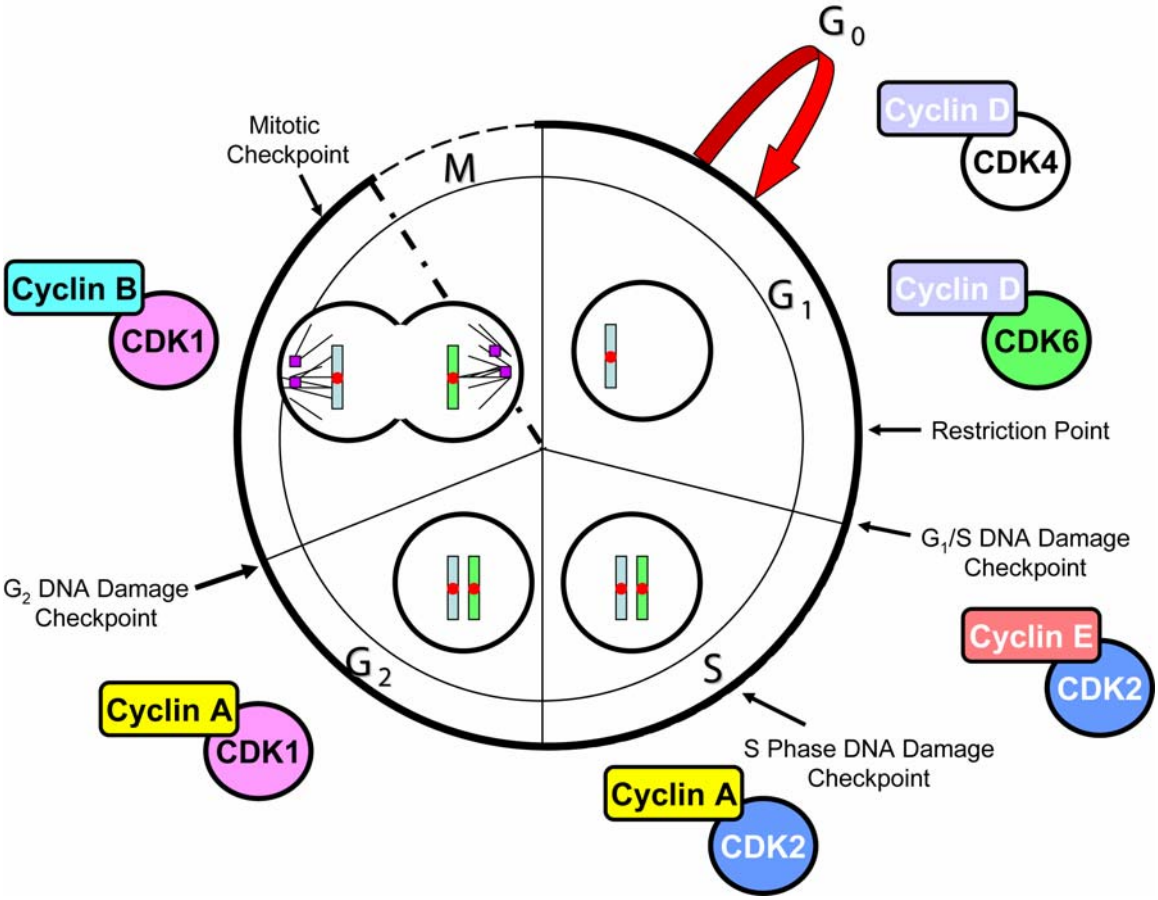

Figure 6. The Eukaryotic Cell Cycle, Cell Cycle Regulators, and Checkpoints.
The eukaryotic cell cycle is divided into two stages: mitosis and interphase. Interphase is subdivided into Gap1 (G_1), Synthesis (S), and Gap2 (G_2). During G_1 phase, cells grow and prepare for DNA replication. During S phase, chromosomes are duplicated forming sister chromatids. The sister chromatids are held together by centromeres. The G_2 phase is the stage where cell growth and protein synthesis occurs. Mitosis (nuclear division) or M phase is the phase where the daughter cells separate and the cells divide (cytokinesis). Cells do not progress to the restriction point located at late G_1 phase, if the environment is not favorable for cell division. Then the cells progress into the resting state, the G_0 phase. Checkpoints are located throughout the cell cycle to function as monitoring devices for DNA damage and proper spindle formation. The interaction between cyclins and cyclin-dependent kinases (CDK) regulates progression through the cell cycle.

chromatids into individual chromosomes as the cell and spindles elongate to begin cytokinesis. Fifth, during telophase, a new nuclear envelope forms, the spindles depolymerize, and the chromosomes decondense. Sixth, cytokinesis completes mitosis with division of the cytoplasm to create two daughter cells. Then the cells enter the G_1 phase for another round of cell duplication [152, 153].

Although the cell cycle of budding yeast is similar to higher eukaryotes, *S. cerevisiae* duplicate their cells by budding and the nuclear envelope does not breakdown at late mitosis (Figure 7) [150]. Briefly, the beginning of the G_1 phase is signified by a mother cell. As the G_1 phase progresses, protein synthesis occurs as the cell simultaneously grows until it reaches a sufficient size to activate gene expression and the microtubule spindles assemble at the spindle pole bodies. If the cell is switched to a low nutrient medium without the appropriate growth-promoting signals, then the cell enters the G_0 phase where the cell grows slowly until the cell reaches an optimal size to progress through the cell cycle. Once the cell reaches a critical size, the cell commits to transitioning through the cell cycle at the start point [154]. During S phase, a bud emerges on the cell and the spindle pole bodies duplicate. As the cell reaches the G_2 phase, the bud continues to grow and the spindle pole bodies separate as the microtubule spindles formulate and elongate [155]. The exact timing of spindle elongation is controversial because spindle elongation has also been documented as entry into mitosis [156]. The spindles continue to elongate as well as the nucleus while the bud simultaneously grows larger at the G_2/M transition stage [155]. During mitosis, the chromosomes segregate and the nucleus divides [155].

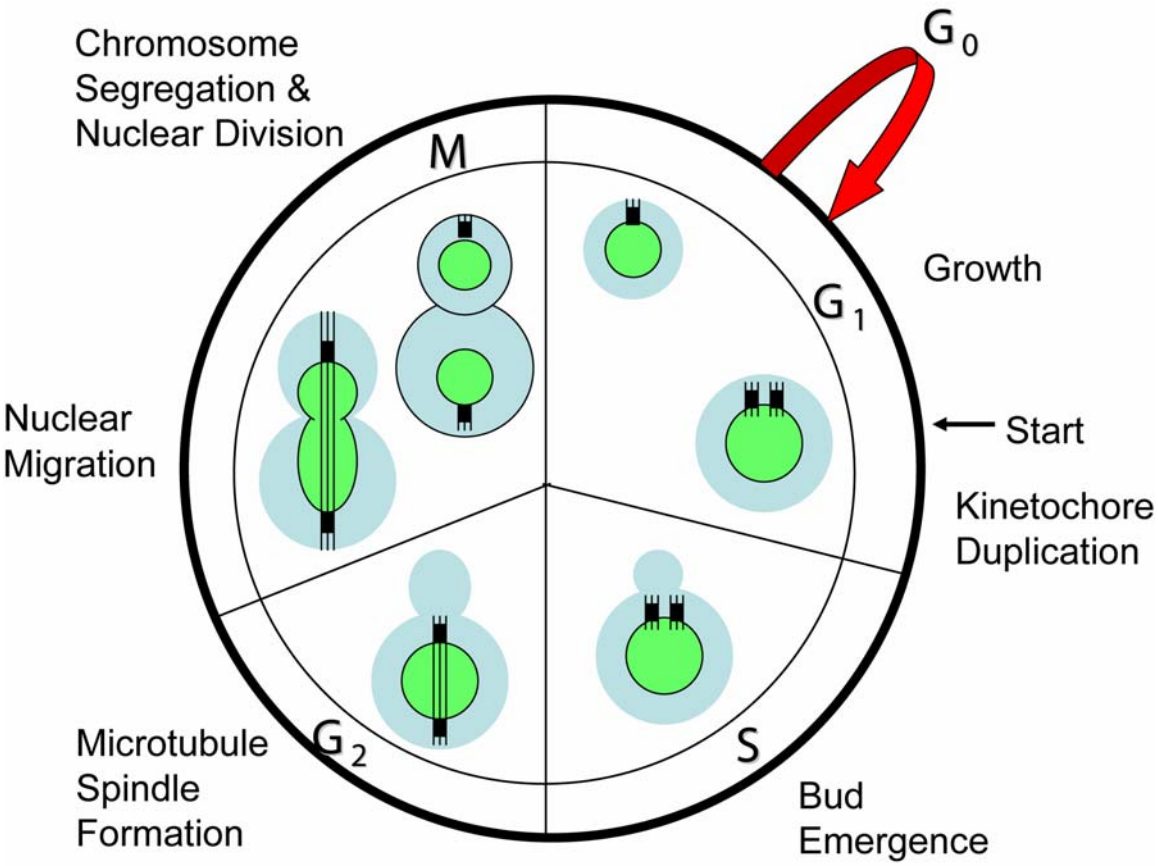

Figure 7. The yeast *S. cerevisiae* cell cycle.
S. cerevisiae duplicate by budding. During the G_1 phase, the cell grows until it reaches a sufficient size to activate gene expression and the microtubule spindles assemble at the spindle pole bodies. If the cell is switched to a low nutrient medium then the cell enters G_0 phase where it grows slowly until the cells reaches an optimal size to progress through the cell cycle. Once the cell reaches a critical size, the cell commits to transitioning through the cell cycle at the start point. During S phase, a bud emerges on the cell and the spindle pole bodies duplicate. As the cell reaches G_2 phase, the spindle pole bodies separate as the microtubule spindles formulate and elongate. The spindles continue to elongate as the nucleus migrates to each side of the cell at the G_2/M stage. During mitosis, the chromosomes segregate and the nucleus divides.

1.11a Regulation of the Eukaryotic Cell Cycle

Progression through the eukaryotic cell cycle is regulated by many factors. One of these is the cell cycle checkpoints. The checkpoints function as monitoring devices. Different checkpoints are put in place throughout the cell cycle to ensure different processes have been completed properly in order to maintain the integrity of the genome (Figure 6) [157, 158]. The cell cycle is stopped at distinct checkpoints if all the conditions are not favorable and the processes have not occurred appropriately to transition to the next phase. These halts in the cell cycle allow time to repair the problem. If the problem can not be repaired then the cells are targeted for programmed cell death (apoptosis).

There are four main checkpoints: G_1/S, S phase, G_2 phase, and the mitotic (spindle) checkpoint (Figure 6) [158]. The G_1/S checkpoint detects DNA damage such as double-strand breaks, UV photo products or incomplete DNA replication. The S phase checkpoint also detects DNA damage. The G_2 phase checkpoint detects DNA damage after DNA replication has been completed. The mitotic checkpoint ensures that mitotic spindles form properly [158-160]. In addition, DNA damage checkpoints are activated throughout the cell cycle and function by activating critical proteins that work to repair each type of DNA damage [161]. Another regulatory mechanism is the restriction point. Cells do not progress to the restriction point (start in yeast) located at late G_1 phase of the cell cycle if the cells have not received the appropriate growth-promoting signals. These cells progress into the resting state, the G_0 phase. Some cells stay in the G_0 phase forever [157, 162].

Key regulators of the cell cycle are cyclins and a family of cyclin-dependent kinases (CDK) [154, 163]. CDKs are a part of a family of serine/threonine protein

kinases that trigger activation of downstream factors by phosphorylating specific proteins [164, 165]. Interaction between cyclins and CDKs activates the kinase of the bound CDK [165, 166]. The cellular levels of cyclins control progression through the cell cycle. The levels of these cyclins vary at certain stages of the cell cycle while the CDK levels remain relatively stable [167, 168].

The cyclins and CDKs form different complexes at distinct phases of the cell cycle (Figure 6). Interaction between the cyclin D proteins (cyclin D1, cyclin D2, and cyclin D3) with CDK4 and CDK6 are required for entry into G_1 phase [169]. Cyclin E interacts with CDK2 to regulate the G_1/S phase transition [170]. Cyclin A also binds CDK2 but it regulates S phase entry and S phase progression [171, 172]. Lastly, cyclins A and B separately interact with CDK1 during late G_2 to M phase to regulate entry into mitosis and M phase progression [173, 174]. The activity of the CDKs is not only regulated by interaction with cyclins, but CDK function can be negatively regulated by CDK inhibitors (CKI) that bind CDK alone or CDK-cyclin complexes [175]. In *S. cerevisiae*, there is only one CDK protein which regulates cell cycle progression, the cell-division cycle protein, Cdc28 [176, 177].

1.12 Interplay of Nuclear Transport and Cell Cycle Progression

There is a long history suggesting nuclear transport factors play key roles in regulating the cell cycle. The original indicators come from defects in cell cycle progression associated with mutations in nuclear transport factors [178-182]. For example, the first evidence of interplay between nuclear transport and the cell cycle was observed with the nuclear transport factor, Ran. A study utilizing cultured baby hamster kidney cells containing a conditional allele of RCC1 (RanGEF), revealed premature entry

into mitosis in the presence of unreplicated DNA [178]. Furthermore, in a conditional allele of RanGEF in fission yeast cells, the mutant cells progress through one round of DNA replication and mitosis before arresting at the mitosis-interphase transition of the cell cycle due to the failure of chromatin decondensation [179]. Subsequent studies have revealed RanGTP regulates the activity of several mitotic proteins primarily by modulating interactions with nuclear import factors [181-185].

Importin α orthologs in *S. cerevisiae* and the fission yeast, *Schizosaccharomyces pombe*, have also been linked to the cell cycle [113, 180, 186]. Interestingly, a conditional allele of *S. cerevisiae* importin α (*SRP1*), *srp1-31*, which contains an amino acid substitution within the first ARM domain just N-terminal of the cNLS binding pocket, was shown to cause cell cycle defects [113, 180]. The srp1-31 mutant has been reported to delay cells at the G_2/M transition of the cell cycle [180]. This mutant also shows defects in nuclear protein import [180], suggesting the cell cycle delay could be due to the inability to import key proteins functioning in the G_2/M transition. However, the *srp1-31* mutation is not located within a functional region of importin α, making it unclear how this amino acid change impacts the molecular function of importin α in nuclear import (Figure 2).

Many proteins have been identified whose functions in different cellular processes are dependent upon their ability to be imported into the nucleus at distinct stages of the cell cycle. A subset of these cargo proteins that contribute to control of the cell cycle, are likely to be targeted into the nucleus through a cNLS sequence [47].

1.12a Cell Cycle Regulated Proteins

As mentioned earlier, progression through the eukaryotic cell cycle is regulated by the cellular levels of cyclins and interaction of the cyclins with CDKs [167, 168]. Specifically, cyclin A and cyclin B are required for entry into mitosis and their expression level is regulated [173, 174]. The function of the cell cycle regulators, cyclin A and cyclin B, is dependent on import into the nucleus during different phases of the cell cycle when the nuclear envelope is intact [187]. Cyclin A is imported into the nucleus during the S phase and is degraded during metaphase of mitosis [187]. Cyclin B accumulates in the cytoplasm during the S and the G_2 phases and then cyclin B is imported into the nucleus at the start of mitosis before the nuclear envelope is broken down [187, 188].

1.12b Nuclear Transport, Cell Cycle, and Cancer

The activity of tumor suppressors and transcription factors involved in controlling cell growth and cell death is also regulated by their location in the cell during distinct stages of the cell cycle [189]. The mislocalization of these proteins can potentially lead to the development of different cancers [190-194]. For example, the activity of the multifunctional tumor suppressor, p53, is highly regulated by its cell cycle dependent localization to the nucleus. The expression of p53 is controlled by its degradation in the cytoplasm. Stressors such as DNA damage induce the transient stabilization of p53 and localization of p53 into the nucleus [195]. The p53 protein enters the nucleus at various stages of the cell cycle in different tissue types to activate transcription factors that initiate apoptosis [196-199]. The nuclear import of p53 is poorly understood but published reports show nuclear accumulation of p53 between the G_1 and the S phases of

the cell cycle [200]. It has been reported that mislocalization of p53 to the cytoplasm plays a role in tumorigenesis [201].

The mislocalization of the tumor suppressors, nuclear factor kappa B (NF-κB) and breast cancer 1 (BRCA1), also plays a role in the development of various types of cancers [202]. NF-κB accumulates in the nucleus at the G_1 to S phase transition of the cell cycle [203] and BRCA1 is located in the nucleus at all phases of the cell cycle [204]. The distinct nuclear localization-dependent function of proteins like NF-κB and BRCA1 demonstrates a fundamental role of nuclear import-mediated cell cycle transitions. These examples reveal direct consequences of defects in nuclear transport of critical proteins that regulate cell growth. Therefore, studying the interplay of nuclear transport and the cell cycle could be important for the development of therapeutic approaches to prevent and fight cancers caused by the mislocalization of proteins that regulate cell proliferation.

1.13 *S. cerevisiae* as a Model to Study Nuclear Transport and the Cell Cycle

S. cerevisiae is the ideal model organism to study the interplay between nuclear transport and the cell cycle because the proteins and cellular functions of nuclear transport and the cell cycle are conserved. A fundamental difference between *S. cerevisiae* and higher eukaryotes is the fact that nuclear envelope does not break down during late mitosis in yeast [201]. Therefore, all proteins in *S. cerevisiae* must be actively transported across the nuclear envelope at all stages of the cell cycle. Genetic manipulations in yeast also make it possible to generate conditional alleles to utilize in studying the function of essential genes that would otherwise cause the cell to die in another organism.

1.14 Dissertation Overview

The goal of Chapter II was to develop a quantitative model to identify the upper and lower limits of importin α binding affinity for cNLS cargoes. The hypothesis of this study was the binding affinity between importin α and a cNLS cargo dictates cNLS cargo import into the nucleus. In this study, our lab in collaboration with the Hodel laboratory characterized different cNLS cargo variants possessing a broad range of binding affinities for importin α. We demonstrate the higher the binding affinity of a cNLS cargo for importin α, the higher the probability of the cNLS cargo accumulating in the nucleus.

The goal of Chapter III was to define a role between nuclear transport and cell cycle progression. In this study, we used two mutants of importin α with defined molecular defects in nuclear import to determine the role nuclear transport plays in cell cycle progression. We show the G_1/S transition of the cell cycle is affected by these importin α mutants. In addition, we identified possible cNLS cargoes that function in the G_1 and/or S phases of the cell cycle and show that their localization is affected by defects in nuclear import.

Furthermore, these studies investigate how the nuclear import of key cNLS cargoes involved in cell cycle control are affected by the function of the nuclear import receptor, importin α. As a result of these studies we have defined a specific role of the nuclear transport machinery in cell cycle progression in *S. cerevisiae*.

Chapter IV consists of an overall discussion of the data presented in this dissertation and how this body of work increases the knowledge in the nuclear transport and cell cycle field. Future directions will also be presented.

CHAPTER 2

Nuclear Signal-Receptor Affinity Localization Correlates with *in vivo* Localization

Alec E. Hodel*, Michelle T. Harreman*, Kanika F. Pulliam*, *et al.*

*Department of Biochemistry, Emory University School of Medicine, Atlanta, GA 30322
and †Department of Physics, Emory University, Atlanta, GA, 30322

Published in *Journal of Biological Chemistry* 281(33):23545-23556 August 2006

Although this work was published in collaboration with A. Hodel, only my contributions are presented.

Abstract

Nuclear localization signals (NLSs) target proteins into the nucleus through mediating interactions with nuclear import receptors. Here, we perform a quantitative analysis of the correlation between NLS-receptor affinity and the steady-state distribution of NLS-bearing cargo proteins between the cytoplasm and the nucleus of live yeast, which reflects the relative import rates of various NLS sequences. We find that there is a complicated, but monotonic quantitative relationship between the affinity of an NLS for the import receptor, importin α, and the steady-state accumulation of the cargo in the nucleus. This analysis assesses the impact of protein size. In addition, the hypothetical upper limit to an NLS affinity for the receptors is explored through genetic approaches. Overall, our results indicate that there is a correlation between the binding affinity of an NLS cargo for the NLS receptor, importin α, and the import rate for this cargo. This correlation, however, is not maintained for cargoes that bind to the NLS receptor with very weak or very strong affinity.

2.1 Introduction

The segregation of the nuclear genetic material from the cytoplasmic machinery that translates it into proteins provides the eukaryotic cell with complex mechanisms for controlling gene expression. This segregation, however, also presents the cell with a mechanistic problem. Since most intra- and extracellular signaling pathways culminate with changes in gene expression within the nucleus, signals must cross the nuclear envelope to gain access to the genetic material. This signal is almost invariably a protein, such as a transcription factor, that enters the nucleus. In addition, once a gene is transcribed, the messenger RNA must then be exported across the nuclear envelope into the cytoplasm where it is translated into protein. In fact, the nuclear envelope is a critical information barrier across which both RNA and proteins are selectively transported in a highly regulated manner to establish orderly communication and behavior within the cell [205].

The best-characterized mechanism for translocation across the nuclear envelope is protein import which depends on the 'classical' nuclear localization signal or NLS [40]. A classical NLS consists of a cluster of basic residues (monopartite) or two clusters of basic residues separated by 10-12 residues (bipartite) [41, 44]. A complete understanding of nuclear import signals requires a quantitative model for the import reaction that correlates NLS amino acid sequence, *in vitro* interaction energies, and *in vivo* functionality. We have previously attempted to decipher the energetic details of NLS recognition by importin α through quantitative analysis of variant NLSs. The relative importance of each residue in two monopartite NLS sequences was determined using an alanine scanning approach [43]. This analysis was performed using the ΔIBB-importin α

variant, which lacks the N-terminal auto-inhibitory domain, as a model for the high affinity importin α/importin β complex. Variants of NLS sequences were generated with affinities for ΔIBB-importin α that ranged between a K_D of a few micromolar to a K_D of a few picomolar (see Table I). In addition, the energy of inhibition of the importin α IBB domain was measured and found to be approximately 3 Kcal/mole regardless of the sequence of the NLS. These data allow the generation of an energetic scale of nuclear localization sequences where a signal has a high affinity for the cytoplasmic importin α/importin β complex and an affinity 3 Kcal/mole weaker for the auto-inhibited importin α in the nucleus [43].

One goal of this quantitative analysis is to provide a thermodynamic foundation for a numerical model of the process of nuclear transport (for examples see [85, 206, 207]). One would expect that the *in vivo* process of nuclear import would correlate in some manner with the energetics of the individual protein-protein interactions that drive the process. One finding from a recent modeling study is that the rates of nuclear protein import are largely governed by the level of the NLS receptor, importin α [207]. One implication of this finding is that the binding affinity of the NLS receptor for its cargo should be an important determinant of how efficiently that cargo is transported into the nucleus. Indeed, there is empirical evidence to indicate that there is some sort of functional threshold of affinity that an NLS must possess for importin α in order for the cargo to be imported into the nucleus [42]. When the SV40 NLS (PKKKRKVE) is mutated to the SV40T3 sequence (PKTKRKVE), its affinity for ΔIBB-importin α decreases by ~ 3 Kcal/mol (from K_D=9 nM to K_D=3 μM) and it also loses its ability to function as a nuclear localization signal *in vivo* [42]. Thus the energetic threshold

dividing a functional NLS from a non-functional NLS exists somewhere between the binding affinity of the SV40T3 variant NLS (K_D=3 μM) and the SV40 wildtype NLS (K_D= 9 nM).

There have been a handful of reports comparing the measured binding affinity between an NLS and its receptors with the rate of import of a cargo fused to that NLS *in vivo*. Work by Jans *et al.* [208-210] involved the measurement of the binding constant between several NLSs and full length importin α through an ELISA assay followed by measurement of the import rate of these NLSs microinjected into rat hepatoma cells. They reported that the initial rate of protein import is linearly correlated with the equilibrium constant for the interaction between the NLS-cargo and importin α. This is an interesting result as this relationship would hold true in a simple model where the rate of protein import would depend on the equilibrium concentration of the importin α/importin β/cargo-NLS ternary complex. Although provocative, the dynamic range of the measurements used in this study was limited: the range of K_D measurements used in this report varied only by a factor of four. Thus it would be interesting to see if this correlation suggested in these studies is general to a wider range of NLS affinities.

The quantitative data generated by our examination of the energy landscape of importin α yields a numerical skeleton on which to build a comprehensive model for the complicated process of protein import. A given NLS can be situated on a linear scale that describes its affinity for the importin α/importin β complex (using ΔIBB importin α as a model) as well as its affinity for importin α alone [43]. For an NLS to function in nuclear import, one might hypothesize that it must have an affinity for the importin α/β complex that is tight enough to stimulate the uptake of the NLS-cargo into the nuclear pore, but it

must also have an affinity for lone importin α that is weak enough to allow efficient release of the cargo into the nucleus. Thus, we might hypothesize that there are both upper and lower limits to the affinity of an NLS for its receptors that define a functional localization signal.

Here, we report the results of our initial experiments designed to address the correlation between *in vitro* binding energies and *in vivo* import function. We quantify the initial import rates of various NLSs in live yeast cells of the NLS-bearing cargo protein. Our results indicate that there is a complicated but monotonic quantitative relationship between the affinity of an NLS for the import receptors and the initial rate of nuclear accumulation of the cargo in the nucleus.

2.2 Material and Methods

Construction of Plasmids

All plasmids used in this study are listed in Table 2. NLS-GFP fusion proteins were expressed in the yeast S. cerevisiae under the control of the *MET25* promoter using the plasmid pGFP-C-FUS [211]. The NLS-GFP fusion proteins expressed in yeast were identical to the proteins expressed in E. coli for in vitro binding studies [43] except that the first 17 residues of the N-terminus were removed, including the N-terminal 6xHis tag, to facilitate expression in yeast. The DNA sequences encoding the SV40-GFP fusion were amplified from the bacterial expression vector (see [43] using the DNA oligonucleotide GCTCTAGATGGGCAGCCATATGGCTAG as a 5' primer and the oligo ACTCATCTCGACGGTATCG as the 3' primer. The DNA encoding the SV40-GFP fusion protein was then ligated into the yeast expression vector pGFP-C-Fus [211] using *Xba*I and *Cla*I restriction sites, placing the gene as an in-frame 5' fusion with a

second GFP molecule encoded in the vector DNA (pAC1065). The fidelity of the resulting vector was confirmed by sequencing and by appropriate expression of the target protein in yeast. Other NLS sequences were placed in this vector by PCR amplification and then ligated into the SV40-GFP-GFP vector using *Xba*I and *Hind*III.

NLS-reporters carrying a single copy of the GFP protein were constructed from the NLS-GFP-GFP reporter plasmids by digesting with *Sal*I, then performing an intramolecular ligation with the resulting large fragment.

To construct a plasmid encoding the NLS-GFP-NES reporter, first an intermediate vector was generated encoding GFP-NES. The bacterial expression vector SV40-GFP [43] was amplified using the primers GTCCGGCGTAGAGGATCGAG, which primed 5' to the gene in the vector, and GCGCCTCGAGTTAGCGGCCGCGGA GGAGCCGGAGCCTTTGTATAGTTCATCCATGC, which added a *Not*I site at the 3' end of the GFP gene. The resulting DNA fragment was cut with *Hin*dIII and *Xho*I and ligated into pET28a (Novagen). After verification by sequencing, this new vector, GFP-Not, was then amplified with primers GTCCGGCGTAGAGGATCGAG at the 5' end and GCGCCTCGAGTTAGGACCCGGACCCTATGTCCAAGCCTGCGAGTTTCA GTGCCAGGGCGGCCGCGGAGGAGCCGG, which added the NES sequence to the 3' end of the GFP gene after the *Not*I site. This PCR fragment was again cut with *Hin*dIII and *Xho*I and ligated into pET28a. After verification by sequencing, the DNA fragment encoding GFP-NES was then excised using *Hin*dIII and *Xho*I. This fragment was then ligated into each yeast NLS reporter expression plasmid cut with the same enzymes creating NLS-GFP-NES reporters with unique NLS sequences that could be expressed in yeast.

Microscopy

Indirect immunofluorescence was performed as described elsewhere [212]. To detect myc-tagged importin α or the NLS-GFP reporter, myc (EMD Bioscience) and GFP antibodies [213] were diluted 1:3000 and incubated with fixed cells overnight at 4ºC. The Texas Red-labeled anti-mouse secondary (Jackson ImmnunoResearch) and FITC anti-rabbit secondary antibodies (1:1000) were incubated with cells for 2 h at room temperature. Cells were also labeled with DAPI (1 μg/ml) to mark the position of the nucleus. Samples were viewed through a Texas Red-optimized filter and a GFP-optimized filter (Chroma Technology) using an Olympus BX60 epifluorescence microscope equipped with a Photometrics Quantix digital camera.

Direct fluorescence microscopy was used to localize GFP fusion proteins in live cells. For all experiments, cells were incubated with DAPI to visualize the DNA and confirm the location of the nucleus. The localization of the fusion protein was monitored by directly viewing the GFP signal in living cells through a GFP-optimized filter as described for indirect immunofluorescence microscopy.

NLS-GFP Import Assay

The NLS-GFP import assay was performed as described previously [214]. Briefly, cells were grown to early mid-log phase in synthetic media containing 2% glucose (w/v) at 30ºC, pelleted, resuspended in 1 ml of glucose-free synthetic media containing 10 mM sodium azide, 10 mM 2-deoxy-D-glucose, and incubated at 30ºC for 45 min. The cells were then pelleted, washed with 1 ml of ice-cold ddH_20, repelleted, resuspended in 100 μl of glucose-containing synthetic media pre-warmed to 30ºC, and incubated at 30ºC. For scoring, 2-μl samples were removed every 2.5 min following resuspension in pre-warmed glucose-containing synthetic media. Individual cells were analyzed and counted

using a GFP-optimized filter (Chroma Technology) using an Olympus BX60 epifluorescence microscope. Cells were scored as "nuclear" if the nucleus was both brighter than the surrounding cytoplasm and a nuclear-cytoplasmic boundary was visible. At least 100 cells were counted for each time point. Cells were also examined to assure the complete relocalization of nuclear proteins upon energy depletion.

Overexpression of NLS Cargo

Wild-type cells (ACY192) or *srp1-55* cells (ACY642) were transformed with β-galactose inducible plasmids encoding GFP (pAC1350), SV40 NLS (ESPKKKRKVE)-GFP (pAC1352), a bipartite SV40 NLS (KRTADGSEFESPKKKRKVE)-GFP (pAC1353) or as a control a known dominant negative mutant of NTF2 (N77Y NTF2, pAC253) [43, 118, 215]. Single transformants were grown in liquid culture to saturation, serially diluted (1:10) and spotted on minimal media plates containing 2% galactose or, as a control, 2% glucose. Galactose induces expression of the plasmid encoded proteins. Plates were incubated at 25°C for 3 days. For all experiments we employed quantitative immunoblotting to examine the level of expression of both the NLS reporter proteins and the importin alpha proteins. This analysis revealed that the expression levels of either the reporters or the importin alpha proteins were equivalent for all experiments (data not shown).

2.3 Results

Measurements of in vivo import rates

Our first goal was to determine the correlation between the affinity of an NLS for receptor and the rate of import of the NLS-cargo into the nucleus. This is an important question as this relationship would have direct implications for the mechanism of nuclear transport. We have previously generated a diverse set of NLS variants comprising a wide range of defined affinities for importin α [43]. To measure the *in vivo* import rate associated with these variant NLSs, we constructed a reporter cargo for use in live yeast that is nearly identical to the NLS-GFP fusion proteins used in the *in vitro* measurements with two exceptions [43]. First, the N-terminal 17 residues of the protein used in the *in vitro* studies was removed to facilitate expression in yeast. Although this reduces the number of residues N-terminal to the NLS (from 27 to 10 in the case of the bipartite NLS), the local context of the NLS remains identical. The second modification is the addition of a second GFP peptide to the C-terminus of the reporter. This addition yields a double GFP molecule (molecular weight of ~55kD) with a presumably slowed rate of passive diffusion through the nuclear pore. The similarity between the *in vitro* and *in vivo* reporter molecules near the N-terminal NLS ensures that the results of one assay are directly comparable to the results of the other.

In Figure 8A, yeast cells expressing four different NLS-GFP-GFP reporters are imaged by direct fluorescence microscopy. The level of nuclear fluorescence compared to cytoplasmic fluorescence increases with the measured strength of the affinity between the reporter and importin α. The tight binding SV40 NLS shows more marked nuclear localization than the weak SV40T3 mutant or the GFP-GFP without an NLS (Figure 8A,

panels A-C). The very tight binding BPSV40 NLS is only observed in the nucleus (Figure 8A, panel D). Thus, the relative 'strength' of an NLS sequence is apparently reflected qualitatively in the steady-state distribution of the fluorescent reporter in yeast cells.

One possibility is that since the BPSV40 reporter binds to importin α with high affinity, the enhanced nuclear localization simply reflects an increase in the reporter-receptor complex rather than free reporter within the nucleus. To determine whether the BPSV40 reporter remains bound to importin α in the nucleus, we localized importin α and the BPSV40 reporter in yeast overexpressing the importin α export receptor, Cse1p. Because Cse1 relocalizes importin α to the cytoplasm [103, 104, 216], if the nuclear concentration of the BPSV40 reporter were due solely to binding to importin α, the nuclear cargo concentration would be expected to decrease when importin α is no longer concentrated in the nucleus. Thus, localization of both importin α and the BPSV40 reporter was analyzed by indirect immunofluorescence in control cells or cells overexpressing Cse1p. Control cells show primary nuclear localization of both the BPSV40 reporter and importin α (Figure 8B, panels A and C). Overexpression of *CSE1* causes relocalization of importin α to the cytoplasm (Figure 8B, panel D), while the BPSV40 reporter remains within the nucleus (Figure 8B, panel B). This result shows that the nuclear localization of the BPSV40 reporter does not depend on a nuclear pool of importin α.

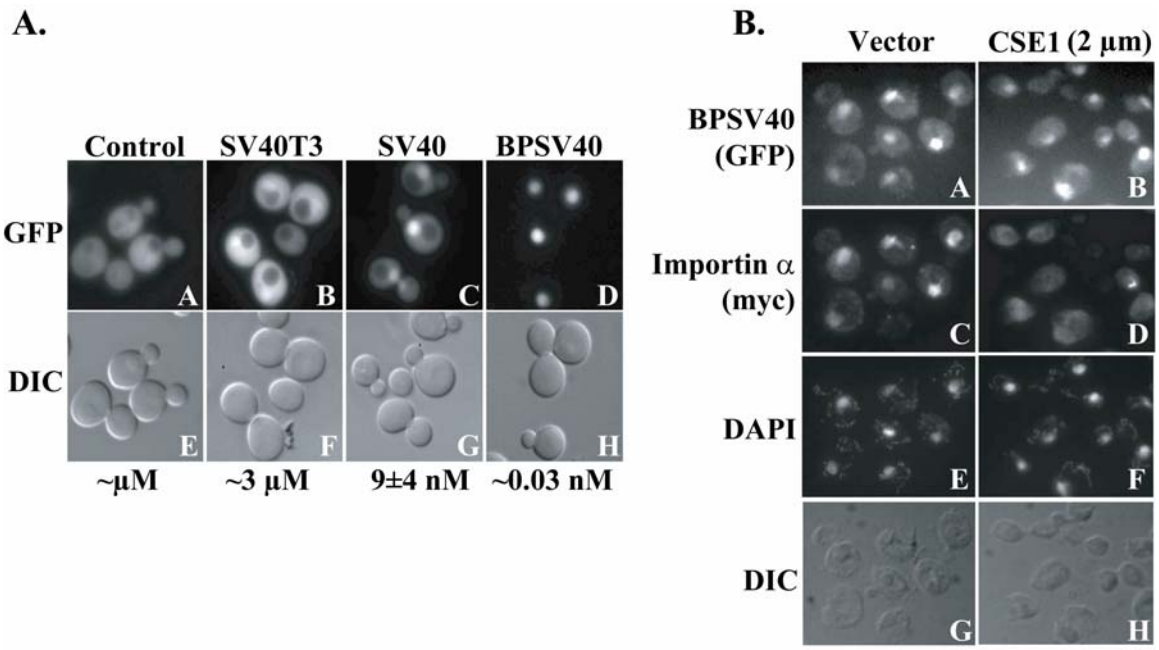

Figure 8. Localization of NLS Variants.
Steady-state fluorescence distribution in yeast expressing NLS-GFP-GFP variants as viewed through a standard fluorescence microscope. (A) The top panels show GFP fluorescence (panels A-D). The bottom panels show the corresponding DIC image (panels E-H). The binding constant for each NLS-cargo binding to importin α is indicated below the images. (B) Localization of importin α–myc (pAC963) and the BPSV40-GFP-GFP reporter (pAC1056) by indirect immunofluorescence in control cells (pRS425) or cells overexpressing *CSE1* (pAC958). Images of wild type cells expressing the BPSV40-GFP-GFP reporter (panels A and B) and importin α-myc (panels C and D) are shown. Corresponding DAPI and DIC images are shown below (panels E-H).

To confirm the validity of our results using steady-state measurements to estimate import rates, we carried out a kinetic NLS-GFP import assay [214] on selected reporters. This assay provides a kinetic measurement of initial import rates in live yeast cells (Figure 9). The NLS-GFP import assay was performed using GFP-GFP, as a control, and the SV40T3, SV40, and BPSV40 variants. In this assay, cells expressing NLS reporters are depleted of energy by incubation with azide and 2-deoxy-glucose, which causes the redistribution of any nuclear protein [214]. Import kinetics are then measured by counting the percentage of cells showing nuclear localization of the reporter over time after azide and 2-deoxy-glucose are removed. As predicted by our steady-state analysis, the import kinetics increase as the binding affinity of the reporter for importin α increases (Figure 9A). In fact, import of the BPSV40 reporter is so fast that it is virtually all nuclear at the earliest time point we can measure. To assure that the BPSV40 reporter was redistributed upon incubation of cells with azide and 2-deoxy-glucose, we examined cells expressing this reporter at each point in the assay (Figure 9B). Cells show diffuse localization of the BPSV40 reporter in media containing azide and 2-deoxy-glucose in comparison to cells not treated (Figure 9B, compare panels A and B). After cells are washed with H_20, BPSV40 remains diffusely localized throughout the cell (Figure 9B, panel C). However, as soon as cells are placed in pre-warmed glucose-containing media, BPSV40 accumulates within the nucleus (Figure 9B, panels D and E).

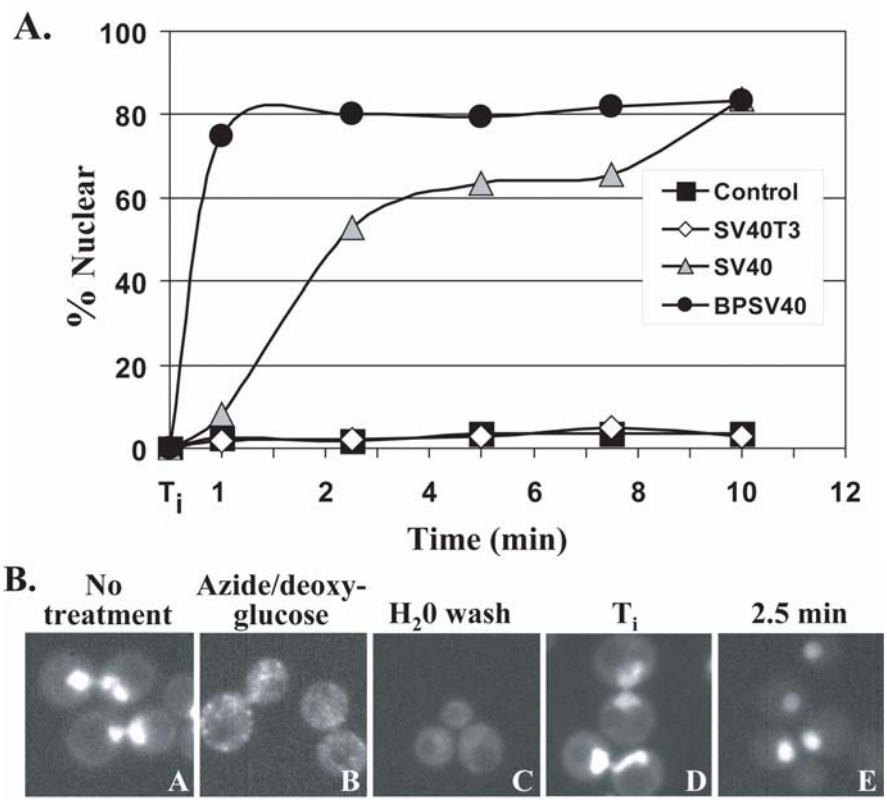

Figure 9. A kinetic assay for NLS reporter import in wild type cells.
The import of GFP (pAC1069), SV40T3 (pAC1067), SV40 (pAC1065), and BPSV40 (pAC1056) reporters were analyzed using a kinetic import assay [214]. (A) Import kinetics were measured by counting the percentage of cells showing nuclear accumulation of the NLS reporters every 2.5 min over a 10 min time period. T_i denotes the initial import time point which was taken before cells were resuspended in prewarmed glucose-containing media. (B) Images of yeast expressing the BPSV40-GFP-GFP reporter at different points in the assay. Panel A shows cells before treatment. Panel B shows cells resuspended in media containing azide and 2-deoxy-glucose. Panel C shows cells washed with H_20. Panel D shows the initial time point for cells resuspended in synthetic media (T_i). Panel E shows cells incubated for 2.5 min in synthetic media at 30ºC.

Addition of an NES to increase the dynamic range of the analysis

A limitation of this study is the dynamic range of $R_{N/C}$ values available using GFP as a cargo. Due to the inherent nuclear targeting of GFP, the range is limited to values greater than 1.4. In an attempt to increase the dynamic range of the measurements, a nuclear export signal (NES) was added to the C-terminus of a single GFP reporter (sequence: AAALALKLAGLNI) [50]. The goal was to cause the cytoplasmic accumulation of reporters carrying weaker NLSs, but still allow the nuclear accumulation of stronger NLSs. Surprisingly, we found the NES, at least in this context, to be a much stronger targeting signal than the import signal imparted by most of the NLSs used in this study. An SV40-GFP-NES reporter showed an exclusively cytoplasmic steady-state localization (data not shown). This suggests that this particular NES dominates the trafficking of the NLS/NES combination. Strikingly, when the stronger BPSV40 NLS was paired with the NES, the reporter appeared to accumulate at the nuclear rim as shown in Figure 10. To ensure that accumulation at the nuclear rim is due to NES-dependent export, the BPSV40-GFP-NES reporter was expressed in the yeast strain crm1-3, which contains a mutation in the yeast NES export receptor, Crm1p/Xpo1p [136]. In this mutant, the BPSV40-GFP-NES reporter accumulates within the nucleus (Figure 10) consistent with the hypothesis that nuclear rim localization is a direct effect of rapid export after import. This observation suggests that the residence time of the BPSV40-GFP-NES reporter in the nuclear pore complex is large relative to the time the reporter remains in either the nucleus or the cytoplasm. One interpretation of this observation is

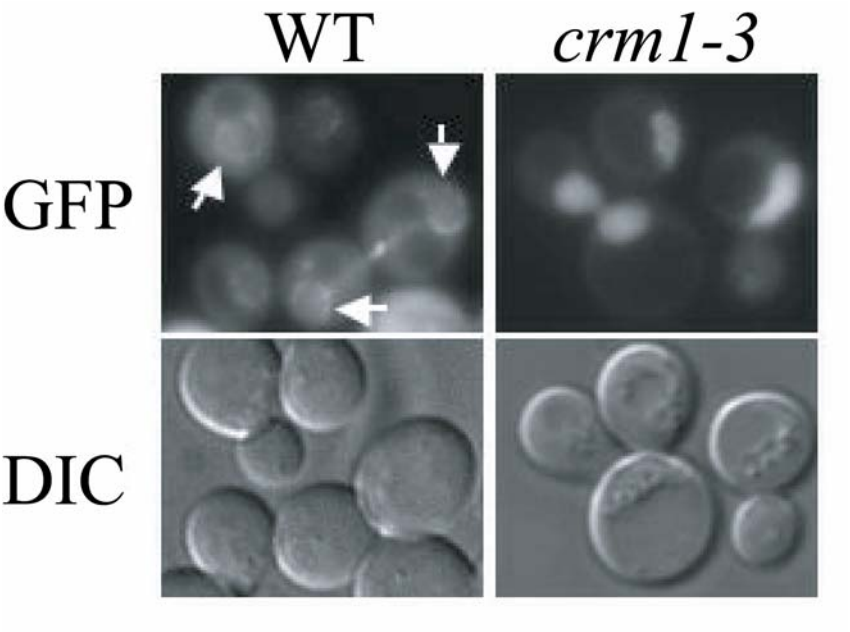

Figure 10. Effect of an NES on reporter localization.
Images of yeast expressing the BPSV40-GFP-NES reporter taken with a standard fluorescence microscope. The top panels show GFP fluorescence. The bottom panels show the corresponding DIC images. The left panels show the reporter expressed in wild type yeast cells. The right panels show the reporter expressed in *crm1-3* mutant cells [201].

that the initial steps of import and export are relatively fast compared to the rate of either translocation through the pore or release from the pore.

Upper limit to functional NLS affinity

In our original hypothesis, we proposed that for an NLS to be functional in vivo, it must have an adequate affinity for the import receptors in the cytoplasm to allow capture, but it must also have a weak enough affinity for the receptors in the nucleus to allow efficient release of the cargo. This admittedly simplistic model for protein import predicts that there is an upper limit to the affinity of a functional NLS for the import receptors. Surprisingly, we did not see evidence for such an upper limit in our imaging studies above. There is a saturation behavior observed for the high affinity bipartite NLSs in that the relative localization of these NLSs are apparently insensitive to changes in the NLS affinity, but these high affinity NLSs efficiently localize their cargoes to the nucleus.

From our simple model of protein import, which assumes that no other factors are involved in the release of cargo except importin α, importin β, and Ran-GTP, we would expect that high affinity NLS-cargoes would remain bound to importin α even after the dissociation of importin β from the trimeric import complex. Importin α cannot interact with its export factor, Cse1p, when an NLS is bound [104, 105, 121]. Thus, we would expect the high affinity NLS-cargo/importin α complexes to accumulate in the nucleus and deplete cytoplasmic importin α to the detriment of cellular growth.

Because no obvious growth defects were observed in our imaging studies with the bipartite NLSs, we further examined the toxicity, or lack thereof, of high affinity NLSs by expressing the NLS-GFP-GFP cargoes at a higher level and directly analyzing cell growth. Using a galactose inducible expression vector, we tested the effects of

overexpressing both the SV40-GFP-GFP and the BPSV40-GFP-GFP reporters on growth of wildtype yeast cells. As controls, we also tested the empty vector and a known dominant negative variant of the protein NTF2 [215]. As shown in Figure 11 (top panel), the overexpression of either NLS-cargo had no apparent effect on cell growth. This result is somewhat surprising given that the BPSV40 NLS is predicted to have nanomolar affinity for importin α in the nucleus [43]. Similar results were obtained when we expressed the NLS reporters from a very strong *GPD1* promoter on a multicopy plasmid (data not shown). This analysis suggests that the affinity, or lack thereof, of the NLS for importin α in the nucleus is not the limiting factor in the release of cargoes in the nucleus.

In fact, several factors contribute to the release of the NLS cargo from the importin α within the nucleus [118, 121]. These factors include the nucleoporin, Nup2 [121], the export receptor for importin α, Cse1p [105], and the auto-inhibitory domain of the importin receptor itself [118]. To determine whether any of these factors are critical for release of the NLS cargo within the nucleus, we examined overexpression of the nM binding cargo in cells that express a variant of yeast importin α, encoded by the *SRP1* gene [215], that has compromised auto-inhibitory function. This variant, which is encoded by *srp1-55*, has an alanine substitution in the NLS-like sequence of the IBB domain reducing its ability to compete with NLS binding through an intra-molecular interaction with the NLS-binding site [136]. This yeast mutant thus harbors a defect in the ability of importin α to release the NLS cargo in the nucleus. When the NLS-GFP-GFP reporters were overexpressed in the *srp1-55* mutant, a mild growth defect was observed with BPSV40-GFP-GFP expression where no defect was observed with SV40-

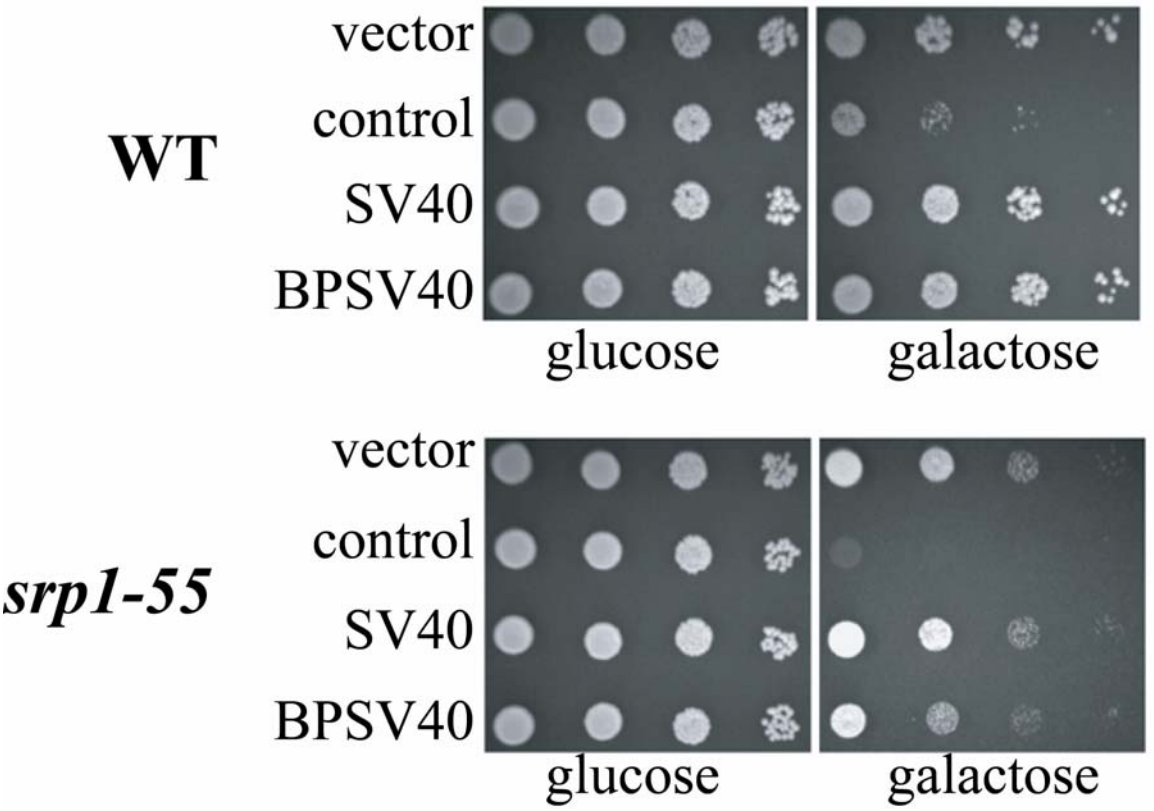

Figure 11. Overexpression of NLS cargo.
Wild type (WT) yeast cells or cells that express an auto-inhibitory mutant form of the NLS receptor importin α (*srp1-55*) as the only copy of the NLS receptor [217] were transformed with the following galactose-inducible plasmids expressing: vector (pAC1350); a control protein that inhibits cell growth when it is overexpressed (pAC253); an SV40-NLS reporter (pAC1352); or a BPSV40-NLS reporter (pAC1353). Cells were grown to saturation in glucose media (no expression) and then serially diluted and spotted on glucose (left) or galactose (right) plates.

GFP-GFP expression. This finding suggests that when the NLS releasing mechanism of the protein import machinery is perturbed, cells become sensitive to high affinity NLS-cargoes.

2.4 Discussion

Intuitively, one would expect the function of a nuclear localization signal (NLS) to be related to its affinity for the NLS receptor. Jans *et al.* have hypothesized that the import rate of an NLS-bearing cargo is linearly related to $1/K_D$ based on measurements of a small range of K_D values [208-210]. This hypothesis is consistent with a model where a number of NLS cargoes compete for limited number of import receptors resulting in a relative rate of import that is proportional to the relative concentrations of NLS-cargo/receptor complexes. In this study, we have investigated a much larger dynamic range of NLS affinities compared to that examined by Jans *et al.* We find that the initial rate at which a cargo is imported, is monotonically correlated with the binding affinity of the NLS for the import receptor complex. However, the analytical relationship between these parameters is not yet completely clear. A clearer picture of the analytical form of the relationship between affinity and import rate would provide a powerful means by which various models [207] for the complicated process of nuclear import could be tested at an experimental and quantitative level. Along with the work of Jans *et al.*, this report provides another early step in the quantitative description of NLS-mediated nucleocytoplasmic transport.

The relationship between initial import rate and the cytoplasmic affinity for import transporters can be described as having three regimes. NLSs with affinities weaker than 10^{-7}M yield initial import rate values indistinguishable from GFP-GFP

alone. NLSs with affinities between 10^{-7}M and 10^{-9}M yield initial import rate values that generally increase with increasing affinity. NLSs with affinities greater than 10^{-9}M yield broad initial import rate distributions that are invariant with the NLS affinity. From this data, one can hypothesize that the initial import rate of an NLS is a continuous function of its affinity for the import receptors, but at high affinities, the initial import rate is limited by some mechanism (assuming that the export rate constant for the NLS-GFP-GFP is identical to that of GFP-GFP alone). Thus, on average, the highest rate constant for NLS-mediated import appears to be about four times larger than the rate constant for the SV40 NLS. This may be an indication that the saturation phenomenon observed for strong NLSs may be due to a unique aspect of the fact that they are bipartite NLSs rather than just a function of their high affinity for the import receptors.

With our increased understanding of the interactions that govern the nuclear transport process, particularly the importin α/importin β-mediated import of cargoes containing a classical NLS, it has become possible to model the overall process. In recent years, two laboratories have established such models [85, 206, 207]. Largely these studies indicate that the level of nuclear Ran governs the import process. Recent work also indicates that the cellular level of the import receptor, importin α, is an important determinant of nuclear import [207]. Implicit within these results is the suggestion that it is not actually the amount of importin α that governs the import of a particular cargo but rather the amount of cargo bound to the import receptor that governs import rates. If more receptor is available, then more cargo will be bound. Alternatively, if the affinity of the receptor/cargo interaction is increased, this should also lead to enhanced nuclear import. The results presented here provide the experimental data in support for this idea.

Ultimately, we will need a combination of modeling studies and experimental tests of those models to fully understand the molecular mechanisms that govern the rate of nuclear protein transport.

A somewhat surprising observation in this report is that the nuclear import machinery of yeast is robust enough to handle NLS affinities that vary over several orders of magnitude. Particularly noteworthy is that exceptionally high affinity NLSs appear to be properly localized to the nucleus and released in the nucleoplasm without causing any severe disruption to cellular growth. This finding supports the suggestion that the processes of nuclear import could be regulated on a kinetic level rather than a thermodynamic level. Provocative evidence for the importance of kinetic regulation has been offered by Gilchrist *et al.* specifically regarding the release of NLS-cargo in the nucleus [121]. Their work demonstrates that both the nucleoporin Nup2 and the export receptor for importin α, Cse1, can enhance the rate of disassembly of the importin α/NLS-cargo complex in vitro [88, 121]. Recent structural studies have revealed details of how both Nup2 [22] and Cse1 [105] interact with importin α. Despite the information that the three-dimensional structures of these complexes provide, it is still not clear how these factors act in a coordinated manner to facilitate NLS-cargo release in vivo. Such questions highlight the importance of future experimentation defining both the energetic and kinetic behaviors of the nuclear trafficking machinery. These experiments will then provide a foundation for a more advanced model describing the nuclear transport process.

2.5 Acknowledgments

We would like to thank our colleagues in the Corbett, Berland, and Hodel labs who contributed to this study. This work is dedicated to the memory of our friend and colleague, Dr. Alec Hodel.

Table 1. NLS variants and their affinity for ΔIBB-importin α

NLS Variant Name	NLS sequence[a]	K_D ΔIBB Importin α
		nM
BPSV40	KR-X_8- PKKKRKV	(0.03)[b]
BPSV40A5	KR-X_8- PKKK**A**KV	(0.2)
BPSV40A6	KR-X_8- PKKKR**A**V	0.9 ± 1
BPSV40A4	KR-X_8- PKK**A**RKV	1 ± 1
Myc	PAAKRVKLD	6 ± 3
SV40	PKKKRKV	9 ± 4
MycA9	PAAKRVKL**A**	13.5 ± 8
BPSV40T3	KR-X_8- PK**T**KRKV	13.5 ± 6
SV40A2	P**A**KKRKV	16.5 ± 1
MycA6	PAAKR**A**KLD	25 ± 11
SV40A5	PKKK**A**KV	38 ± 2
SV40A1	**A**KKKRKV	36 ± 2
SV40A7	PKKKRK**A**	53 ± 4
MycA8	PAAKRVK**A**D	85 ± 7
MycA1	**A**AAKRVKLD	120 ± 14
SV40A4	SPKK**A**RKV	335 ± 7
SV40A6	PKKKR**A**VE	310 ± 100
MycA7	PAAKRV**A**LD	650 ± 70
SV40R3	PK**R**KRKV	850 ± 200
MycA5	PAAK**A**VKLDE	1400 ± 850
BP-GFP	KR	~2000 ± 1000
SV40T3	PK**T**KRKV	~3000 ± 1414
SV40A3	SPK**A**KRKV	~3000 ± 1400
MycA4	PAA**A**RVKLDE	~15000 ± 7000

[a] Bold and underlined font represents amino acid changes in each variant NLS

[b] Calculated values inferred from binding affinity for full-length importin α.

The K_D values for full length importin α can be approximated from these numbers as follows: K_D (full-length importin α) ~ 120 K_D (ΔIBB Importin α).

Table 2. Yeast strains and plasmids used in study

Strain/plasmid	Description	References
ACY192 (wild-type)	*MATa ura3-52 leu2Δ1 trp1*	[187, 197, 199]
ACY817 (*Nup49-GFP*)	*MATa ura3-52 leu2Δ1 trp1 nup49-GFP::TRP1*	[187]
ACY339 (*crm1-3*)	*MATa ura3-52 his3Δ200 leu2Δ1 trp1 ade2 ade3*	[187]
ACY642 (*srp1-55*)	*MATα ura3-52 his3Δ200 leu2Δ1 trp1 srp155::LEU2*	[197]
pRS425	2μ, *LEU2, AMP^R*	[47]
pAC253	*ntf2N77Y, GAL1-10,* 2 μ, *URA3, AMP^R*	[41, 44]
pAC958	*CSE1,* 2 μ, *LEU2, AMP^R*	This Study
pAC963	*SRP1-c-myc* (3X), *CEN, TRP1, AMP^R*	[97, 98, 218]
pAC1056	*BPSV40-NLS-GFP-GFP, CEN, URA3, AMP^R*	This Study
pAC1057	*BPSV40A5-NLS-GFP-GFP, CEN, URA3, AMP^R*	This Study
pAC1058	*BPSV40A6-NLS-GFP-GFP, CEN, URA3, AMP^R*	This Study
pAC1059	*BPSV40T3-NLS-GFP-GFP, CEN, URA3, AMP^R*	This Study
pAC1060	*MYC-NLS-GFP-GFP, CEN, URA3, AMP^R*	This Study
pAC1061	*MYCA1-NLS-GFP-GFP, CEN, URA3, AMP^R*	This Study
pAC1063	*MYCA6-NLS-GFP-GFP, CEN, URA3, AMP^R*	This Study
pAC1065	*SV40-NLS-GFP-GFP, CEN, URA3, AMP^R*	This Study
pAC1066	*SV40A5-NLS-GFP-GFP, CEN, URA3, AMP^R*	This Study
pAC1067	*SV40T3-NLS-GFP-GFP, CEN, URA3, AMP^R*	This Study
pAC1069	*GFP-GFP, CEN, URA3, AMP^R*	This Study
pAC1350	*pGAL1-GFP, CEN, URA3, AMP^R*	This Study
pAC1352	*pGAL1-SV40-NLS-GFP, CEN, URA3, AMP^R*	This Study
pAC1353	*pGAL1-BP-SV40-NLS-GFP*, *CEN, URA3*, *AMP^R*	This Study
pAC2046	*BPMYC-NLS-GFP-GFP, CEN, URA3, AMP^R*	This Study
pAC2047	*SV40A2-NLS-GFP-GFP, CEN, URA3, AMP^R*	This Study
pAC2048	*SV40A7-NLS-GFP-GFP, CEN, URA3, AMP^R*	This Study
pAC2049	*BPSV40-NLS-GFP, CEN, URA3, AMP^R*	This Study
pAC2050	*SV40-NLS-GFP, CEN, URA3, AMP^R*	This Study
pAC2051	*BPSV40-NLS-GFP-NES, CEN, URA3, AMP^R*	This Study

CHAPTER 3

The Classical Nuclear Localization Signal Receptor, Importin α, is Required for Efficient Transition through the G_1/S Stage of the Cell Cycle in *Saccharomyces cerevisiae*

Kanika F. Pulliam, Milo B. Fasken, Laura M. McLane, John V. Pulliam, and Anita H. Corbett

Department of Biochemistry, Emory University School of Medicine, Atlanta, GA 30322

Published in *Genetics* 181(1):105-18 January 2009

Abstract

There is significant evidence linking nucleocytoplasmic transport to cell cycle control. The budding yeast, *Saccharomyces cerevisiae*, serves as an ideal model system to study transport events critical to cell cycle progression because the nuclear envelope remains intact throughout the cell cycle. Previous studies linked the classical nuclear localization signal (cNLS) receptor, importin α/Srp1, to the G_2/M transition of the cell cycle. Here, we utilize two engineered mutants of importin α/Srp1 with specific molecular defects to explore how protein import impacts cell cycle progression. One mutant, Srp1-E402Q, is defective in binding to cNLS cargoes that contain two clusters of basic residues termed a bipartite cNLS. The other mutant, Srp1-55, has defects in release of cNLS cargoes into the nucleus. Consistent with distinct *in vivo* functional consequences for each of the Srp1 mutants analyzed, we find that overexpression of different nuclear transport factors can suppress the temperature sensitive growth defects of each mutant. Studies aimed at understanding how each of these mutants impacts cell cycle progression reveal a profound defect at the G_1 to S phase transition in both the *srp1-E402Q* and *srp1-55* mutants as well as a modest G_1/S defect in the temperature sensitive *srp1-31* mutant, which was previously implicated in G_2/M. We take advantage of the characterized defects in the *srp1-E402Q* and *srp1-55* mutants to predict candidate cargo proteins likely to be impacted in these mutants and provide evidence that three of these cargoes, Cdc45, Yox1, and Mcm10, are not efficiently localized to the nucleus in importin α mutants. These results reveal that the classical nuclear protein import pathway makes important contributions to the G_1/S cell cycle transition.

3.1 Introduction

The compartmentalized transport of macromolecules including proteins and RNAs into and out of the nucleus is a highly regulated process essential for all eukaryotic cells. Bidirectional movement of these macromolecules controls cell growth through coordinating nuclear and cytoplasmic aspects of gene expression [118, 119]. The orchestration of the cell cycle is one of the most complex processes cells must undergo requiring coordination of numerous cytoplasmic and nuclear events. Many previous studies have uncovered links between cell cycle control and nuclear transport [93, 94, 96] but how these two cellular processes control and influence one another is not yet understood in detail.

The nuclear envelope provides a physical mechanism for regulation of numerous events that contribute to cell cycle transitions. In higher eukaryotic cells the nuclear envelope breaks down during mitosis, allowing for redistribution of macromolecules between the nucleus and the cytoplasm [104, 120]. Despite this transient disappearance of the barrier separating the nucleus and the cytoplasm, there are numerous protein transport events that occur during stages of the cell cycle where the nuclear envelope remains intact.

Many of the cargo proteins that contribute to control of the cell cycle are likely to be targeted to the nucleus through a classical nuclear localization signal (cNLS) [105]. Significant evidence has accumulated to support the idea that rates of import into the nucleus are largely determined by interaction between the NLS cargo and the NLS receptor [219] making recognition of the NLS cargo by the NLS receptor essentially the rate-limiting step in the process of nuclear protein import.

Therefore, the goal of this study is to understand how specific engineered amino acid changes that cause defects in importin α cNLS cargo binding and release into the nucleus affect cell cycle progression. Results of this analysis reveal an important role for the classical nuclear import pathway in G_1/S transition of the cell cycle, suggesting key cargoes containing bipartite cNLS motifs need to be imported to the nucleus to allow cells to properly enter S phase and replicate DNA.

3.2 Materials and Methods

Yeast strains and plasmids

All chemicals were obtained from Sigma or USBiological unless otherwise noted. All DNA manipulations were performed by standard protocols [220], and all media were prepared by standard procedures [221]. All yeast strains and plasmids used in this study are listed in Table 3 and 4.

To generate mutants of importin α that could be directly compared to one another, each mutant was integrated into the same strain background as the previously generated allele *srp1-55* (ACY641) [136]. The E402Q importin α mutant replaced the wild type copy of importin α. To integrate E402Q importin α, the E402Q mutation was subcloned into the open reading frame of the *LEU2* integrating plasmid, pRS406 [217], to create *srp1-E402Q* (pAC1999). E402Q importin α was then integrated at the endogenous *SRP1* locus by linearization of the *srp1-E402Q* (pAC1999) plasmid and transformed into the S288C wild type diploid cells (ACY247). Transformants that grew on plates lacking leucine were selected for further analysis. The presence of the E402Q importin α mutation was confirmed by PCR and sequencing. The heterozygous diploid was then sporulated and tetrads were dissected to generate the haploid, *srp1-E402Q* (ACY1560).

This integration strategy is designed to make E402Q importin α the only copy of importin α expressed in the haploid strain.

Although the *srp1-31* (ACY639) mutant already existed in an S288C background, the mutant was further backcrossed to an S288C wild type strain (PSY580) [136]. The heterozygous diploid strain was sporulated and tetrads dissected to generate *srp1-31* haploids (ACY1561 and ACY1562).

To generate cells where microtubules could be visualized directly with GFP, *TUB1-GFP* (pAC1344) was integrated at the *URA3* locus as described previously [222]. The Cdc45, Mcm10 and Yox1 proteins were visualized by monitoring the localization of previously described integrated C-terminal GFP fusion proteins: Cdc45-GFP (YLR103C), Mcm10-GFP (YIL150C), or Yox1-GFP (YML027W) [223]. Each of these strains was crossed to either the *srp1-31* (ACY1561) or *srp1-55* (ACY642) mutant. The resulting diploid strains were sporulated and tetrads dissected to generate *srp1* mutant strains expressing Cdc45-GFP, Yox1-GFP, or Mcm10-GFP (Table 3).
[49].

In vivo functional analysis

The function of importin α variants *in vivo* was assessed by examining the growth of the integrated alleles**,** *srp1-31***,** *srp1-55*, and *srp1-E402Q***.** As a control, each mutant was covered with a wild type *SRP1 URA3* plasmid (pAC876) to ensure conditional phenotypes were complemented prior to the growth assays. Single colonies were grown to saturation in liquid culture, serially diluted (1:10), and spotted on minimal medium plates as a control or on fluoroorotic acid (5-FOA) plates. The drug 5-FOA eliminates

the *URA3* plasmid-encoded wild type *SRP1* (pAC876) to reveal the phenotype of the mutants [224]. Plates were incubated at the indicated temperatures for 3-7 days.

Immunoblot analysis

Immunoblot analysis was performed using standard methods [225]. Cultures were grown to log phase in yeast extract peptone dextrose (YEPD) media at 25ºC and then shifted to the indicated temperature. Cells were then harvested by centrifugation and washed twice in water and once in PBSMT (100 mM KH_2PO_4, pH 7.0, 15 mM $(NH_4)_2SO_4$, 75 mM KOH, 5 mM $MgCl_2$, 0.5% Triton X-100). Cells were subsequently lysed in PBSMT with protease inhibitors (0.5 mM phenylmethylsulfonyl fluoride, 3 μg/ml each of aprotinin, leupeptin, chymostatin, and pepstatin) by glass bead lysis. Equal amounts of total protein were resolved by SDS-PAGE and immunoblotted with polyclonal anti-importin α antibody (1:5000 dilution) raised against recombinant GST-importin α followed by anti-rabbit secondary antibody (1:5000 dilution).

NLS-GFP import assay

The NLS-GFP import assay was performed as described previously [214]. Briefly, cells were grown to early mid-log phase in synthetic media containing 2% glucose (w/v) at 25ºC, pelleted, resuspended in 1 ml glucose-free synthetic media containing 10 mM sodium azide, 10 mM 2-deoxy-D-glucose and incubated at 25ºC for 45 min. Cells were then pelleted, washed with 1 ml of ice-cold ddH_20, repelleted, and resuspended in 50 μl of glucose-containing synthetic media pre-equilibrated to 25ºC (permissive), 37 ºC (*srp1-31*, *srp1-E402Q*), or 18 ºC (*srp1-55*). For scoring, 2-μl samples were removed every 2.5 min from the pre-equilibrated media, and images were collected through a GFP-optimized filter (Chroma Technology) using an Olympus BX60 epifluorescence

microscope. Cells were scored as "nuclear" if the nucleus was both brighter than the surrounding cytoplasm and a nuclear-cytoplasmic boundary was visible. At least 100 cells were counted at each time point. Images of cells in sodium azide and 2-deoxy-D-glucose were also collected and analyzed to ensure the complete redistribution of nuclear proteins at time T_0.

Microscopy

Direct fluorescence microscopy was performed to localize GFP fusion proteins in live cells. For all experiments, cultures were also labeled with Hoescht dye (1 μg/ml) to visualize DNA and confirm the location of the nucleus. The localization of GFP fusion proteins was monitored by directly viewing the GFP signal in living cells through a GFP-optimized filter (Chroma Technology) using an Olympus BX60 epifluorescence microscope equipped with a Photometrics Quantix digital camera. For localization of candidate cargoes, cells expressing Cdc45-GFP, Mcm10-GFP, or Yox1-GFP were grown to log phase at the permissive temperature and then shifted to the nonpermissive temperature for 3 hours.

High copy suppressor analysis

For high-copy suppressor analysis, high copy plasmids (2μ *TRP1*) encoding the nuclear transport factors, importin β (pAC592), Cse1 (pAC1303), and Nup2 (pAC1385) were transformed into *srp1-55* (ACY641), *srp1-E402Q* (ACY1560), and *srp1-31* (ACY1561) cells covered by an *SRP1 URA3* maintenance plasmid (pAC876). Genetic suppression was assessed by growing single colonies in liquid culture to saturation, serially diluting (1:10), and spotting on minimal medium plates as a control or on 5-FOA plates. Plates were incubated at the indicated temperatures for 3-6 days.

Cell cycle arrest and release

For cell cycle studies, cultures were synchronized by treatment with alpha factor or hydroxyurea. For arrest with alpha factor, cells were grown to early mid-log phase (OD_{600} 0.25-0.35) in YEPD media at 25ºC. Cell cycle arrest was accomplished by pelleting the cells, washing with YEPD (pH 3.9), and resuspending in fresh YEPD (pH 3.9) containing a 1:500 dilution of 5 mg/ml of alpha factor (Sigma) followed by a 90 min incubation at 25ºC. Additional alpha factor (1:1000 dilution) was added every 30 min. Cells were released from alpha factor arrest by pelleting the cells, washing twice with YEPD and resuspending in fresh YEPD for release at the indicated temperatures for an additional 3 hrs [226].

For hydroxyurea arrest, cells were arrested with alpha factor as described above. Then cells were pelleted, washed twice with YEPD and resuspended in YEPD containing 200 mM hydroxyurea. Cultures were incubated for an additional 2 hrs at 25ºC. Cells were then pelleted, washed twice with YEPD and resuspended in fresh YEPD for release at the indicated temperatures for an additional 3 hrs [226].

Flow cytometry analysis

Cells were prepared for flow cytometry analysis by staining with propidium iodide [227]. Briefly, asynchronous or synchronous cultures were ethanol fixed overnight at 4ºC, washed, and resuspended in 50 mM sodium citrate. Cells were then treated with 0.1 mg/ml RNase A for 2 hrs at 37ºC and 10 mg/ml of Proteinase K for 1 hr at 50ºC. Cells were stained with 8 μg/ml of propidium iodide. Each sample was analyzed with a FACSVantage SE (Becton Dickinson, Franklin Lakes, NJ). Data was analyzed using FloJo 7.2.2 software.

Plasmid loss

Plasmid loss was determined in wild type or mutant cells containing plasmids with an early (*ARS305*), middle (*ARS1*), or late (*ARS1412*) firing autonomously replicating sequence (ARS) [228]. Cells were grown to log phase after which at least 200 cells were plated on nonselective YEPD plates. Colonies that grew on YEPD plates were then replica plated to *ura*$^-$ selective plates to determine plasmid loss. The percentage of plasmid loss was calculated as [100-(the ratio of colonies on the *ura*$^-$ selective plate/colonies on the YEPD plate) X 100]. The experiment was performed in triplicate.

Statistical analysis

Statistical methods were employed to determine if a significant difference was observed in the plasmid loss percentage of the *srp1* mutant cells as compared to wild type cells. Data was analyzed using a one-way analysis of variance (ANOVA) for origin of replication followed by a Dunnett's multiple comparison test using Graph Pad Prism 3.0. The significance level (alpha) was set at 0.05 for all statistical tests. If the calculated p value was less than alpha, then the difference in plasmid loss was reported as being statistically significant.

3.3 Results

In order to examine links between the classical nuclear protein import pathway and cell cycle progression, we exploited two mutants of importin α with specific molecular defects (Figure 12A). The *srp1-E402Q* mutant alters a critical glutamic acid residue in the minor pocket of the cNLS cargo binding domain to glutamine [93, 96]. This conservative amino acid substitution at position 402 creates the conditional allele of

importin α, *srp1-E402Q*, that causes a decrease in bipartite cNLS cargo binding *in vitro* and impacts the steady-state localization of a bipartite NLS cargo *in vivo* [135].

As a complement to the analysis of the NLS-cargo binding pocket, a variant of importin α that affects cargo delivery was also employed. A conserved NLS-like sequence within the N-terminal IBB domain of importin α, ^{54}KRR^{56}, is essential for the auto-inhibitory function of importin α [118]. An arginine to alanine substitution at position 55 within this auto inhibitory sequence (KRR→KAR) creates a conditional allele of importin α, *srp1-55*, that specifically affects cargo delivery/release into the nucleus [136].

Functional analysis of srp1 mutants

To compare the consequences of defects in cargo binding and cargo release *in vivo*, we generated alleles of the *srp1-55* and *srp1-E402Q* importin α mutants that could be directly compared to one another (See Materials and Methods). As a control, we also generated the previously characterized, *srp1-31* mutant [180], in the same genetic background. As an initial characterization and comparison of these mutants, we analyzed their growth at various temperatures. To ensure that equal numbers of cells were grown and spotted, the *srp1-31*, *srp1-55*, and *srp1-E402Q* mutants were transformed with a wild type *SRP1* plasmid. To assay growth, ten-fold serial dilutions of the samples were spotted on control plates where wild type *SRP1* is maintained or 5-FOA plates where the plasmid encoding wild type *SRP1* is lost. In comparison to wild type cells, *srp1-55* mutant cells show a growth defect at 18ºC as previously reported [136]. In contrast, *srp1-31* and *srp1-E402Q* mutants show growth defects at 37ºC (Figure 12B).

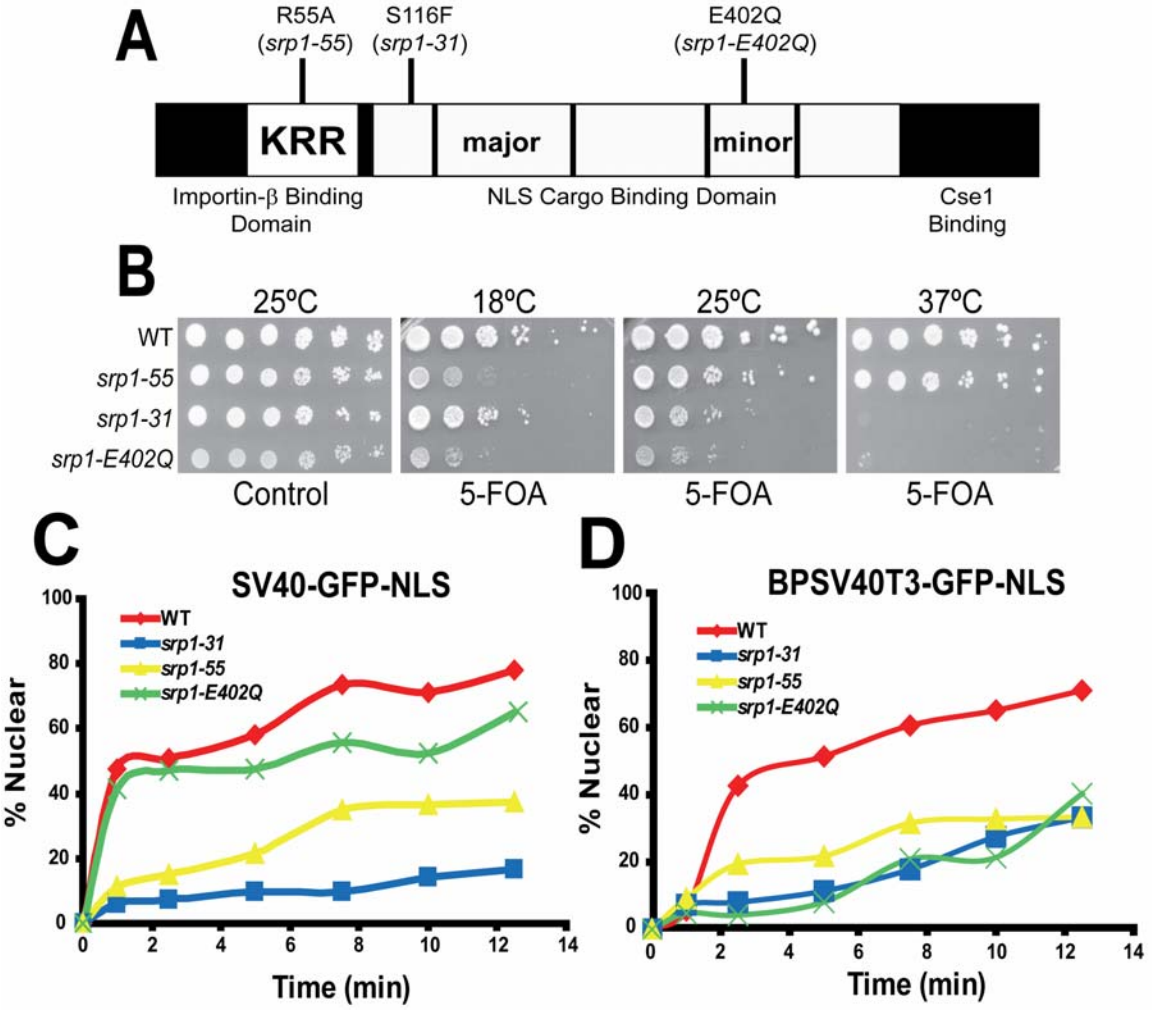

Figure 12. Functional analysis of importin α mutants *in vivo*.
(A) A Schematic diagram of importin α is shown with the three major domains indicated. The position of the auto-inhibitory NLS-like sequence (^{54}KRR^{56}) is also indicated. The approximate location as well as the amino acid change for each of the *srp1* mutant alleles employed in the study is shown. (B) Growth of each srp1 mutant was assessed at 18°C, 25°C, and 37°C. Each mutant was covered with a wild type *SRP1 URA3* plasmid (pAC876) and analyzed by serial dilution and spotting on control plates (where the wild type *SRP1* plasmid is maintained) or 5-FOA plates (where the wild type *SRP1* plasmid is lost). Plates were incubated at the indicated temperatures for 3-7 days. (C) Kinetic assay for monopartite SV40-GFP NLS and (D) bipartite BPSV40T3-GFP NLS import reporters. The initial import rates for the cNLS import cargoes and

reporter were analyzed using a kinetic import assay as described in Materials and Methods. Cultures were grown to early-mid log phase at 25ºC and then shifted to the nonpermissive temperature (37°C for *srp1-31* and *srp1-E402Q* cells and 18°C for *srp1-55* cells). Initial import kinetics was measured by determining the percentage of cells showing nuclear accumulation of the cNLS reporter at a given time. For scoring, 2 µl samples were removed every 2.5 min. Cells were scored as "nuclear" if the nucleus was both brighter than the surrounding cytoplasm and a nuclear-cytoplasmic boundary was visible. At least 100 cells were counted at each time point. Results are plotted as the percentage of cells showing nuclear cNLS reporter signal versus time for WT (♦), *srp1-31*(■), *srp1-55* (▲), and *srp1-E402Q* (×) cells.

Immunoblot analysis indicates no significant change in the level of any of the Srp1 mutant proteins at the nonpermissive temperatures as compared to wild type importin α, indicating that the growth defects observed are not due simply to loss of the essential importin α protein (data not shown).

NLS-GFP import assay

Prior studies examined the cargo binding properties of the *srp1-55* and *srp1-E402Q* variants *in vitro* as well as their impact on the steady-state localization of cNLS cargo *in vivo* [135, 136]. To further characterize the impact of each of these alleles as well as the *srp1-31* mutant on nuclear protein import, we used a semi-quantitative kinetic NLS-GFP import assay that assesses the initial rate of NLS cargo import [214]. For this assay, import of both a monopartite SV40 and a bipartite BPSV40T3 NLS cargo was examined. The SV40 and BPSV40T3 cargoes were selected for the NLS-GFP import assay because they both bind to importin α with a similar affinity (K_D~10 nM) and importantly the bipartite cargo is engineered such that productive binding to importin α absolutely depends on the basic cluster of amino acids that binds to the minor NLS binding pocket [43]. Experiments were carried out at the nonpermissive temperatures in live cells as described in Materials and Methods. In comparison to wild type cells, the *srp1-31* and *srp1-55* mutants showed a decrease in the initial rate of nuclear import of the monopartite cNLS cargo SV40-GFP (Figure 12C). As expected there was no observed change in the initial import rate of the monopartite cargo in *srp1-E402Q* cells (Figure 12C) because the E402Q amino acid substitution decreases bipartite cargo binding without impairing binding to monopartite cNLS cargo [135]. However, all three mutants, *srp1-31*, *srp1-55*, and *srp1-E402Q* show a decrease in the initial rate of nuclear import of the bipartite

cNLS cargo BPSV40T3-GFP (Figure 12D). These results confirm that cells expressing each variant of importin α have defects in cNLS protein import.

Importin α variants differ in their in vivo molecular defects

Although all of the importin α mutant cells showed defects in the kinetic NLS import assay, we hypothesized that the different engineered amino acid changes in each importin α variant should impair nuclear import through distinct mechanisms. In order to address this hypothesis, we tested whether each of the importin α mutants could be suppressed by overexpression of several nuclear transport factors with the assumption that suppression by specific factors could provide information about what interactions are compromised *in vivo*. For this analysis, we examined overexpression of importin β, Cse1, and the nuclear pore protein, Nup2. Importin β interacts with the IBB domain of importin α to target the import complex to the nuclear pore [116, 117]. Cse1 is the export receptor for recycling importin α to the cytoplasm [103, 104] and both Cse1 and Nup2 facilitate cargo delivery in the nucleus [22, 98, 105]. As controls, each *srp1* mutant was also transformed with vector alone or with a wild type importin α plasmid. In order to ensure equal growth and spotting, each mutant was transformed with wild type *SRP1* on a *URA3* plasmid. Cultures were grown to saturation, serially diluted, and then spotted on either control plates where the *SRP1* maintenance plasmid is retained or plates containing 5-FOA where the maintenance plasmid is lost but the overexpression plasmids are retained (Figure 13). The 5-FOA plates were incubated at the nonpermissive temperature as previously determined (See Figure 12B) for each mutant. Interestingly, we find that the temperature-sensitive growth defect of *srp1-31* cells is suppressed by overexpression of

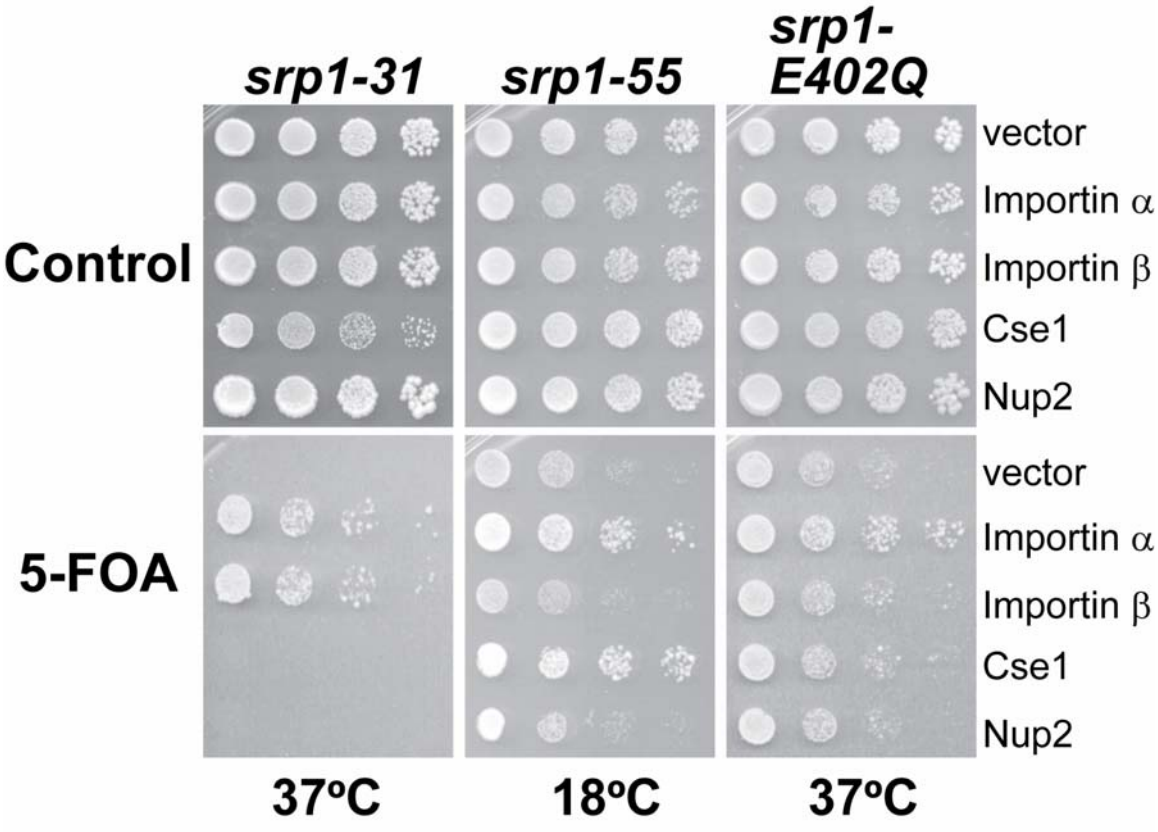

Figure 13. High copy suppressor analysis.
High copy plasmids encoding the nuclear transport factors, importin β (pAC592), Cse1 (pAC1303), and Nup2 (pAC1385), were transformed into *srp1-55*, *srp1-E402Q*, and *srp1-31* cells which also contained a wild type *SRP1 URA3* plasmid (pAC876). As a control, each mutant was also transformed with vector alone (pRS424) or wild type *SRP1* plasmid (pAC1354). Genetic suppression was assessed by spotting saturated cultures on control plates (where the wild type *SRP1* plasmid is retained) or on 5-FOA plates (where the wild type *SRP1* plasmid is lost). Plates were incubated at the indicated temperatures for 3-6 days. Suppression was scored as enhanced growth at the nonpermissive temperature as compared to the vector control.

importin β (Figure 13). As previously observed [136], the cold-sensitive growth defect of *srp1-55* mutant cells is suppressed by overexpression of the nuclear export factor, Cse1 (Figure 13). In contrast, the temperature-sensitive growth defect of *srp1-E402Q* cells is not suppressed by any of the nuclear transport factors (Figure 13). Taken together, these results suggest that the *in vivo* defects that underlie diminished protein import in each of these mutants are likely to be distinct from one another.

Mutants of importin α affect cell cycle progression

In order to probe the link between importin α and cell cycle events, we exploited these *srp1* mutants that impact the classical nuclear protein import pathway through distinct mechanisms. As a first step to determine whether all defects in importin α impair G_2/M of the cell cycle as previously described for the *srp1-31* mutant [180], each importin α mutant was spotted on plates containing either hydroxyurea, which inhibits DNA replication [229], or benomyl, which blocks mitosis prior to the onset of anaphase [230]. Consistent with previous reports, the *srp1-31* mutant shows sensitivity to growth on benomyl suggesting a defect in G_2/M of the cell cycle (Figure 14A) [180]. In contrast, the *srp1-55* and *srp1-E402Q* mutant cells show no obvious sensitivity to benomyl. Surprisingly, in comparison to wild type cells, s*rp1-31*, *srp1-55* and *srp1-E402* mutants all show sensitivity to hydroxyurea suggesting a defect in processes critical to the G_1/S cell cycle transition including DNA replication, DNA repair and/or checkpoint function (Figure 14A).

To begin to assess how the cell cycle is affected in each of the *srp1* mutants, the DNA content of each mutant was measured in an asynchronous cell population using flow cytometry (Figure 14B). Samples were analyzed at 30 minute intervals over 6 hours

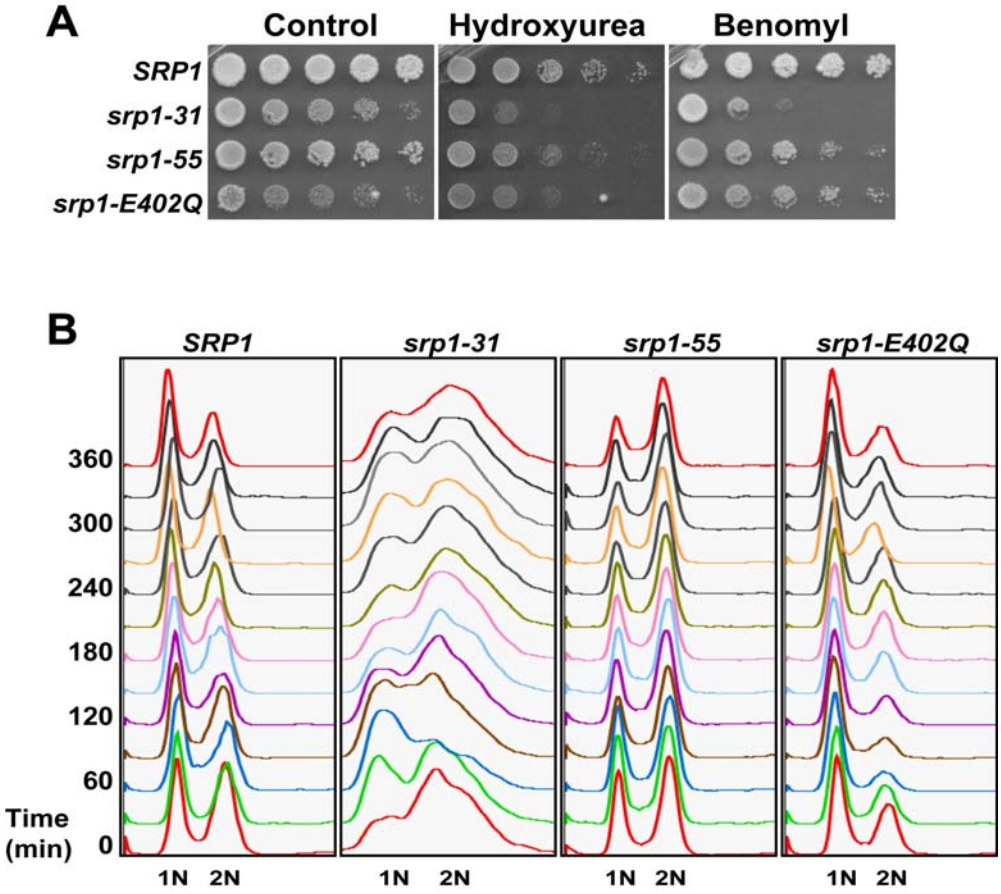

Figure 14. Analysis of cell cycle defects in srp1 mutants.
(A) Analysis of cell growth on hydroxyurea and benomyl plates. In order to determine whether any of the *srp1* mutant alleles show hypersensitivity to growth on plates containing hydroxyurea or benomyl, cultures were grown to saturation at the permissive temperature, then serially diluted and spotted on control YEPD plates, YEPD containing 100 mM hydroxyurea or YEPD plates containing 10 mg/ml benomyl. Plates were incubated at the permissive temperature for 3-7 days. (B) Analysis of cell cycle progression in unsynchronized cells. Wild type (*SRP1*) and mutant (*srp1-31*, *srp1-55*, *and srp1-E402Q*) cells were grown to early mid-log phase at the permissive temperature and then shifted to the nonpermissive temperature (37ºC for *srp1-31* and *srp1-E402Q* cells; 18ºC for *srp1-55* cells). Samples were collected every 30 min for 6 hours for flow cytometry to analyze DNA content. The positions of unreplicated DNA (1N) and replicated DNA (2N) are indicated below the graphs.

at both the permissive and nonpermissive temperatures. The cells are scored as having 1N (G_1) or 2N (G_2/M) DNA content. All importin α mutants show a distribution of 1N and 2N DNA content that is indistinguishable from wild type (*SRP1*) cells at the permissive temperature (data not shown). In wild type (*SRP1*) cells the distribution of 1N and 2N DNA content is unchanged relative to the permissive temperature. Consistent with previous results [180], *srp1-31* mutant cells show some accumulation of cells in the G_2/M phase of the cell cycle as compared to G_1. Like the *srp1-31* cells, *srp1-55* cells show some increase in cells with 2N DNA content as compared to wild type cells (*SRP1*), which is consistent with previous analysis of an asynchronous population of these cells [136]. In contrast to the *srp1-31* and *srp1-55* mutants, *srp1-E402Q* mutant cells show an increase in the population of cells with 1N DNA content as compared to wild type (*SRP1*) cells. While these results are consistent with impaired cell cycle transitions due to compromised classical nuclear protein import, defects at multiple points in the cell cycle are not readily uncovered by analysis of asynchronous cultures.

Both sensitivity to hydroxyurea and analysis of DNA content for the *srp1-E402Q* mutant suggest a role for importin α in the G_1/S cell cycle transition. To assess the DNA content of synchronized cultures, cells were arrested in late G_1 phase of the cell cycle with the mating type pheromone, alpha factor [231, 232], and then analyzed by flow cytometry over time following release from alpha factor. Samples were analyzed at 30 minute intervals over 3 hours at both the permissive and nonpermissive temperatures. All importin α mutants show wild type progression at the permissive temperature (data not shown). As expected, wild type cells progress through the cell cycle over the time course of the experiment at all temperatures. As previously reported, *srp1-31* mutant cells

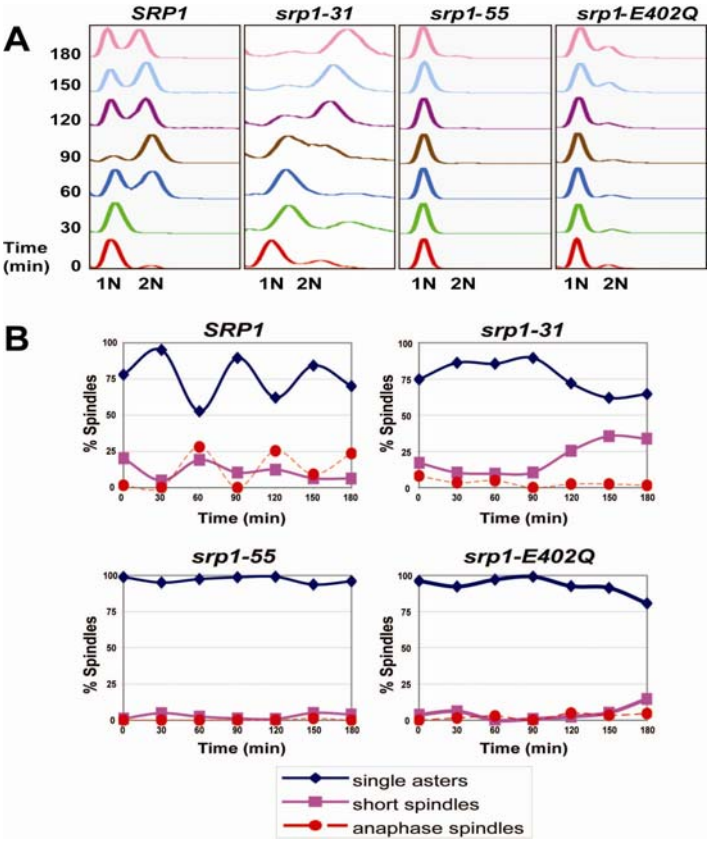

Figure 15. Analysis of cell cycle progression in cells synchronized in G_1 phase of the cell cycle.

(A) Wild type (*SRP1*) and mutant (*srp1-31, srp1-55, srp1-E402Q*) cells were grown to early mid-log phase at the permissive temperature and then arrested at late G_1 phase with alpha factor. Samples were then released to the nonpermissive temperature (37ºC for *srp1-31* and *srp1-E402Q* cells; 18ºC for *srp1-55* cells). Samples were collected every 30 min for 3 hours for flow cytometry to analyze DNA content. The positions of unreplicated DNA (1N) and replicated DNA (2N) are indicated below the graphs. (B) Spindle morphology. Wild type (*SRP1*) and mutant (*srp1-31*, *srp1-55*, *srp1-E402Q*) cells expressing *Tub1-GFP* to visualize microtubules were treated as described above for (A). Spindles were visualized by examining integrated *Tub1-GFP* signal by direct fluorescence microscopy. Results are plotted as the percentage of spindles in the total cell population scored as single asters (no spindles ♦), short spindles (spindle not extending to the duplicated nucleus of the daughter cell ■) or anaphase spindles (spindle extending to the duplicated nucleus ●) versus time.

display a defect in progression through G_2/M (Figure 15A) [180]. The *srp1-31* mutant also shows a slight defect in the G_1/S phase transition which is consistent with growth sensitivity to hydroxyurea. Interestingly, both *srp1-55* and *srp1-E402Q* mutant cells show a profound defect in the G_1/S transition (Figure 15A). These results link importin α and hence the classical nuclear import pathway to the G_1/S transition of the cell cycle as well as the previously reported G_2/M transition.

Using the synchronization method employed for flow cytometry, the spindle morphology of each mutant following the shift to the nonpermissive temperature was assessed over time (Figure 15B). The percentage of spindle formation was defined as: containing single asters (no spindles); short spindles (spindle not extending to the duplicated nucleus of the daughter cell); or anaphase spindles (spindle extending to the duplicated nucleus) [233]. In comparison to wild type cells, *srp1-31* cells show an increased number of short spindles and a decrease in the relative number of anaphase spindles after three hours at the nonpermissive temperature (Figure 15B). In contrast, *srp1-55* and *srp1-E402Q* mutant cells show a constant level of single asters over time which correlates with a defect in the G_1/S phase transition where spindle formation has not yet begun (Figure 15B).

Since a profound delay at the G_1/S transition was observed in *srp1-55* and *srp1-E402Q* mutant cells, we wanted to determine whether these cells were defective not only in transition but also in progression through S phase. To examine progression through S phase, the mutant cells were arrested in G_1 using alpha factor at the permissive temperature and then released into media containing hydroxyurea to synchronize cells in early S phase. After two hours, cells were released at either the permissive or the

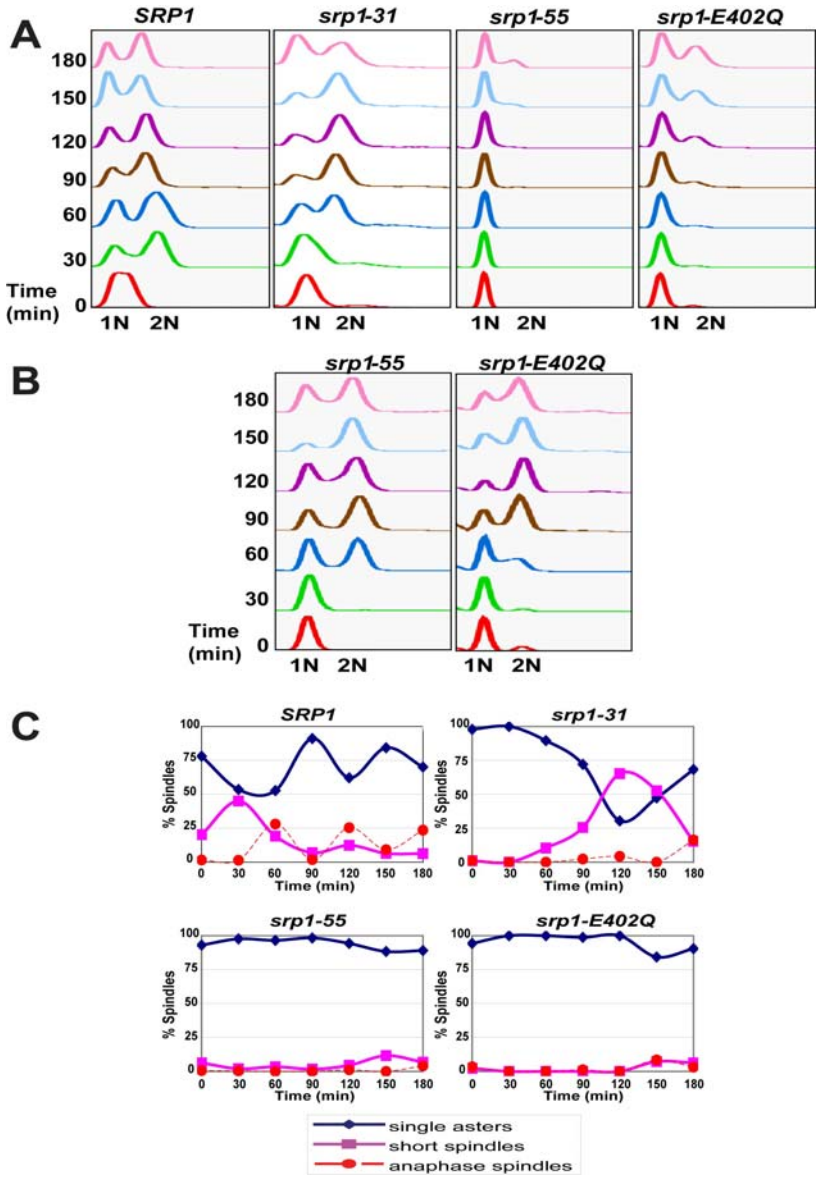

Figure 16. Analysis of cells synchronized in S phase of the cell cycle.
(A) Wild type (*SRP1*) and mutant (*srp1-31*, *srp1-55*, *srp1-E402Q*) cells were grown to early mid-log phase at the permissive temperature and then arrested at late G_1 phase with alpha factor. Samples were then released into hydroxyurea at the permissive temperature and incubated for two hours. Finally, these cells synchronized in early S phase were released to the nonpermissive temperature (37ºC for *srp1-31* and *srp1-E402Q* cells; 18ºC for *srp1-55* cells). Samples were collected every 30 min for 3 hours for analysis by flow cytometry to analyze DNA content. The positions of unreplicated DNA (1N) and replicated DNA (2N) are indicated below the graphs.

(B) Mutant (*srp1-31* and *srp1-E402Q*) cells were grown to early mid-log phase at the permissive temperature and then arrested at late G_1 phase with alpha factor. Samples were then released to the permissive temperature to determine if the cells are released from alpha factor arrest. Samples were collected every 30 min for 3 hours for flow cytometry to analyze DNA content. The positions of unreplicated DNA (1N) and replicated DNA (2N) are indicated below the graphs. (C) Spindle morphology. Wild type (*SRP1*) and mutant (*srp1-31*, *srp1-55*, *srp1-E402Q*) cells expressing *Tub1-GFP* to visualize microtubules were treated as described above for (A). Spindles were visualized by examining integrated *Tub1-GFP* signal by direct fluorescence microscopy. Results are plotted as the percentage of spindles in the total cell population scored as single asters (no spindles ♦), short spindles (spindle not extending to the duplicated nucleus of the daughter cell ■) or anaphase spindles (spindle extending to the duplicated nucleus ●) versus time.

nonpermissive temperature. Samples were then analyzed by flow cytometry. At the permissive temperature, wild type and all mutant cells progress through the cell cycle in a comparable manner (data not shown). However, when mutants are released to the nonpermissive temperature, both *srp1-55* and *srp1-E402Q* cells progress slowly through S phase in comparison to wild type cells (Figure 16A). This experiment also provides further evidence that *srp1-31* cells have defects in S phase progression as well as G_2/M as they also progress through S phase more slowly than wild type cells (Figure 16A). To ensure that *srp1-55* and *srp1-E402Q* cells were both able to release from alpha factor arrest, the DNA content of these mutant cells was also monitored at the permissive temperature (Figure 16B). Flow cytometry analysis shows that both *srp1-55* and *srp1-E402Q* cells can release from alpha factor arrest and enter the cell cycle at the permissive temperature providing evidence that these cells when first synchronized with alpha factor and then released into media containing hydroxyurea should be synchronized in early S phase. We also employed spindle morphology analysis for each mutant as independent confirmation of the cell cycle delays observed in the *srp1-31*, *srp1-55*, and *srp1-E402Q* cells (Figure 16C). As observed for the alpha factor arrest, both *srp1-55* and *srp1-E402Q* cells show nearly 100% of cells with single asters throughout the time course of the experiment. This spindle morphology is consistent with the failure to enter the cell cycle over the time course of the experiment. As suggested by the flow cytometry data, the *srp1-31* cells show a delay in spindle formation relative to wild type (*SRP1*) cells, but spindles do form and elongate in this mutant by about 90 minutes (compare to ~30 minutes for wild type (*SRP1*) cells).

Results indicate that all of the importin α mutants examined show defects in the G_1/S transition and in S phase progression. As an initial approach to understand how *srp1* mutants might affect DNA replication, we utilized a plasmid loss assay [228, 234]. This assay monitors loss of plasmids containing an autonomously replicating sequence (ARS), which function as replication origins in *S. cerevisiae* [234]. Although defects in many cell cycle pathways can contribute to chromosome loss, mutants with general DNA replication defects exhibit loss regardless of the origin of replication used in the plasmid, whereas mutants specific for replication initiation often exhibit differential loss, dependent on the nature of the replication origin [235-237].

Therefore, we compared the rate of loss of plasmids containing an ARS that fires early in S phase (*ARS305*), in the middle of S phase (*ARS1*) or late in S phase (*ARS1412*) [228]. All results are compared to wild type (*SRP1*) cells (Figure 17). In comparison to wild type (*SRP1*) cells, both the *srp1-31* and *srp1-E402Q* mutant cells exhibit plasmid loss of the early firing origin of replication, *ARS305*. As described in Materials and Methods, statistical analysis reveals a significant increase in plasmid loss in the *srp1-31* mutant as compared to the wild type (*SRP1*) cells ($^{**}p<0.01$) (Figure 17A). We also observed increased plasmid loss in *srp1* mutant cells with *ARS1*, which fires in the middle of S phase. Statistical analysis shows a significant increase in plasmid loss in both the *srp1-31* ($^{**}p<0.01$) and the *srp1-55* ($^{**}p<0.01$) mutant cells (Figure 17B). Finally, the *srp1-31* and *srp1-E402Q* mutants show an increase in plasmid loss for the late firing origin of replication, *ARS1412*. Statistical analysis reveals a significant increase in plasmid loss for both *srp1-31* ($^{**}p<0.01$) and *srp1-E402Q* ($^{*}p<0.05$) mutant cells as compared to wild type (*SRP1*) cells (Figure 17C). In order to rule out changes

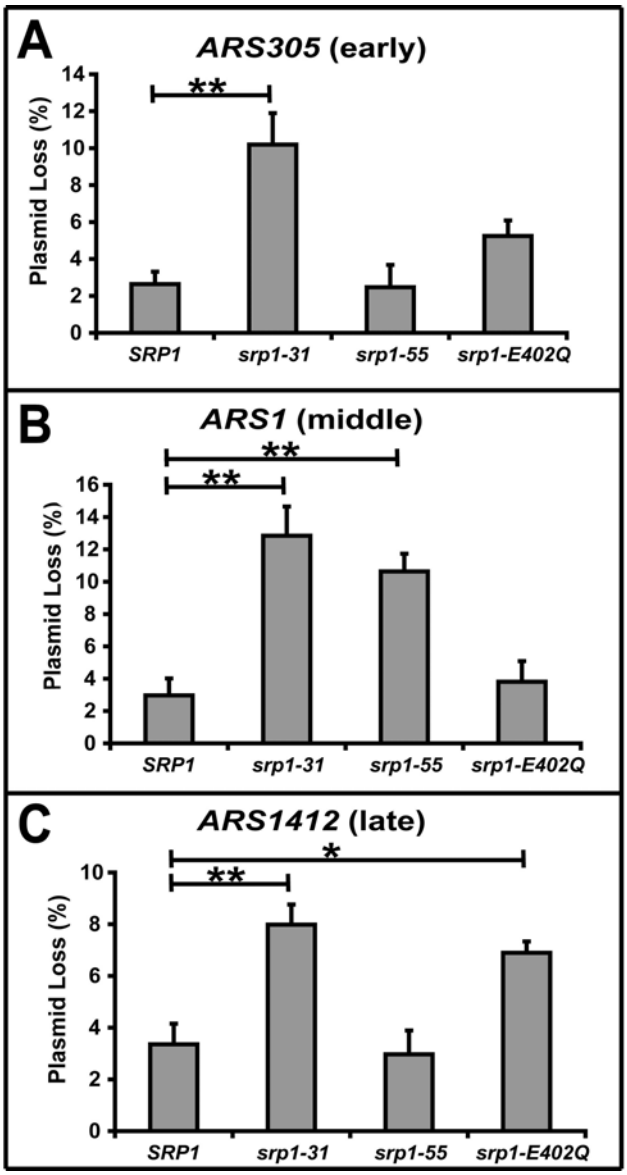

Figure 17. Analysis of plasmid loss.

To determine if *srp1* mutant cells have defects in DNA replication, a plasmid loss assay was performed. Plasmid loss was determined in cells containing plasmids with early (*ARS305*), middle (*ARS1*), or late (*ARS1412*) firing autonomously replicating sequences (ARS) as described in Materials and Methods. Results are plotted as the mean percentage of plasmid loss for (A) *ARS305* (early), (B) *ARS1* (middle), or (C) *ARS1412* (late) firing ARS sequences for each srp1 mutant (*srp1-31*, *srp-55*, and *srp1-E402Q*) as well as wild type (*SRP1*) control cells. Experiments were performed in triplicate. Standard deviations in the data are indicated by the

error bars. A one-way ANOVA followed by a Dunnett's multiple comparison test using an alpha value of 0.05 was used to determine the significance of the results. Significant differences between samples corresponding to the following p-values (* = $p<0.05$, ** = $p<0.01$) are indicated by the lines above the bars.

within the wild type control, plasmid loss for early, middle, and late firing replication origins was compared in wild type cells. This comparative analysis shows no significant difference in plasmid loss between the early, middle and late replication origins in the wild type cells (p=0.8417) (data not shown). Interestingly, the *srp-31* mutant shows a significant increase in plasmid loss at the early, middle, and late firing origins of replication suggesting a general chromosome loss phenotype. The plasmid loss defect in the *srp1-55* mutant suggests a specific defect in the middle firing origin of replication, *ARS1*. In contrast, the *srp1-E402Q* mutant shows a specific defect in the late firing origin of replication, *ARS1412*. Together, these results indicate that these *srp1* alleles have distinct effects on chromosome loss, which may result from differential import of key cell cycle proteins.

Bipartite cNLS candidates involved in G_1/S of the cell cycle

While it is likely that numerous import cargoes are impacted in the *srp1* mutant cells, we wanted to determine whether there were key candidates that would be most likely to be affected. In order to identify candidate cargoes whose import could be impaired in the *srp1-55* and *srp1-E402Q* cells, a bioinformatic approach was taken to identify proteins containing a putative bipartite cNLS that are involved in G_1/S of the cell cycle and are localized to the nucleus (Figure 18A). To identify the entire complement of candidate bipartite cNLS cargoes, the PSORT II algorithm for predicting bipartite cNLS motifs [238] was used to query the *S. cerevisiae* GenBank™ [239]. Out of 5850 proteins, 968 contain a predicted bipartite cNLS. We then used the PSORTII algorithm to query the pool of 1515 nuclear or nucleolar proteins as defined by localization of GFP fusion proteins [223]. Of these 1515 nuclear/nucleolar proteins, 391 contain a predicted

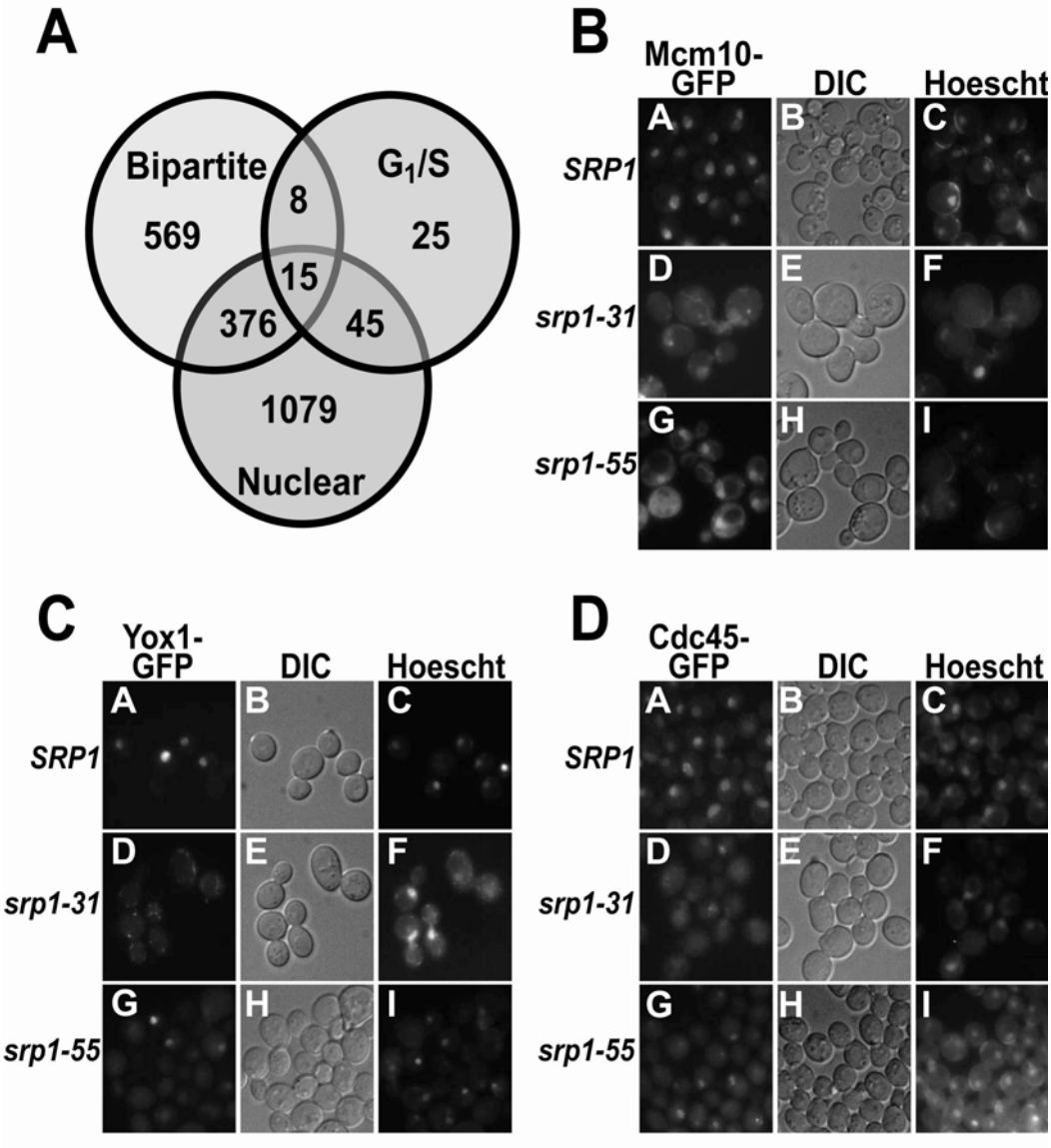

Figure 18. Candidate bipartite proteins implicated in G_1/S of the cell cycle are not efficiently targeted to the nucleus in importin α mutants.

(A) The PSORT II algorithm for bipartite cNLSs was used to query three sets of data: the 5850 proteins in the *S. cerevisiae* GenBank™ (Bipartite) [239], the 1515 proteins localized to either the nucleus or the nucleolus in the global yeast GFP-fusion library (Nuclear) [223], and 93 proteins implicated in G_1/S of the cell cycle based on the Gene Ontology definition (G_1/S) (http://www.geneontology.org/). The overlap between these three data sets identifies 15 proteins that contain a predicted bipartite cNLS, localize to the nucleus, and are already implicated in G_1/S of the cell cycle. Data from this analysis is presented as a Venn diagram. (B-D) Wild type

(*SRP1*) and *srp1* mutant (*srp1-31*, *srp1-55*) cells expressing Mcm10-GFP (B), Yox1-GFP (C), or Cdc45-GFP (D) were analyzed by direct fluorescence microscopy. Cultures were grown to log phase at the permissive temperature then shifted to the nonpermissive temperature (37ºC for *srp1-31* cells; 18ºC for *srp1-55* cells) for three hours. Wild type cells (*SRP1*) were analyzed following shifts to both 37ºC and 18ºC and identical results were obtained with each of the GFP fusion proteins. Results are shown for the wild type cells shifted to 37ºC. Corresponding DIC and Hoechst DNA staining images are shown.

bipartite cNLS [223]. As a preliminary approach to identify a subset of these proteins linked to the G_1/S cell cycle transition, we searched for genes containing the terms G_1, S, or G_1/S in their Gene Ontology definition (http://db.yeastgenome.org/cgi-bin/GO/). Through this initial approach, we identified 93 proteins implicated in G_1/S of the cell cycle. The overlap between these three data sets identifies 15 proteins that contain a predicted bipartite cNLS, localize to the nucleus, and are already implicated in the G_1/S transition (Figure 18A). These 15 candidate proteins that could be affected in cells that are defective in nuclear import of cargoes containing bipartite cNLS are listed in Table 5.

As an initial test of whether the nuclear import of any of these candidate cargoes is impaired in the importin alpha mutants, we selected three candidates that had previously been visualized as nuclear GFP fusion proteins, Cdc45, Mcm10 and Yox1 [223]. Cdc45 is involved in DNA replication and remains nuclear throughout *S. cerevisiae* cell cycle [240, 241]. Cdc45 interacts with the minichromosome maintenance (MCM) proteins which regulate DNA replication [240]. Mcm10 is a constitutively nuclear chromatin-associated protein that plays a role in DNA replication initiation by recruiting both the Mcm2-7 complex and DNA polymerase α to DNA replication origins [242-244]. Yox1 is a homeodomain transcriptional repressor that regulates the expression of genes that are critical for the G_1/S transition [245, 246]. We examined the localization of Mcm10-GFP, Yox1-GFP, and Cdc45-GFP in wild type (*SRP1*), *srp1-31*, and *srp1-55* cells (Figure 18B-D). At the permissive temperature, Mcm10-GFP, Yox1-GFP, and Cdc45-GFP are localized to the nucleus in all cells examined (data not shown). Following a shift to the nonpermissive temperature, both s*rp1-31* and *srp1-55* cells show a decrease in nuclear localization of Mcm10-GFP (Figure 18B) and Yox1-GFP (Figure

18C) in comparison to wild type (*SRP1*) cells. Interestingly, Cdc45-GFP remains nuclear localized in *srp1-55* cells but is mislocalized to the cytoplasm in *srp1-31* cells (Figure 18D).

3.4 Discussion

Results of this study define an important role for the NLS receptor, importin α, in DNA replication. Specifically, we report that two mutants of importin α cause a profound delay in the G_1/S cell cycle transition. Although previous studies described defects in G_2/M associated with other importin α mutants, *srp1-31* [180] and *srp1-55* [136], this is the first report demonstrating that mutations in the NLS receptor and hence defects in the classical protein import pathway impair the G_1/S transition.

Our study also reveals that the *srp1-31* mutant shows a delay in both the G_2/M and G_1/S cell cycle transitions, although the G_1/S delay for the *srp1-31* cells is not as profound as observed for *srp1-55* and *srp1-E402Q* cells. The G_2/M cell cycle defect observed for the *srp1-31* mutant is consistent with previous work [180] and also with the hypersensitivity to both benomyl and hydroxyurea. Genetic analysis indicated that the temperature-sensitive growth defect of *srp1-31* is suppressed by the overexpression of the nuclear import receptor, importin β. This finding suggests that the amino acid change in the *srp1-31* variant protein could impair importin β binding. As interaction between importin α and β is critical to target cargoes to the nuclear pore for import [247], decreased interaction with importin β could lead to profound defects in nuclear import of critical cargoes required for cell cycle transitions.

This study is distinct from the previous analysis of the *srp1-31* allele because the importin α variants employed here have well-characterized molecular defects. The Srp1-

E402Q mutant protein is impaired in binding to cargoes that contain a bipartite cNLS [135]. The Srp1-55 protein shows defects in cargo delivery into the nucleus [136]. We find that cells that express each of these importin α variants as the sole cellular copy of importin α both have defects in the G_1/S cell cycle transition. The finding that importin α variants with defects in cargo binding and cargo delivery cause similar cell cycle defects may be surprising; however, the most logical interpretation of this result may be that both variants are defective in the effective nuclear import of cargo proteins that contain a classical bipartite NLS. This conclusion is fairly obvious for the *srp1-E402Q* protein which has an amino acid substitution in a key residue of the minor NLS binding pocket that makes contact only with cargoes that contain a bipartite cNLS and, in fact, only shows defects in the import of bipartite cNLS cargoes [93, 135]. In the case of the *srp1-55* protein, the auto-inhibitory and hence the inherent cargo release mechanism is impaired [136]. However, in cells, there are additional factors that facilitate cargo release including the export receptor, Cse1, and the nuclear pore protein, Nup2 [104, 121, 131]. Indeed, overexpression of Cse1 suppresses the growth defect of the *srp1-55* mutant. Possibly, cargoes that bind tightly to the NLS receptor may be most impacted *in vivo* when the cargo delivery function inherent to importin α is impaired. These tight binding cargoes are most likely to be those cargoes that contain a bipartite cNLS as bipartite cargoes typically bind with a stronger affinity to the NLS receptor than monopartite cargoes [43]. Thus, *srp1-55* and *srp1-E402Q* cells may both, logically, be most impaired in nuclear delivery of bipartite cNLS cargo proteins.

Although *srp1-55* and *srp1-E402Q* mutant cells show similar defects in the cell cycle, the plasmid loss assay provides further insight into the molecular defect. The

plasmid loss assay indicates that a defect in cNLS cargo binding (*srp1-E402Q*) affects DNA replication late in S phase. Similarly, the plasmid loss assay suggests that a defect in cNLS cargo release (*srp1-55*) also affects DNA replication but in the middle of S phase. Furthermore, like *srp1-31* cells, our results suggest that *srp1-55* cells are impaired in both the G_1/S and G_2/M cell cycle transitions. Interestingly, these results suggest that different defects in the NLS receptor importin α are likely to affect the import of distinct complements of nuclear import cargoes including some that may be uniformly affected and some that may be distinct for each mutant. Presumably what cargoes are affected in each mutant depends on both cargo recognition in the cytoplasm and release into the nucleus. Other factors that effect recognition and release could also influence the phenotype of these mutants.

The use of variants of importin α with specific molecular defects allowed us to identify a number of candidate proteins that may be impacted in these mutants. For three of these candidate proteins, Mcm10, Yox1, and Cdc45 we show that nuclear localization is differentially impaired in the importin α mutants. While Mcm10 and Yox1 are mislocalized in each importin α mutant examined, Cdc45 is mislocalized to the cytoplasm only in *srp1-31* cells. Overall, these results show that different defects in importin α affect distinct cargoes. In the future, genetic approaches that exploit the conditional growth phenotypes of these *srp1* mutants may be useful in identifying additional cargo proteins impacted in these mutants including some that may be specific for each mutant.

Collectively, our data demonstrate a molecular role for the nuclear localization signal receptor, importin α, during the G_1/S stage of the cell cycle. This finding adds to

our previous understanding of the link between nuclear transport and cell cycle progression as previously only defects in the G_2/M transition had been linked to mutants in the nuclear import receptor. Future studies will be aimed at identifying key cargoes that must enter the nucleus to mediate these critical cell cycle transitions.

3.5 Acknowledgements

We are very grateful to Dr. Deanna Koepp for her help with cell cycle studies as well as her comments on the manuscript. We would like to thank Dr. Ryan Mills for his help with bioinformatics analysis as well as members of the Corbett laboratory for helpful suggestions. This work was supported by a National Institute of Health grant to AHC. KFP was supported by a National Institute of Health and Facilitating Academic Careers in Engineering and the Sciences supplement.

Table 3. *S. cerevisiae* strains used in this study

Name	Strains	Genotype	References
Wild type	pSY580 (ACY192)	*Mata ura3-52 leu2Δ1 trp1*	[203]
Wild type	ACY247	*Mata/α ura3-52 leu2Δ1/leu2Δ1 his3Δ200/ his3Δ200 ade2/ADE2 ade3/ADE3 lys2/LYS2 trp1/TRP1*	[248]
srp1-55	ACY641	*Mata ura3-52 his3Δ200 leu2Δ1 trp1 ade2 srp1-55::LEU2*	[136]
srp1-55	ACY642	*Matα ura3-52 his3Δ200 leu2Δ1 trp1 srp1-55::LEU2*	[136]
srp1-E402Q	ACY1560	*Mata ura3-52 his3Δ200 leu2Δ1 trp1 ade2 lys2 srp1-E402Q::LEU2*	This study
srp1-31	ACY1561	*Matα ura3-52 leu2Δ1 trp1 his3Δ200 lys2*	This study
srp1-31	ACY1562	*Mata ura3-52 leu2Δ1 trp1*	This study
Cdc45-GFP	YLR103C (ACY1886)	*Mata his3Δ1 leu2Δ0 met15Δ0 ura3Δ0*	[223]
srp1-31-Cdc45-GFP	ACY1889	*Mata leu2Δ0 met15Δ0 ura3Δ0 trp1*	This study
srp1-55-Cdc45-GFP	ACY1890	*Mata met15Δ0 ura3Δ0*	This study
Mcm10-GFP	YIL150C (ACY1887)	*Mata his3Δ1 leu2Δ0 met15Δ0 ura3Δ0*	[223]
srp1-31-Mcm10-GFP	ACY1891	*Mata leu2Δ0 met15Δ0 ura3Δ0*	This study
srp1-55-Mcm10-GFP	ACY1892	*Mata met15Δ0 ura3Δ0*	This study
Yox1-GFP	YML027W (ACY1888)	*Mata his3Δ1 leu2Δ0 met15Δ0 ura3Δ0*	[223]
srp1-31-Yox1-GFP	ACY1893	*Mata leu2Δ0 met15Δ0 ura3Δ0*	This study
srp1-55-Yox1-GFP	ACY1894	*Mata met15Δ0 ura3Δ0*	This study

Table 4. List of plasmids

Plasmid	Description	References
pRS406	*LEU2*, integration, *AMP^R*	[249]
pRS424	*2μ, TRP1, AMP^R*	[217]
pAC592	*RSL2, 2μ, TRP1, AMP^R*	[136]
pAC876	*SRP1, CEN, URA3, AMP^R*	[118]
pAC1059	*pMET25-BPSV40T3-NLS-GFP-GFP, CEN, URA3, AMP^R*	[250]
pAC1065	*pMET25-SV40-NLS-GFP-GFP, CEN, URA3, AMP^R*	[250]
pAC1303	*CSE1, 2μ, TRP1, AMP^R*	[136]
pAC1344	*TUB1-GFP,* integration*, URA3, AMP^R*	[251]
pAC1354	*SRP1, CEN, TRP1, AMP^R*	[136]
pAC1385	*NUP2, 2μ, TRP1, AMP^R*	[136]
pAC1999	*E402Q-SRP1, LEU2,* integrating*, AMP^R*	This study
p305.2	*ARS305 CEN5 URA3*	[228]
pARS1	*ARS1 CEN5 URA3*	[228]
p12	*ARS1412 CEN5 URA3*	[228]

Table 5. List of bipartite cNLS candidates involved in G_1/S

Protein	Function
Bck2	Molecular function unknown
Cdc40	RNA splicing factor activity
Cdc45	DNA Replication
Mcm10	DNA Replication and chromatin binding
Rsc3	DNA binding
Swi5	DNA replication and transcriptional activator activity
Tos4	Transcription factor activity
Tye7	Transcription factor activity
Pog1	RNA POL II transcription factor activity
Taf1	RNA POL II transcription factor activity
Taf13	RNA POL II transcription factor activity
Taf14	RNA POL II transcription factor activity
Yap5	RNA POL II transcription factor activity
Yhp1	DNA binding
Yox1	DNA binding

CHAPTER 4. GENERAL DISCUSSION

The studies described in this dissertation examine the quantitative mechanism of classical nuclear import and then extend our analysis of protein import to address how this mechanism regulates a fundamental process in biology, the cell cycle. Importantly, these studies reveal the nuclear import pathway is required for efficient progression through the G_1/S cell cycle transition.

4.1 cNLS Cargo Binding Affinity for Importin α Dictates Nuclear Import

The complex process of nuclear protein import consists of a number of potential rate-limiting steps. These steps include: (1) receptor-cargo assembly in the cytoplasm, (2) translocation through the nuclear pore complex, (3) delivery of cargo into the nucleus, and (4) recycling of import receptors back to the cytoplasm (Figure 3).

The goal of Chapter 2 was to determine how the binding affinity of a cNLS cargo for importin α in the cytoplasm dictates the rate of import of the cNLS cargo into the nucleus. This study used variants of the cNLS cargoes, SV40 and Myc, to examine a broad range of *in vitro* binding affinities of the cNLS cargoes for importin α (Table 1). The *in vitro* binding affinity of the SV40 and Myc variant cargoes for importin α was correlated with *in vivo* nuclear localization data to determine a relationship between the cNLS cargo affinity for importin α and the initial rate of nuclear accumulation.

Other approaches to examine a correlation between cNLS cargo binding affinity for importin α and the initial rate of nuclear accumulation have been undertaken [207, 209, 210]. Jans *et al*. utilized an *in vitro* permeabilized cell assay and microinjection of exogenous cargo proteins into cells to examine import of proteins into the nucleus [209,

210]. Jans' studies examined cargoes with a narrow range of binding affinities for importin α [209, 210], which only gives information about a subset of cargoes. Consistent with our conclusions, they found that nuclear transport is dependent on the binding affinity between importin α and its cargo [209, 210], but these results were obtained with an artificial system.

Riddick *et al*. performed a computer modeling study to examine import rates using a similar microinjection assay [207]. Through examination of cNLS cargo localization at steady-state and measurement of the rate of nuclear accumulation, Riddick *et al.* concluded that the cellular levels of importin α dictate the rate of nuclear import [207]. Specifically, increased levels of importin β, reduced nuclear accumulation of a cargo, while increased levels of importin α enhanced nuclear accumulation [207]. The weakness of this study lies in the fact that they only examined one type of cNLS cargo.

The same group also wanted to compare the efficiency of importin α-mediated nuclear import in comparison to direct nuclear import with only importin β [252]. Riddick *et al.* hypothesized, the use of adapters such as importin α increases the initial rate of nuclear import because export of importin α is coupled to GTP hydrolysis [252]. Using the same computer modeling system, Riddick *et al*. determined that the initial rate of cargo nuclear accumulation by directly binding importin β is actually faster than importin α-mediated import. This initial rate of import is increased with importin β-mediated transport, because importin β has a higher rate of passage through the NPC and a faster cycling time than importin α [252]. They suggested that cargoes use importin α for nuclear import because the importin α system is more efficient [252].

Jans and Riddick were correct in their interpretations, but our *in vivo* studies demonstrate for the first time in living cells, formation of the nuclear import complex dictates the rate of import of a cNLS cargo into the nucleus. Therefore, a rate-limiting step in classical nuclear import is assembly of the nuclear import complex in the cytoplasm. The probability of formation of the import complex is increased by an increase in importin α levels and an increase in the affinity of the cNLS cargo for importin α.

Validity of a Predicted cNLS cargo

Studies in Chapter 2 create a quantitative model to assess whether cNLS cargo affinity for importin α dictates nuclear import. One prediction from our quantitative studies is both lower and upper limits exist for the binding affinities of functional cNLS cargoes for importin α. For a cNLS cargo to fall between the upper and lower limit boundaries, a cNLS cargo must possess a high enough affinity for importin α, for the cargo to be recognized by the receptor in the cytoplasm, yet a weak enough affinity for importin α, for the cargo to be efficiently released into the nucleus. We show there is a linear relationship between cNLS cargo binding affinity for importin α and the initial rate of nuclear accumulation of cNLS cargo (Figure 9). cNLS cargoes with affinities between 10^{-7}M and 10^{-9}M, yield initial import rates that generally increase with increasing binding affinity (Figure 19). One implication of this finding is when the affinity between the cNLS cargo and importin α is very high, more cNLS cargoes accumulates in the nucleus. On the contrary, a low affinity between the cNLS cargo and importin α, leads to less nuclear accumulation of the cNLS cargo. Therefore we wanted to determine which affinity is too low to yield efficient nuclear import.

A Lower Limit for cNLS Cargo Binding Affinity for Importin α

In our studies, we find there is a lower limit for cNLS cargo binding affinity for importin α. A subset of cNLS SV40 and Myc variants that have a very low binding affinity for importin α do not show accumulation in the nucleus. Based on this localization study, our data suggest the lower limit to confer nuclear import of a cNLS cargo is a binding affinity of ~10^{-7}M or lower (Figure 19). Therefore, if the interaction between a cargo and importin α is too weak, then the cargo will not efficiently interact with importin α in the cytoplasm to allow localization to the nucleus. These studies demonstrate predicted cNLS cargoes with very low affinities for importin α do not contain a functional cNLS. In summary, classical nuclear import is directly related to the interaction between the cNLS cargo and importin α, which ultimately leads to the assembly of the cNLS cargo/importin α/β import complex.

Is There an Upper Limit for cNLS Cargo Binding Affinity for Importin α?

Since a lower limit for cNLS cargo binding affinity for importin α exists, we predicted an upper limit must also exist. Although there are cNLS cargoes that bind importin α very tightly in the cytoplasm, this high affinity interaction between the cargo and importin α must be disrupted to allow release of the cargo into the nucleus [136]. If the cargo is not efficiently released into the nucleus, then a defect in dissociation of the cargo from importin α could deplete the pool of free importin α available to mediate

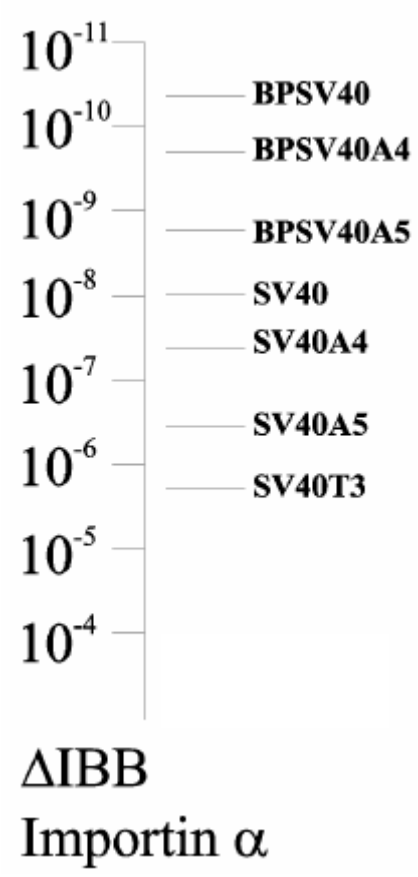

Figure 19. An *in vitro* Energy Scale for Nuclear Localization.
The relative binding affinities for various NLS variant sequences in complex with importin α are shown on a logarithmic scale. The scale represents the binding affinity of NLS cargo variants for importin α in the cytoplasm (as approximated using ΔIBB importin α). NLS cargoes with affinities between 10^{-7}M and 10^{-9}M yield initial import rate values that generally increase with increasing binding affinity. A lower limit for NLS cargo binding affinity for importin α is below 10^{-7} M. Our studies revealed no detectable upper limit for NLS cargo binding affinity for importin α *in vivo* [43].

nuclear import. As discussed in the Introduction, importin α is essential [112, 113]; therefore the removal of importin α would lead to cell death.

Experiments in Chapter 2 show in contrast to a lower limit for binding affinity, no upper limit for cNLS cargo binding affinity for importin α *in vivo* was defined. Contrary to our prediction that very strong binding cargoes would cause cells to die, we show overexpression of these strong binding cargoes is not toxic to wild type cells (Figure 11), implying strong binding cargoes are able to dissociate from importin α in the nucleus. In contrast, overexpression of high affinity cargoes in cells that show a defect in cargo release (*srp1-55*), causes a mild growth defect indicating the sensitivity of defects in cargo release with high affinity cargoes (Figure 11).

A limitation of this study is the cellular levels of the cNLS cargoes have not been quantified. Since more cNLS cargoes exist in the cell than importin α, the import function of importin α must be fast enough to accommodate import of many different cargoes with a wide range of affinities for importin α. Therefore, quantification of the cargo levels would help determine the amount of cNLS cargoes required to deplete the cell of importin α and identify an upper limit to cNLS cargo binding affinity for importin α. Another approach to define an upper limit is to identify proteins that are sensitive to defects in cargo release (s*rp1-55*).

One explanation for the efficient release of very strong binding cNLS cargoes from importin α lies in the characterization of additional factors involved in release of the cargoes into the nucleus. As discussed in the Introduction, biochemical and structural analyses have determined the auto-inhibition motif of importin α plays a role in regulating the release of cNLS cargo into the nucleus [118, 119, 136]. *In-vitro* binding

studies suggest that the auto-inhibition motif of importin α alone may not be sufficient to compete with a strong binding cNLS cargo. Other factors that help facilitate release of cNLS cargo into the nucleus *in vivo* are the nuclear pore protein, Nup2, and the importin α export receptor, Cse1 [103, 104, 129, 131]. As described in the Introduction, Nup2 competes with cNLS cargo for binding to the cNLS cargo binding pocket of importin α [22, 23] and Cse1 is responsible for recycling cargo-free importin α back to the cytoplasm [103-105].

Taken together, cooperation of the auto-inhibition motif of importin α, Nup2, and Cse1, facilitates efficient release of strong binding cNLS cargoes into the nucleus and these factors participate in exporting cargo-free importin α back to the cytoplasm for another round of nuclear import. Although no upper limit for cNLS cargo binding affinity for importin α *in vivo* was defined, these studies suggest the classical nuclear transport machinery is robust enough to allow productive import of tightly bound cNLS cargoes. Since these studies, did not examine all possible cNLS sequences, a cNLS cargo showing an upper limit for affinity for importin α may exist and could cause a defect in cargo release into the nucleus.

A New Quantitative Model for Classical Nuclear Transport

Our studies provide significant insight into a quantitative model for classical nuclear transport that incorporates the thermodynamics and kinetics of cNLS cargo recognition by importin α and the import of the cNLS cargo to the nucleus. For thermodynamics, the nuclear import variables utilized are the binding affinity of the cargo for importin α and the cellular levels of the nuclear transport machinery. The kinetic experiments examine the initial rate of nuclear accumulation. Our quantitative

model changes the simple dynamics of cNLS cargo binding and release [247]. Previously, nuclear import was predicted to be dependent on thermodynamics [43, 85, 206, 207, 209, 210, 252]. In contrast to previous studies, our results suggest that both thermodynamics and kinetics play a role in formation of the nuclear import complex through the interaction of the cNLS cargo and importin α. The cNLS cargo:importin α interaction is the rate-limiting step in nuclear import.

$$\textbf{cNLS cargo} + \textbf{Importin } \alpha \underset{K_{ON}}{\overset{K_{OFF}}{\leftrightarrows}} \textbf{cNLS cargo•Importin } \alpha$$

The rate-limiting step is affected by both the amount of importin α and the binding affinity of the cNLS cargo for importin α. Consistent with our work, a study published after our analysis of importin α examined how the binding affinity of non-classical NLS cargoes for the importin β import receptor, Kap123, correlates with nuclear import [137]. These authors also found that the amount of the Kap123 receptor changes the rate of import of its NLS cargoes [137]. In conclusion, assembly of the import complex in the cytoplasm dictates transport of classical and non-classical cargoes into the nucleus.

A caveat of the cNLS cargo:importin α interaction rate-limiting step is the assumption that the rate-limiting step only affects cNLS cargo binding in the cytoplasm. The rate-limiting step can also affect cNLS cargo release into the nucleus. As mentioned above, our studies suggest a cargo with a low affinity for importin α has a slow initial rate of nuclear accumulation (K_{ON}) because it takes a longer time for the cNLS cargo to bind importin α in the cytoplasm. Our experiments which employ ΔIBB importin α show increased binding affinity of cNLS for importin α in the cytoplasm. The K_d we measure is a combination of $K_{ONcytoplasm}$ and $K_{OFFcytoplasm}$. Our experiments do not distinguish between faster binding and slower release for high affinity cargoes. But the

experiments do show an increase in the steady-state levels of the import complex yields faster import. Further binding analysis would need to be performed to examine the affects of cNLS cargo release into the nucleus and initial rates of nuclear accumulation.

Examination of Targeting Sequences not Imported into the Nucleus via the Classical Nuclear Transport Machinery

The quantitative approach of examining binding affinities can be applied to other targeting signal-receptor pairs that do not use the classical nuclear transport pathway for entry into the nucleus. The challenge is very few targeting signals that mediate transport receptor binding have been identified as of yet. For example, this model could examine nuclear/cytoplasmic accumulation of putative non-classical NLS or NES, cNES and PY-NLS sequences, and their binding affinity for the export receptor, Crm1, or importin β superfamily receptors [48-51]. In addition, experiments could examine proteins that contain more than one predicted signal sequence. The study of proteins containing multiple signal sequences is important because experiments in Chapter 2 examined subcellular localization of both NLS and NES sequences fused to the same GFP reporter. These localization studies demonstrated the binding affinity of the NLS or NES for its receptor dictates where the cargo will accumulate (Figure 10). Therefore, if the binding affinity of the NES for the NES receptor is higher than the affinity between the NLS and its receptor, then the cargo will accumulate in the cytoplasm. Use of a quantitative model to test the function of predicted import and export signal sequences, could establish a foundation to discover associations between the functional subellular location of a particular cargo and the binding affinity of a cargo for its import or export receptor.

4.2 Classical Nuclear Transport Regulates Cell Cycle Transitions

Because our study revealed the rate-limiting step of classical nuclear import is cNLS cargo interaction with importin α, we wanted to examine this interaction in a fundamental biological process. We chose to investigate the cell cycle because links between classical nuclear transport and the cell cycle have been reported [179-181, 253-256]. Therefore, the goal of Chapter 3 was to examine the interplay between nuclear transport and cell cycle control by specifically determining how modifications in the nuclear import machinery affect the nuclear import of critical cNLS cargoes involved in regulating cell cycle progression.

Importin α mutants with Defects in Cargo Binding and Cargo Release

Studies in Chapter 3 identified specific molecular functions of nuclear import implicated in controlling the transport of critical proteins that regulate cell cycle transitions. Previous studies have shown that the importin α mutant, *srp1-31*, is defective in the transition through the G_2/M stage of the cell cycle [180]. Although *srp1-31* cells showed a defect in progression through mitosis, the specific molecular impact the S→P amino acid substitution within the Srp1-31 mutant protein has on importin α function is not known. Therefore, a molecular role importin α plays in cell cycle progression is not defined with the Srp1-31 mutant. Importantly, our study demonstrates for the first time, engineered mutants in importin α affect cNLS cargo binding in the cytoplasm or cNLS cargo release into the nucleus affect efficient transition through the G_1/S stage of the cell cycle.

Since *SRP1* is an essential gene and import of cNLS cargo into the nucleus is critical for cell function [112, 180], a major challenge was to identify conditional mutants

of importin α that impair but do not eliminate *SRP1* function. One mutant we exploited is Srp1-E402Q, which has an amino acid substitution in the minor binding pocket of importin α. Therefore, this amino acid substitution decreases the binding affinity of importin α for bipartite cNLS cargoes [135] (Figure 12A). Bipartite cNLS cargoes must bind both the major and minor binding pocket of importin α for efficient nuclear import to occur [44]. Chapter 3 revealed the decrease in the bipartite cNLS cargo affinity for importin α decreases the initial rate of nuclear accumulation of a bipartite cNLS cargo **(**Figure 8**)**.

We also exploited a second conditional mutant of *SRP1*, *srp1-55*. An amino acid substitution at position 55 within the auto-inhibition sequence (KRR→KAR) of importin α, creates this conditional allele that leads to inefficient cNLS cargo release into the nucleus. The impact the Srp1-55 mutant has on cNLS cargo release has previously been tested in binding studies with a monopartite cNLS cargo. These studies revealed that the Srp1-55 mutant causes a defect in monopartite cNLS cargo release [136].

The two importin α mutants, Srp1-E402Q and Srp1-55, and the previously characterized Srp1-31 mutant were employed to determine how defects in the nuclear import process affect transition through the cell cycle. A series of studies examined cell growth, DNA content and spindle morphology at different stages of the cell cycle to determine how a defect in cNLS cargo binding (*srp1-E402Q*) or cNLS cargo release (*srp1-55*) affects cell cycle progression. These studies revealed for the first time that mutants of importin α affect transition through the G_1/S stage of the cell cycle.

To begin to identify the specific regions of S phase impacted by the importin α mutants, we utilized different origins that initiate DNA replication at different stages

within S phase. We determined the function of *srp1-31* is required throughout S phase, while cargo release (*srp1-55*) plays a role in progression through the middle of S phase and cargo binding (*srp1-E402Q*) is involved in late S phase progression. This study suggests that the individual importin α mutants cause differential defects on distinct cargoes that are involved in S phase progression. The finding that multiple stages of S phase are affected in these importin α mutants suggests cargo binding and cargo release in the nuclear import process are critical for the function of a subset of cNLS cargoes involved in different stages of S phase progression. Future studies could examine the subcellular localization and interaction of cNLS cargoes involved in initiating early, mid, or late S phase.

Although there are proteins involved in initiating DNA replication at all origins of replication, there are key proteins that are involved in replication timing. For example, the protein Ku is involved in the regulation of replication timing specifically at telomeric regions of DNA [257]. Replication of telomere regions occurs late in S phase [258, 259]. Interestingly, the Ku70 subunit of Ku contains a bipartite cNLS [260]. As *srp1-E402Q* mutant cells cause a defect in DNA replication late in S phase, *srp1-E402Q* could affect cargo binding of Ku70. Further binding studies using wild type importin α and the Srp1-E402Q mutant with Ku70 would need to be performed to test this hypothesis.

The timing of DNA replication is more complex than the use of distinct proteins to initiate replication at different origins. Replication timing is speculated to also be dependent on developmental stage, chromatin structure, and/or changes in gene expression [261-263]. Therefore proteins functioning in development, DNA structure

and transcription may be key cargoes affected by defects in cNLS cargo binding and cargo release.

Identification of Candidate Bipartite cNLS Cargoes involved in Cell Cycle Progression

The most critical question raised by the cell cycle studies presented here is how to identify the cNLS cargoes that must be imported into the nucleus for efficient progression through the G_1/S stage of the cell cycle. The importin α mutants employed in this study most likely have defects in import of cNLS cargoes containing a bipartite cNLS. Because bipartite cargoes have two binding sites, they typically have stronger binding affinities for importin α in the cytoplasm than monopartite cargoes. The *srp1-E402Q* mutant impacts bipartite cNLS cargo binding and the *srp1-55* mutant impacts bipartite cNLS cargo release. Since the bipartite cNLS cargoes bind importin α more tightly than monopartite cNLS cargoes, we hypothesize it is more difficult for strong binding bipartite cNLS cargoes to release from importin α once inside the nucleus. Although an upper limit to cNLS cargo release was not discovered in our studies, there could be cNLS cargoes with a sufficiently strong binding affinity for importin α that could have difficulty releasing from importin α in the nucleus.

In Chapter 3, we identified 15 candidate bipartite cargoes previously implicated in the G_1 and/or S phase(s) of the cell cycle (Figure 18A, Table 5). Nuclear import of these bipartite cNLS cargoes may be required for the G_1/S transition of the cell cycle. The most logical candidates to start examining were Mcm10, Yox1, and Cdc45 because they are directly implicated in S phase/DNA replication [240-243, 264-266].

We utilized the importin α mutants to examine the subcellular localization of the GFP-tagged bipartite candidates, Mcm10, Yox1, and Cdc45 in *srp1-31* and *srp1-55* mutant cells. Mcm10 and Yox1 are mislocalized to the cytoplasm in *srp1-31* and *srp1-55* mutant cells; however the import of Cdc45 to the nucleus is only defective in *srp1-31* mutant cells suggesting a defect in cargo release does not affect Cdc45 nuclear import. Importantly, these studies confirm our hypothesis that import of key cargoes is affected in mutants of importin α. These localization studies imply each individual cargo is affected differently depending on the molecular defect in nuclear import.

A Role for Importin α at the G_1/S and G_2/M Stages of the Cell Cycle

Prior to these studies, importin α had been implicated in the G_2/M stage of the cell cycle (see Figure 6) based on defects in the *srp1-31* and *srp1-55* mutants [136, 180]. These studies suggested cNLS cargoes that play a role in the G_2/M stage of the cell cycle depend on the function of importin α for import into the nucleus. Although our studies focused on the defect in the G_1/S transition, this finding does not eliminate possible involvement of the nuclear import machinery in regulating other phases of the cell cycle. Additional studies would need to be performed to examine a possible role of importin α in regulating these stages. For example, a genome-wide overexpression suppression study in each importin α mutant would be useful to identify candidate cNLS cargoes that are dependent on interactions with importin α for entry into the nucleus. An overexpression suppression screen would be useful because prior analysis showed a genetic interaction between *srp1-55* and *CSE1* and also *srp1-31* and importin β (*RSL2*) (Figure 13) [136]. Although the previous overexpression suppression analysis did not examine genetic interactions between importin α and candidate cargoes, this study found

other components of the nuclear transport machinary. Candidates identified in the suppressor screen could be classified as (1) cNLS cargoes whose nuclear import is affected by defects in cargo binding and/or cargo release, (2) whether the cNLS cargo is involved in the cell cycle and if it is, (3) which stage of the cell cycle requires the function of that cNLS cargo. We can predict cargoes affected by molecular defects in nuclear import may be involved in multiple stages of the cell cycle and some cargoes will be affected by the same molecular defect. We can also expect to identify proteins that function at different cell cycle checkpoints.

Bipartite cNLS cargoes with a low affinity for importin α would be most affected by a defect in cargo binding (*srp1-E402Q*) in the cytoplasm. Bipartite cNLS cargoes with a high affinity for importin α would be most affected by a defect in cargo release (*srp1-55*) into the nucleus. A series of four binding studies would need to be performed to determine if the cargo contains a functional cNLS [47]. First, mutational analysis of the predicted cNLS sequence should cause a defect in nuclear import. Second, fusion of the predicted cNLS sequence to an unrelated protein localizes the fusion protein into the nucleus. Third, binding assays should show a direct interaction of the predicted cNLS cargo with importin α. Fourth, the *srp1-E402Q* and/or *srp1-55* mutants should disrupt import of the predicted cNLS cargo into the nucleus [47].

Specifically, cNLS cargoes involved in the G_1 and/or S phases could be checkpoint proteins or components of the DNA replication machinery [157, 158]. These proteins should be localized to the nucleus. Defects in cNLS cargo binding (*srp1-E402Q*) or cargo release (*srp1-55*) could potentially lead to a defect in the import of these key checkpoint or DNA replication machinery proteins. Mislocalization of the

checkpoint proteins could lead to improper progression through the restriction point, the G_1/S DNA damage checkpoint, and/or the S phase DNA damage checkpoint. As a result of mislocalization of the checkpoint proteins, cells may contain duplicated DNA with mutations that will eventually lead to cell death or uncontrolled cell growth. Likewise, the mislocalization of DNA replication machinery could result in lack of chromosome duplication or a defect in replication timing. Therefore the nuclear import of key cNLS cargoes is required for efficient cell cycle progression.

Limitations of using *S. cerevisiae* as model system to study nuclear transport and the cell cycle

Although using yeast *S. cerevisiae* as a model to study cellular processes is very simple and the proteins are conserved with higher eukaryotes as was discussed in the Introduction, the yeast model has some limitations. In contrast to yeast, the nuclear envelope breaks down at late mitosis in higher eukaryotes such that the nuclear import machinery is not required at late mitosis. Therefore prior studies showing mutants of importin α in *S. cerevisiae* cause a defect in the G_2/M stage of the cell cycle [136, 180] may translate to higher eukaryotes.

In addition, there are fewer proteins in yeast in comparison to higher eukaryotes. For instance, there is only one *S. cerevisiae* CDK protein, Cdc28, which is required for cell cycle checkpoint activity while there are a total of four human CDKs, CDK1, CDK2, CDK4, and CDK6 [164, 165]. As mentioned in the Introduction, *S. cerevisiae* contains only one importin α protein while humans contain six isoforms of importin α. The identification of four CDK proteins and six isoforms of importin α in humans suggest the classical nuclear import process is more complex than the nuclear import model in yeast. This complexity in humans provides further evidence for a highly coordinated system

where cNLS cargoes can be imported into the nucleus by different importin α isoforms. Interaction of the importin α isoforms with their cNLS cargoes, possibly depends on the cargoes binding affinity for a specific isoform, the function of the cargo, and the tissue specific expression of the isoform and/or cargo. Previous studies have begun to examine the preference of cNLS cargoes for specific isoforms of importin α in humans [267].

4.3 GENERAL CONCLUSIONS

Overall, this dissertation demonstrates how the classical nuclear import machinery makes critical contributions to the cell cycle. First, we showed the rate-limiting step of nuclear import is formation of the nuclear import complex through interaction of the cNLS cargo with importin α in the cytoplasm. Second, we provided evidence that the rate-limiting step in nuclear import also dictates the progression of the cell cycle. Our studies show, for the first time, classical nuclear import regulates progression through the G_1/S stage of the cell cycle.

As mentioned in the Introduction, many different factors play a role in progression through the eukaryotic cell cycle (Figure 6). The cyclins and cyclin-dependent kinases (CDKs) function in regulating processes that occur in each part of the cell cycle. The different checkpoints located throughout the cell cycle function in making sure each process occurs efficiently before the next steps can transpire. This dissertation shows that the nuclear import receptor, importin α is also required for efficient progression through the G_1/S transition of the cell cycle (Figure 20). Specifically, importin α imports key cNLS cargoes into the nucleus during the G_1 and/or S phase(s) of the cell cycle. These cargoes are directly or indirectly involved in the G_1/S transition. Although our studies show importin α plays a role in the cell cycle by importing cNLS

cargoes involved in cell cycle progression, importin α could also have an independent role in cell cycle progression.

Our newly proposed mechanism of cell cycle regulation suggests a subset of critical proteins that play key roles in cell cycle control, must be transported into the nucleus at a specific point in the cell cycle by the classical nuclear transport machinery. This dissertation presents supporting evidence for the involvement of cNLS cargoes in the G_1/S stage of the cell cycle where a defect in cargo binding or cargo release leads to profound delays in the cell cycle. These subtle mutations in importin α impact cell cycle progression and could possibly contribute to human disease such as cancer.

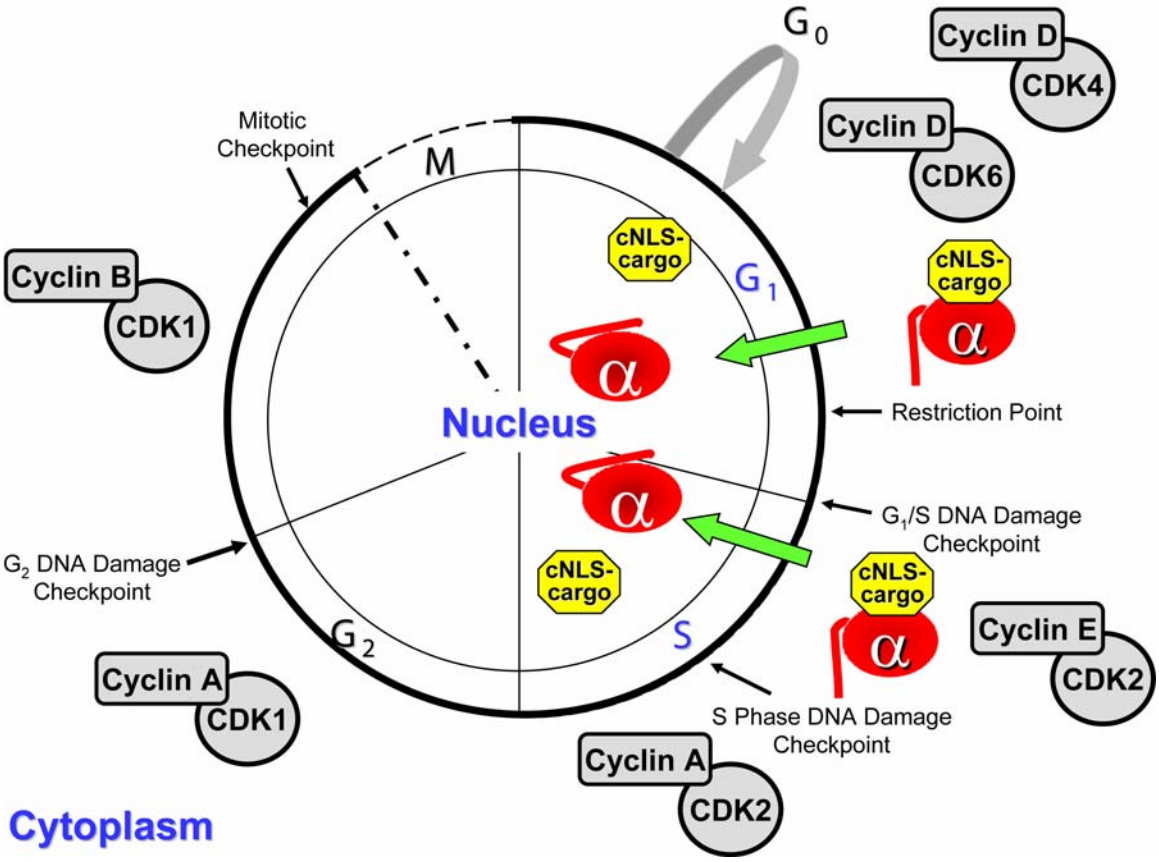

Figure 20. A Role for Importin α in Regulating Transition through G_1/S stage of the Cell Cycle

Schematic of a cell during different phases of the cell cycle. Inside the circle is the nucleus and outside the circle is the cytoplasm. The outer rim of the circle represents the nuclear envelope. The arrows represent flow of proteins into the nucleus during nuclear import. cNLS cargo recognition by importin α can be added to the knowledge of mechanisms (checkpoints, cyclin/CDK interaction, etc.) that regulate progression through the cell cycle.

CHAPTER 5. REFERENCES

1. Kornberg, R.D., *Eukaryotic transcriptional control.* Trends Cell Biol, 1999. **9**(12): p. M46-9.

2. Jacob, F. and J. Monod, *Genetic regulatory mechanisms in the synthesis of proteins.* J Mol Biol, 1961. **3**: p. 318-56.

3. Gorlich, D. and U. Kutay, *Transport between the cell nucleus and the cytoplasm.* Annu Rev Cell Dev Biol, 1999. **15**: p. 607-60.

4. Wente, S.R., *Gatekeepers of the nucleus.* Science, 2000. **288**(5470): p. 1374-7.

5. Vasu, S.K. and D.J. Forbes, *Nuclear pores and nuclear assembly.* Curr Opin Cell Biol, 2001. **13**(3): p. 363-75.

6. Rabut, G., P. Lenart, and J. Ellenberg, *Dynamics of nuclear pore complex organization through the cell cycle.* Curr Opin Cell Biol, 2004. **16**(3): p. 314-21.

7. Griffis, E.R., S. Xu, and M.A. Powers, *Nup98 localizes to both nuclear and cytoplasmic sides of the nuclear pore and binds to two distinct nucleoporin subcomplexes.* Mol Biol Cell, 2003. **14**(2): p. 600-10.

8. Daigle, N., et al., *Nuclear pore complexes form immobile networks and have a very low turnover in live mammalian cells.* J Cell Biol, 2001. **154**(1): p. 71-84.

9. Tran, E.J. and S.R. Wente, *Dynamic nuclear pore complexes: life on the edge.* Cell, 2006. **125**(6): p. 1041-53.

10. Akey, C.W., *Structural plasticity of the nuclear pore complex.* J Mol Biol, 1995. **248**(2): p. 273-93.

11. Pante, N. and M. Kann, *Nuclear pore complex is able to transport macromolecules with diameters of about 39 nm.* Mol Biol Cell, 2002. **13**(2): p. 425-34.

12. Fried, H. and U. Kutay, *Nucleocytoplasmic transport: taking an inventory.* Cell Mol Life Sci, 2003. **60**(8): p. 1659-88.

13. Rout, M.P., et al., *The yeast nuclear pore complex: composition, architecture, and transport mechanism.* J Cell Biol, 2000. **148**(4): p. 635-51.

14. Goldberg, M.W. and T.D. Allen, *The nuclear pore complex: three-dimensional surface structure revealed by field emission, in-lens scanning electron*

microscopy, with underlying structure uncovered by proteolysis. J Cell Sci, 1993. **106 (Pt 1)**: p. 261-74.

15. Beck, M., et al., *Nuclear pore complex structure and dynamics revealed by cryoelectron tomography.* Science, 2004. **306**(5700): p. 1387-90.

16. Akey, C.W. and D.S. Goldfarb, *Protein import through the nuclear pore complex is a multistep process.* J Cell Biol, 1989. **109**(3): p. 971-82.

17. Rout, M.P. and J.D. Aitchison, *Pore relations: nuclear pore complexes and nucleocytoplasmic exchange.* Essays Biochem, 2000. **36**: p. 75-88.

18. Rout, M.P. and G. Blobel, *Isolation of the yeast nuclear pore complex.* J Cell Biol, 1993. **123**(4): p. 771-83.

19. Reichelt, R., et al., *Correlation between structure and mass distribution of the nuclear pore complex and of distinct pore complex components.* J Cell Biol, 1990. **110**(4): p. 883-94.

20. Cronshaw, J.M., et al., *Proteomic analysis of the mammalian nuclear pore complex.* J Cell Biol, 2002. **158**(5): p. 915-27.

21. Doye, V. and E.C. Hurt, *Genetic approaches to nuclear pore structure and function.* Trends Genet, 1995. **11**(6): p. 235-41.

22. Matsuura, Y., et al., *Structural basis for Nup2p function in cargo release and karyopherin recycling in nuclear import.* Embo J, 2003. **22**(20): p. 5358-69.

23. Matsuura, Y. and M. Stewart, *Nup50/Npap60 function in nuclear protein import complex disassembly and importin recycling.* Embo J, 2005. **24**(21): p. 3681-9.

24. Allen, T.D., et al., *The nuclear pore complex: mediator of translocation between nucleus and cytoplasm.* J Cell Sci, 2000. **113 (Pt 10)**: p. 1651-9.

25. Rout, M.P. and S.R. Wente, *Pores for thought: nuclear pore complex proteins.* Trends Cell Biol, 1994. **4**(10): p. 357-65.

26. Zeitler, B. and K. Weis, *The FG-repeat asymmetry of the nuclear pore complex is dispensable for bulk nucleocytoplasmic transport in vivo.* J Cell Biol, 2004. **167**(4): p. 583-90.

27. Strawn, L.A., et al., *Minimal nuclear pore complexes define FG repeat domains essential for transport.* Nat Cell Biol, 2004. **6**(3): p. 197-206.

28. Ben-Efraim, I. and L. Gerace, *Gradient of increasing affinity of importin beta for nucleoporins along the pathway of nuclear import.* J Cell Biol, 2001. **152**(2): p. 411-7.

29. Bayliss, R., et al., *GLFG and FxFG nucleoporins bind to overlapping sites on importin-beta.* J Biol Chem, 2002. **277**(52): p. 50597-606.

30. Hetzer, M.W., T.C. Walther, and I.W. Mattaj, *Pushing the envelope: structure, function, and dynamics of the nuclear periphery.* Annu Rev Cell Dev Biol, 2005. **21**: p. 347-80.

31. Fahrenkrog, B., et al., *Domain-specific antibodies reveal multiple-site topology of Nup153 within the nuclear pore complex.* J Struct Biol, 2002. **140**(1-3): p. 254-67.

32. Paulillo, S.M., et al., *Nucleoporin domain topology is linked to the transport status of the nuclear pore complex.* J Mol Biol, 2005. **351**(4): p. 784-98.

33. Olsson, M., S. Scheele, and P. Ekblom, *Limited expression of nuclear pore membrane glycoprotein 210 in cell lines and tissues suggests cell-type specific nuclear pores in metazoans.* Exp Cell Res, 2004. **292**(2): p. 359-70.

34. Fan, F., et al., *cDNA cloning and characterization of Npap60: a novel rat nuclear pore-associated protein with an unusual subcellular localization during male germ cell differentiation.* Genomics, 1997. **40**(3): p. 444-53.

35. Cai, Y., et al., *Characterization and potential function of a novel testis-specific nucleoporin BS-63.* Mol Reprod Dev, 2002. **61**(1): p. 126-34.

36. Makhnevych, T., et al., *Cell cycle regulated transport controlled by alterations in the nuclear pore complex.* Cell, 2003. **115**(7): p. 813-23.

37. Galy, V., et al., *Nuclear retention of unspliced mRNAs in yeast is mediated by perinuclear Mlp1.* Cell, 2004. **116**(1): p. 63-73.

38. Green, D.M., et al., *The C-terminal domain of myosin-like protein 1 (Mlp1p) is a docking site for heterogeneous nuclear ribonucleoproteins that are required for mRNA export.* Proc Natl Acad Sci U S A, 2003. **100**(3): p. 1010-5.

39. Dingwall, C., S.V. Sharnick, and R.A. Laskey, *A polypeptide domain that specifies migration of nucleoplasmin into the nucleus.* Cell, 1982. **30**(2): p. 449-58.

40. Dingwall, C. and R.A. Laskey, *Nuclear targeting sequences--a consensus?* Trends Biochem Sci, 1991. **16**(12): p. 478-81.

41. Kalderon, D., et al., *Sequence requirements for nuclear location of simian virus 40 large-T antigen.* Nature, 1984. **311**(5981): p. 33-8.

42. Kalderon, D., et al., *A short amino acid sequence able to specify nuclear location.* Cell, 1984. **39**(3 Pt 2): p. 499-509.

43. Hodel, M.R., A.H. Corbett, and A.E. Hodel, *Dissection of a nuclear localization signal.* J Biol Chem, 2001. **276**(2): p. 1317-25.

44. Robbins, J., et al., *Two interdependent basic domains in nucleoplasmin nuclear targeting sequence: identification of a class of bipartite nuclear targeting sequence.* Cell, 1991. **64**(3): p. 615-23.

45. Dingwall, C., et al., *The nucleoplasmin nuclear location sequence is larger and more complex than that of SV-40 large T antigen.* J Cell Biol, 1988. **107**(3): p. 841-9.

46. Dingwall, C., J. Robbins, and S.M. Dilworth, *Characterisation of the nuclear location sequence of Xenopus nucleoplasmin.* J Cell Sci Suppl, 1989. **11**: p. 243-8.

47. Lange, A., et al., *Classical nuclear localization signals: definition, function, and interaction with importin alpha.* J Biol Chem, 2007. **282**(8): p. 5101-5.

48. Lee, B.J., et al., *Rules for nuclear localization sequence recognition by karyopherin beta 2.* Cell, 2006. **126**(3): p. 543-58.

49. Lange, A., et al., *A PY-NLS nuclear targeting signal is required for nuclear localization and function of the Saccharomyces cerevisiae mRNA-binding protein, Hrp1*. J Biol Chem, 2008.

50. Wen, W., et al., *Identification of a signal for rapid export of proteins from the nucleus.* Cell, 1995. **82**(3): p. 463-73.

51. Fischer, U., et al., *The HIV-1 Rev activation domain is a nuclear export signal that accesses an export pathway used by specific cellular RNAs.* Cell, 1995. **82**(3): p. 475-83.

52. Adam, S.A., R.S. Marr, and L. Gerace, *Nuclear protein import in permeabilized mammalian cells requires soluble cytoplasmic factors.* J Cell Biol, 1990. **111**(3): p. 807-16.

53. Adam, S.A. and L. Gerace, *Cytosolic proteins that specifically bind nuclear location signals are receptors for nuclear import.* Cell, 1991. **66**(5): p. 837-47.

54. Moore, M.S. and G. Blobel, *The two steps of nuclear import, targeting to the nuclear envelope and translocation through the nuclear pore, require different cytosolic factors.* Cell, 1992. **69**(6): p. 939-50.

55. Moore, M.S. and G. Blobel, *The GTP-binding protein Ran/TC4 is required for protein import into the nucleus.* Nature, 1993. **365**(6447): p. 661-3.

56. Adam, E.J. and S.A. Adam, *Identification of cytosolic factors required for nuclear location sequence-mediated binding to the nuclear envelope.* J Cell Biol, 1994. **125**(3): p. 547-55.

57. Gorlich, D., et al., *Isolation of a protein that is essential for the first step of nuclear protein import.* Cell, 1994. **79**(5): p. 767-78.

58. Moore, M.S. and G. Blobel, *Purification of a Ran-interacting protein that is required for protein import into the nucleus.* Proc Natl Acad Sci U S A, 1994. **91**(21): p. 10212-6.

59. Strom, A.C. and K. Weis, *Importin-beta-like nuclear transport receptors.* Genome Biol, 2001. **2**(6): p. REVIEWS3008.

60. Gorlich, D., et al., *A novel class of RanGTP binding proteins.* J Cell Biol, 1997. **138**(1): p. 65-80.

61. Fornerod, M., et al., *The human homologue of yeast CRM1 is in a dynamic subcomplex with CAN/Nup214 and a novel nuclear pore component Nup88.* Embo J, 1997. **16**(4): p. 807-16.

62. Lee, S.J., et al., *The structure of importin-beta bound to SREBP-2: nuclear import of a transcription factor.* Science, 2003. **302**(5650): p. 1571-5.

63. Cingolani, G., et al., *Molecular basis for the recognition of a nonclassical nuclear localization signal by importin beta.* Mol Cell, 2002. **10**(6): p. 1345-53.

64. Andrade, M.A., et al., *Comparison of ARM and HEAT protein repeats.* J Mol Biol, 2001. **309**(1): p. 1-18.

65. Conti, E., C.W. Muller, and M. Stewart, *Karyopherin flexibility in nucleocytoplasmic transport.* Curr Opin Struct Biol, 2006. **16**(2): p. 237-44.

66. Rout, M.P., G. Blobel, and J.D. Aitchison, *A distinct nuclear import pathway used by ribosomal proteins.* Cell, 1997. **89**(5): p. 715-25.

67. Jakel, S. and D. Gorlich, *Importin beta, transportin, RanBP5 and RanBP7 mediate nuclear import of ribosomal proteins in mammalian cells.* Embo J, 1998. **17**(15): p. 4491-502.

68. Mosammaparast, N., et al., *Nuclear import of histone H2A and H2B is mediated by a network of karyopherins.* J Cell Biol, 2001. **153**(2): p. 251-62.

69. Muhlhausser, P., et al., *Multiple pathways contribute to nuclear import of core histones.* EMBO Rep, 2001. **2**(8): p. 690-6.

70. Stade, K., et al., *Exportin 1 (Crm1p) is an essential nuclear export factor.* Cell, 1997. **90**(6): p. 1041-50.

71. Kutay, U. and S. Guttinger, *Leucine-rich nuclear-export signals: born to be weak.* Trends Cell Biol, 2005. **15**(3): p. 121-4.

72. Yoshida, K. and G. Blobel, *The karyopherin Kap142p/Msn5p mediates nuclear import and nuclear export of different cargo proteins.* J Cell Biol, 2001. **152**(4): p. 729-40.

73. Mingot, J.M., et al., *Importin 13: a novel mediator of nuclear import and export.* Embo J, 2001. **20**(14): p. 3685-94.

74. Mosammaparast, N. and L.F. Pemberton, *Karyopherins: from nuclear-transport mediators to nuclear-function regulators.* Trends Cell Biol, 2004. **14**(10): p. 547-56.

75. Cingolani, G., et al., *Structure of importin-beta bound to the IBB domain of importin-alpha.* Nature, 1999. **399**(6733): p. 221-9.

76. Moroianu, J., G. Blobel, and A. Radu, *Previously identified protein of uncertain function is karyopherin alpha and together with karyopherin beta docks import substrate at nuclear pore complexes.* Proc Natl Acad Sci U S A, 1995. **92**(6): p. 2008-11.

77. Huber, J., et al., *Snurportin1, an m3G-cap-specific nuclear import receptor with a novel domain structure.* Embo J, 1998. **17**(14): p. 4114-26.

78. Goldfarb, D.S., et al., *Importin alpha: a multipurpose nuclear-transport receptor.* Trends Cell Biol, 2004. **14**(9): p. 505-14.

79. Bischoff, F.R. and H. Ponstingl, *Catalysis of guanine nucleotide exchange on Ran by the mitotic regulator RCC1.* Nature, 1991. **354**(6348): p. 80-2.

80. Klebe, C., et al., *Interaction of the nuclear GTP-binding protein Ran with its regulatory proteins RCC1 and RanGAP1.* Biochemistry, 1995. **34**(2): p. 639-47.

81. Ohtsubo, M., H. Okazaki, and T. Nishimoto, *The RCC1 protein, a regulator for the onset of chromosome condensation locates in the nucleus and binds to DNA.* J Cell Biol, 1989. **109**(4 Pt 1): p. 1389-97.

82. Corbett, A.H., et al., *Rna1p, a Ran/TC4 GTPase activating protein, is required for nuclear import.* J Cell Biol, 1995. **130**(5): p. 1017-26.

83. Becker, J., et al., *RNA1 encodes a GTPase-activating protein specific for Gsp1p, the Ran/TC4 homologue of Saccharomyces cerevisiae.* J Biol Chem, 1995. **270**(20): p. 11860-5.

84. Hopper, A.K., H.M. Traglia, and R.W. Dunst, *The yeast RNA1 gene product necessary for RNA processing is located in the cytosol and apparently excluded from the nucleus.* J Cell Biol, 1990. **111**(2): p. 309-21.

85. Smith, A.E., et al., *Systems analysis of Ran transport.* Science, 2002. **295**(5554): p. 488-91.

86. Kalab, P., K. Weis, and R. Heald, *Visualization of a Ran-GTP gradient in interphase and mitotic Xenopus egg extracts.* Science, 2002. **295**(5564): p. 2452-6.

87. Izaurralde, E., et al., *The asymmetric distribution of the constituents of the Ran system is essential for transport into and out of the nucleus.* Embo J, 1997. **16**(21): p. 6535-47.

88. Gilchrist, D. and M. Rexach, *Molecular basis for the rapid dissociation of nuclear localization signals from karyopherin alpha in the nucleoplasm.* J Biol Chem, 2003. **278**(51): p. 51937-49.

89. Moore, M.S. and G. Blobel, *A G protein involved in nucleocytoplasmic transport: the role of Ran.* Trends Biochem Sci, 1994. **19**(5): p. 211-6.

90. Melchior, F., et al., *Inhibition of nuclear protein import by nonhydrolyzable analogues of GTP and identification of the small GTPase Ran/TC4 as an essential transport factor.* J Cell Biol, 1993. **123**(6 Pt 2): p. 1649-59.

91. Kadowaki, T., et al., *Regulation of RNA processing and transport by a nuclear guanine nucleotide release protein and members of the Ras superfamily.* Embo J, 1993. **12**(7): p. 2929-37.

92. Ribbeck, K. and D. Gorlich, *Kinetic analysis of translocation through nuclear pore complexes.* Embo J, 2001. **20**(6): p. 1320-30.

93. Conti, E., et al., *Crystallographic analysis of the recognition of a nuclear localization signal by the nuclear import factor karyopherin alpha.* Cell, 1998. **94**(2): p. 193-204.

94. Conti, E. and J. Kuriyan, *Crystallographic analysis of the specific yet versatile recognition of distinct nuclear localization signals by karyopherin alpha.* Structure, 2000. **8**(3): p. 329-38.

95. Cingolani, G., et al., *Nuclear import factors importin alpha and importin beta undergo mutually induced conformational changes upon association.* FEBS Lett, 2000. **484**(3): p. 291-8.

96. Fontes, M.R., T. Teh, and B. Kobe, *Structural basis of recognition of monopartite and bipartite nuclear localization sequences by mammalian importin-alpha.* J Mol Biol, 2000. **297**(5): p. 1183-94.

97. Bayliss, R., T. Littlewood, and M. Stewart, *Structural basis for the interaction between FxFG nucleoporin repeats and importin-beta in nuclear trafficking.* Cell, 2000. **102**(1): p. 99-108.

98. Liu, S.M. and M. Stewart, *Structural basis for the high-affinity binding of nucleoporin Nup1p to the Saccharomyces cerevisiae importin-beta homologue, Kap95p.* J Mol Biol, 2005. **349**(3): p. 515-25.

99. Lee, S.J., et al., *Structural basis for nuclear import complex dissociation by RanGTP.* Nature, 2005. **435**(7042): p. 693-6.

100. Vetter, I.R., et al., *Structural view of the Ran-Importin beta interaction at 2.3 A resolution.* Cell, 1999. **97**(5): p. 635-46.

101. Iovine, M.K. and S.R. Wente, *A nuclear export signal in Kap95p is required for both recycling the import factor and interaction with the nucleoporin GLFG repeat regions of Nup116p and Nup100p.* J Cell Biol, 1997. **137**(4): p. 797-811.

102. Kose, S., N. Imamoto, and Y. Yoneda, *Distinct energy requirement for nuclear import and export of importin beta in living cells.* FEBS Lett, 1999. **463**(3): p. 327-30.

103. Hood, J.K. and P.A. Silver, *Cse1p is required for export of Srp1p/importin-alpha from the nucleus in Saccharomyces cerevisiae.* J Biol Chem, 1998. **273**(52): p. 35142-6.

104. Solsbacher, J., et al., *Cse1p is involved in export of yeast importin alpha from the nucleus.* Mol Cell Biol, 1998. **18**(11): p. 6805-15.

105. Matsuura, Y. and M. Stewart, *Structural basis for the assembly of a nuclear export complex.* Nature, 2004. **432**(7019): p. 872-7.

106. Cook, A., et al., *The structure of the nuclear export receptor Cse1 in its cytosolic state reveals a closed conformation incompatible with cargo binding.* Mol Cell, 2005. **18**(3): p. 355-67.

107. Macara, I.G., *Transport into and out of the nucleus.* Microbiol Mol Biol Rev, 2001. **65**(4): p. 570-94, table of contents.

108. Imamoto, N., et al., *In vivo evidence for involvement of a 58 kDa component of nuclear pore-targeting complex in nuclear protein import.* Embo J, 1995. **14**(15): p. 3617-26.

109. O'Neill, R.E. and P. Palese, *NPI-1, the human homolog of SRP-1, interacts with influenza virus nucleoprotein.* Virology, 1995. **206**(1): p. 116-25.

110. Cuomo, C.A., et al., *Rch1, a protein that specifically interacts with the RAG-1 recombination-activating protein.* Proc Natl Acad Sci U S A, 1994. **91**(13): p. 6156-60.

111. Kussel, P. and M. Frasch, *Yeast Srp1, a nuclear protein related to Drosophila and mouse pendulin, is required for normal migration, division, and integrity of nuclei during mitosis.* Mol Gen Genet, 1995. **248**(3): p. 351-63.

112. Yano, R., et al., *Cloning and characterization of SRP1, a suppressor of temperature-sensitive RNA polymerase I mutations, in Saccharomyces cerevisiae.* Mol Cell Biol, 1992. **12**(12): p. 5640-51.

113. Yano, R., et al., *Yeast Srp1p has homology to armadillo/plakoglobin/beta-catenin and participates in apparently multiple nuclear functions including the maintenance of the nucleolar structure.* Proc Natl Acad Sci U S A, 1994. **91**(15): p. 6880-4.

114. Herold, A., et al., *Determination of the functional domain organization of the importin alpha nuclear import factor.* J Cell Biol, 1998. **143**(2): p. 309-18.

115. Andrade, M.A., C. Perez-Iratxeta, and C.P. Ponting, *Protein repeats: structures, functions, and evolution.* J Struct Biol, 2001. **134**(2-3): p. 117-31.

116. Gorlich, D., et al., *A 41 amino acid motif in importin-alpha confers binding to importin-beta and hence transit into the nucleus.* Embo J, 1996. **15**(8): p. 1810-7.

117. Weis, K., U. Ryder, and A.I. Lamond, *The conserved amino-terminal domain of hSRP1 alpha is essential for nuclear protein import.* Embo J, 1996. **15**(8): p. 1818-25.

118. Harreman, M.T., et al., *The auto-inhibitory function of importin alpha is essential in vivo.* J Biol Chem, 2003. **278**(8): p. 5854-63.

119. Kobe, B., *Autoinhibition by an internal nuclear localization signal revealed by the crystal structure of mammalian importin alpha.* Nat Struct Biol, 1999. **6**(4): p. 388-97.

120. Schroeder, A.J., et al., *Genetic evidence for interactions between yeast importin alpha (Srp1p) and its nuclear export receptor, Cse1p.* Mol Gen Genet, 1999. **261**(4-5): p. 788-95.

121. Gilchrist, D., B. Mykytka, and M. Rexach, *Accelerating the rate of disassembly of karyopherin.cargo complexes.* J Biol Chem, 2002. **277**(20): p. 18161-72.

122. Chi, N.C., E.J. Adam, and S.A. Adam, *Sequence and characterization of cytoplasmic nuclear protein import factor p97.* J Cell Biol, 1995. **130**(2): p. 265-74.

123. Enenkel, C., N. Schulke, and G. Blobel, *Expression in yeast of binding regions of karyopherins alpha and beta inhibits nuclear import and cell growth.* Proc Natl Acad Sci U S A, 1996. **93**(23): p. 12986-91.

124. Chi, N.C. and S.A. Adam, *Functional domains in nuclear import factor p97 for binding the nuclear localization sequence receptor and the nuclear pore.* Mol Biol Cell, 1997. **8**(6): p. 945-56.

125. Kutay, U., et al., *Export of importin alpha from the nucleus is mediated by a specific nuclear transport factor.* Cell, 1997. **90**(6): p. 1061-71.

126. Bednenko, J., G. Cingolani, and L. Gerace, *Importin beta contains a COOH-terminal nucleoporin binding region important for nuclear transport.* J Cell Biol, 2003. **162**(3): p. 391-401.

127. Bayliss, R., et al., *Interaction between NTF2 and xFxFG-containing nucleoporins is required to mediate nuclear import of RanGDP.* J Mol Biol, 1999. **293**(3): p. 579-93.

128. Loeb, J.D., L.I. Davis, and G.R. Fink, *NUP2, a novel yeast nucleoporin, has functional overlap with other proteins of the nuclear pore complex.* Mol Biol Cell, 1993. **4**(2): p. 209-22.

129. Hood, J.K., J.M. Casolari, and P.A. Silver, *Nup2p is located on the nuclear side of the nuclear pore complex and coordinates Srp1p/importin-alpha export.* J Cell Sci, 2000. **113 (Pt 8)**: p. 1471-80.

130. Guan, T., et al., *Nup50, a nucleoplasmically oriented nucleoporin with a role in nuclear protein export.* Mol Cell Biol, 2000. **20**(15): p. 5619-30.

131. Solsbacher, J., et al., *Nup2p, a yeast nucleoporin, functions in bidirectional transport of importin alpha.* Mol Cell Biol, 2000. **20**(22): p. 8468-79.

132. Denning, D., et al., *The nucleoporin Nup60p functions as a Gsp1p-GTP-sensitive tether for Nup2p at the nuclear pore complex.* J Cell Biol, 2001. **154**(5): p. 937-50.

133. Dilworth, D.J., et al., *Nup2p dynamically associates with the distal regions of the yeast nuclear pore complex.* J Cell Biol, 2001. **153**(7): p. 1465-78.

134. Fontes, M.R., et al., *Structural basis for the specificity of bipartite nuclear localization sequence binding by importin-alpha.* J Biol Chem, 2003. **278**(30): p. 27981-7.

135. Leung, S.W., et al., *Dissection of the karyopherin alpha nuclear localization signal (NLS)-binding groove: functional requirements for NLS binding.* J Biol Chem, 2003. **278**(43): p. 41947-53.

136. Harreman, M.T., et al., *Characterization of the auto-inhibitory sequence within the N-terminal domain of importin alpha.* J Biol Chem, 2003. **278**(24): p. 21361-9.

137. Timney, B.L., et al., *Simple kinetic relationships and nonspecific competition govern nuclear import rates in vivo.* J Cell Biol, 2006. **175**(4): p. 579-93.

138. Jans, D.A., C.Y. Xiao, and M.H. Lam, *Nuclear targeting signal recognition: a key control point in nuclear transport?* Bioessays, 2000. **22**(6): p. 532-44.

139. Kaffman, A. and E.K. O'Shea, *Regulation of nuclear localization: a key to a door.* Annu Rev Cell Dev Biol, 1999. **15**: p. 291-339.

140. Poon, I.K. and D.A. Jans, *Regulation of nuclear transport: central role in development and transformation?* Traffic, 2005. **6**(3): p. 173-86.

141. Riviere, Y., et al., *Processing of the precursor of NF-kappa B by the HIV-1 protease during acute infection.* Nature, 1991. **350**(6319): p. 625-6.

142. Beals, C.R., et al., *Nuclear localization of NF-ATc by a calcineurin-dependent, cyclosporin-sensitive intramolecular interaction.* Genes Dev, 1997. **11**(7): p. 824-34.

143. Kaffman, A., N.M. Rank, and E.K. O'Shea, *Phosphorylation regulates association of the transcription factor Pho4 with its import receptor Pse1/Kap121.* Genes Dev, 1998. **12**(17): p. 2673-83.

144. Fineberg, K., et al., *Inhibition of nuclear import mediated by the Rev-arginine rich motif by RNA molecules.* Biochemistry, 2003. **42**(9): p. 2625-33.

145. Beg, A.A., et al., *I kappa B interacts with the nuclear localization sequences of the subunits of NF-kappa B: a mechanism for cytoplasmic retention.* Genes Dev, 1992. **6**(10): p. 1899-913.

146. Briggs, L.J., et al., *The cAMP-dependent protein kinase site (Ser312) enhances dorsal nuclear import through facilitating nuclear localization sequence/importin interaction.* J Biol Chem, 1998. **273**(35): p. 22745-52.

147. Harreman, M.T., et al., *Regulation of nuclear import by phosphorylation adjacent to nuclear localization signals.* J Biol Chem, 2004. **279**(20): p. 20613-21.

148. Ely, S., A. D'Arcy, and E. Jost, *Interaction of antibodies against nuclear envelope-associated proteins from rat liver nuclei with rodent and human cells.* Exp Cell Res, 1978. **116**(2): p. 325-31.

149. Gerace, L. and G. Blobel, *The nuclear envelope lamina is reversibly depolymerized during mitosis.* Cell, 1980. **19**(1): p. 277-87.

150. Pfaller, R., C. Smythe, and J.W. Newport, *Assembly/disassembly of the nuclear envelope membrane: cell cycle-dependent binding of nuclear membrane vesicles to chromatin in vitro.* Cell, 1991. **65**(2): p. 209-17.

151. Norbury, C. and P. Nurse, *Animal cell cycles and their control.* Annu Rev Biochem, 1992. **61**: p. 441-70.

152. Mitchison, T.J. and E.D. Salmon, *Mitosis: a history of division.* Nat Cell Biol, 2001. **3**(1): p. E17-21.

153. Pines, J. and C.L. Rieder, *Re-staging mitosis: a contemporary view of mitotic progression.* Nat Cell Biol, 2001. **3**(1): p. E3-6.

154. Hartwell, L.H., et al., *Genetic control of the cell division cycle in yeast.* Science, 1974. **183**(120): p. 46-51.

155. Lew, D.J. and S.I. Reed, *Cell cycle control of morphogenesis in budding yeast.* Curr Opin Genet Dev, 1995. **5**(1): p. 17-23.

156. Forsburg, S.L. and P. Nurse, *Cell cycle regulation in the yeasts Saccharomyces cerevisiae and Schizosaccharomyces pombe.* Annu Rev Cell Biol, 1991. **7**: p. 227-56.

157. Pardee, A.B., *A restriction point for control of normal animal cell proliferation.* Proc Natl Acad Sci U S A, 1974. **71**(4): p. 1286-90.

158. Hartwell, L.H. and T.A. Weinert, *Checkpoints: controls that ensure the order of cell cycle events.* Science, 1989. **246**(4930): p. 629-34.

159. Rudner, A.D. and A.W. Murray, *The spindle assembly checkpoint.* Curr Opin Cell Biol, 1996. **8**(6): p. 773-80.

160. Amon, A., *The spindle checkpoint.* Curr Opin Genet Dev, 1999. **9**(1): p. 69-75.

161. Sancar, A., et al., *Molecular mechanisms of mammalian DNA repair and the DNA damage checkpoints.* Annu Rev Biochem, 2004. **73**: p. 39-85.

162. Planas-Silva, M.D. and R.A. Weinberg, *The restriction point and control of cell proliferation.* Curr Opin Cell Biol, 1997. **9**(6): p. 768-72.

163. Nurse, P. and P. Thuriaux, *Regulatory genes controlling mitosis in the fission yeast Schizosaccharomyces pombe.* Genetics, 1980. **96**(3): p. 627-37.

164. Morgan, D.O., *Principles of CDK regulation.* Nature, 1995. **374**(6518): p. 131-4.

165. Pines, J., *Cyclins and cyclin-dependent kinases: theme and variations.* Adv Cancer Res, 1995. **66**: p. 181-212.

166. Fisher, R.P. and D.O. Morgan, *A novel cyclin associates with MO15/CDK7 to form the CDK-activating kinase.* Cell, 1994. **78**(4): p. 713-24.

167. Evans, T., et al., *Cyclin: a protein specified by maternal mRNA in sea urchin eggs that is destroyed at each cleavage division.* Cell, 1983. **33**(2): p. 389-96.

168. Pines, J., *Cyclins: wheels within wheels.* Cell Growth Differ, 1991. **2**(6): p. 305-10.

169. Sherr, C.J., *G1 phase progression: cycling on cue.* Cell, 1994. **79**(4): p. 551-5.

170. Ohtsubo, M., et al., *Human cyclin E, a nuclear protein essential for the G1-to-S phase transition.* Mol Cell Biol, 1995. **15**(5): p. 2612-24.

171. Walker, D.H. and J.L. Maller, *Role for cyclin A in the dependence of mitosis on completion of DNA replication.* Nature, 1991. **354**(6351): p. 314-7.

172. Girard, F., et al., *Cyclin A is required for the onset of DNA replication in mammalian fibroblasts.* Cell, 1991. **67**(6): p. 1169-79.

173. King, R.W., P.K. Jackson, and M.W. Kirschner, *Mitosis in transition.* Cell, 1994. **79**(4): p. 563-71.

174. Arellano, M. and S. Moreno, *Regulation of CDK/cyclin complexes during the cell cycle.* Int J Biochem Cell Biol, 1997. **29**(4): p. 559-73.

175. Sherr, C.J. and J.M. Roberts, *Inhibitors of mammalian G1 cyclin-dependent kinases.* Genes Dev, 1995. **9**(10): p. 1149-63.

176. Nasmyth, K., *Control of the yeast cell cycle by the Cdc28 protein kinase.* Curr Opin Cell Biol, 1993. **5**(2): p. 166-79.

177. Mendenhall, M.D. and A.E. Hodge, *Regulation of Cdc28 cyclin-dependent protein kinase activity during the cell cycle of the yeast Saccharomyces cerevisiae.* Microbiol Mol Biol Rev, 1998. **62**(4): p. 1191-243.

178. Nishitani, H., et al., *Loss of RCC1, a nuclear DNA-binding protein, uncouples the completion of DNA replication from the activation of cdc2 protein kinase and mitosis.* Embo J, 1991. **10**(6): p. 1555-64.

179. Sazer, S. and P. Nurse, *A fission yeast RCC1-related protein is required for the mitosis to interphase transition.* Embo J, 1994. **13**(3): p. 606-15.

180. Loeb, J.D., et al., *The yeast nuclear import receptor is required for mitosis.* Proc Natl Acad Sci U S A, 1995. **92**(17): p. 7647-51.

181. Gruss, O.J., et al., *Ran induces spindle assembly by reversing the inhibitory effect of importin alpha on TPX2 activity.* Cell, 2001. **104**(1): p. 83-93.

182. Nachury, M.V., et al., *Importin beta is a mitotic target of the small GTPase Ran in spindle assembly.* Cell, 2001. **104**(1): p. 95-106.

183. Wiese, C., et al., *Role of importin-beta in coupling Ran to downstream targets in microtubule assembly.* Science, 2001. **291**(5504): p. 653-6.

184. Du, Q., et al., *LGN blocks the ability of NuMA to bind and stabilize microtubules. A mechanism for mitotic spindle assembly regulation.* Curr Biol, 2002. **12**(22): p. 1928-33.

185. Sazer, S. and M. Dasso, *The ran decathlon: multiple roles of Ran.* J Cell Sci, 2000. **113 (Pt 7)**: p. 1111-8.

186. Umeda, M., et al., *The fission yeast Schizosaccharomyces pombe has two importin-alpha proteins, Imp1p and Cut15p, which have common and unique functions in nucleocytoplasmic transport and cell cycle progression.* Genetics, 2005. **171**(1): p. 7-21.

187. Pines, J. and T. Hunter, *Human cyclins A and B1 are differentially located in the cell and undergo cell cycle-dependent nuclear transport.* J Cell Biol, 1991. **115**(1): p. 1-17.

188. Li, J., A.N. Meyer, and D.J. Donoghue, *Nuclear localization of cyclin B1 mediates its biological activity and is regulated by phosphorylation.* Proc Natl Acad Sci U S A, 1997. **94**(2): p. 502-7.

189. Davis, J.R., M. Kakar, and C.S. Lim, *Controlling protein compartmentalization to overcome disease.* Pharm Res, 2007. **24**(1): p. 17-27.

190. Moll, U.M., G. Riou, and A.J. Levine, *Two distinct mechanisms alter p53 in breast cancer: mutation and nuclear exclusion.* Proc Natl Acad Sci U S A, 1992. **89**(15): p. 7262-6.

191. Fabbro, M. and B.R. Henderson, *Regulation of tumor suppressors by nuclear-cytoplasmic shuttling.* Exp Cell Res, 2003. **282**(2): p. 59-69.

192. Kau, T.R., J.C. Way, and P.A. Silver, *Nuclear transport and cancer: from mechanism to intervention.* Nat Rev Cancer, 2004. **4**(2): p. 106-17.

193. Karin, M., et al., *NF-kappaB in cancer: from innocent bystander to major culprit.* Nat Rev Cancer, 2002. **2**(4): p. 301-10.

194. Henkel, T., et al., *Intramolecular masking of the nuclear location signal and dimerization domain in the precursor for the p50 NF-kappa B subunit.* Cell, 1992. **68**(6): p. 1121-33.

195. Woods, D.B. and K.H. Vousden, *Regulation of p53 function.* Exp Cell Res, 2001. **264**(1): p. 56-66.

196. Shaulsky, G., et al., *Nuclear accumulation of p53 protein is mediated by several nuclear localization signals and plays a role in tumorigenesis.* Mol Cell Biol, 1990. **10**(12): p. 6565-77.

197. David-Pfeuty, T., et al., *Cell cycle-dependent regulation of nuclear p53 traffic occurs in one subclass of human tumor cells and in untransformed cells.* Cell Growth Differ, 1996. **7**(9): p. 1211-25.

198. Shaulsky, G., A. Ben-Ze'ev, and V. Rotter, *Subcellular distribution of the p53 protein during the cell cycle of Balb/c 3T3 cells.* Oncogene, 1990. **5**(11): p. 1707-11.

199. Middeler, G., et al., *The tumor suppressor p53 is subject to both nuclear import and export, and both are fast, energy-dependent and lectin-inhibited.* Oncogene, 1997. **14**(12): p. 1407-17.

200. Deng, C.X., *BRCA1: cell cycle checkpoint, genetic instability, DNA damage response and cancer evolution.* Nucleic Acids Res, 2006. **34**(5): p. 1416-26.

201. Yan, C., L.H. Lee, and L.I. Davis, *Crm1p mediates regulated nuclear export of a yeast AP-1-like transcription factor.* Embo J, 1998. **17**(24): p. 7416-29.

202. Yoneda, Y., et al., *A long synthetic peptide containing a nuclear localization signal and its flanking sequences of SV40 T-antigen directs the transport of IgM into the nucleus efficiently.* Exp Cell Res, 1992. **201**(2): p. 313-20.

203. Winston, F., C. Dollard, and S.L. Ricupero-Hovasse, *Construction of a set of convenient Saccharomyces cerevisiae strains that are isogenic to S288C.* Yeast, 1995. **11**(1): p. 53-5.

204. Bucci, M. and S.R. Wente, *In vivo dynamics of nuclear pore complexes in yeast.* J Cell Biol, 1997. **136**(6): p. 1185-99.

205. Suntharalingam, M. and S.R. Wente, *Peering through the pore: nuclear pore complex structure, assembly, and function.* Dev Cell, 2003. **4**(6): p. 775-89.

206. Gorlich, D., M.J. Seewald, and K. Ribbeck, *Characterization of Ran-driven cargo transport and the RanGTPase system by kinetic measurements and computer simulation.* Embo J, 2003. **22**(5): p. 1088-100.

207. Riddick, G. and I.G. Macara, *A systems analysis of importin-{alpha}-{beta} mediated nuclear protein import.* J Cell Biol, 2005. **168**(7): p. 1027-38.

208. Huber, A.H., W.J. Nelson, and W.I. Weis, *Three-dimensional structure of the armadillo repeat region of beta-catenin.* Cell, 1997. **90**(5): p. 871-82.

209. Efthymiadis, A., et al., *Kinetic characterization of the human retinoblastoma protein bipartite nuclear localization sequence (NLS) in vivo and in vitro. A comparison with the SV40 large T-antigen NLS.* J Biol Chem, 1997. **272**(35): p. 22134-9.

210. Xiao, C.Y. and D.A. Jans, *An engineered site for protein kinase C flanking the SV40 large T-antigen NLS confers phorbol ester-inducible nuclear import.* FEBS Lett, 1998. **436**(3): p. 313-7.

211. Niedenthal, R.K., et al., *Green fluorescent protein as a marker for gene expression and subcellular localization in budding yeast.* Yeast, 1996. **12**(8): p. 773-86.

212. Koepp, D.M., et al., *Dynamic localization of the nuclear import receptor and its interactions with transport factors.* J Cell Biol, 1996. **133**(6): p. 1163-76.

213. Seedorf, M., et al., *Interactions between a nuclear transporter and a subset of nuclear pore complex proteins depend on Ran GTPase.* Mol Cell Biol, 1999. **19**(2): p. 1547-57.

214. Shulga, N., et al., *In vivo nuclear transport kinetics in Saccharomyces cerevisiae: a role for heat shock protein 70 during targeting and translocation.* J Cell Biol, 1996. **135**(2): p. 329-39.

215. Quimby, B.B., et al., *Functional analysis of the hydrophobic patch on nuclear transport factor 2 involved in interactions with the nuclear pore in vivo.* J Biol Chem, 2001. **276**(42): p. 38820-9.

216. Kunzler, M. and E.C. Hurt, *Cse1p functions as the nuclear export receptor for importin alpha in yeast.* FEBS Lett, 1998. **433**(3): p. 185-90.

217. Sikorski, R.S. and P. Hieter, *A system of shuttle vectors and yeast host strains designed for efficient manipulation of DNA in Saccharomyces cerevisiae.* Genetics, 1989. **122**(1): p. 19-27.

218. Gorlich, D., et al., *Two different subunits of importin cooperate to recognize nuclear localization signals and bind them to the nuclear envelope.* Curr Biol, 1995. **5**(4): p. 383-92.

219. Sambrook, J. and D. Russell, *Molecular Cloning: A Laboratory Manual.* Cold Spring Harbor Laboratory Press, 2001.

220. Sambrook, J. and D. Russell, *Molecular Cloning: A Laboratory Manual*. 3rd ed. 2001: Cold Spring Harbor Laboratory Press, Cold Spring Harbor, NY.

221. Adams, A., et al., *Methods in Yeast Genetics*. 1997, Cold Spring Harbor: Cold Spring Harbor Laboratory Press.

222. Straight, A.F. and A.W. Murray, *Methods in Enzymology*. Vol. 283. 1997. 425-440.

223. Huh, W.K., et al., *Global analysis of protein localization in budding yeast.* Nature, 2003. **425**(6959): p. 686-91.

224. Boeke, J.D., et al., *5-Fluoroorotic acid as a selective agent in yeast molecular genetics.* Meth. Enzymol., 1987. **154**: p. 164-175.

225. Towbin, H., T. Staehelin, and J. Gordon, *Electrophoretic transfer of proteins from polyacrylamide gels to nitrocellulose sheets: Procedures and some application.* Proc. Natl. Acad. Sci. USA, 1979. **76**: p. 4350-4354.

226. Swaminathan, S., et al., *Yra1 is required for S phase entry and affects Dia2 binding to replication origins.* Mol Cell Biol, 2007. **27**(13): p. 4674-84.

227. Sazer, S. and S.W. Sherwood, *Mitochondrial growth and DNA synthesis occur in the absence of nuclear DNA replication in fission yeast.* J Cell Sci, 1990. **97 (Pt 3)**: p. 509-16.

228. Friedman, K.L., et al., *Multiple determinants controlling activation of yeast replication origins late in S phase.* Genes Dev, 1996. **10**(13): p. 1595-607.

229. Mitchison, J.M. and J. Creanor, *Induction synchrony in the fission yeast. Schizosaccharomyces pombe.* Exp Cell Res, 1971. **67**(2): p. 368-74.

230. Li, R. and A.W. Murray, *Feedback control of mitosis in budding yeast.* Cell, 1991. **66**(3): p. 519-31.

231. Siede, W. and E.C. Friedberg, *Influence of DNA repair deficiencies on the UV sensitivity of yeast cells in different cell cycle stages.* Mutat Res, 1990. **245**(4): p. 287-92.

232. Siede, W., et al., *Regulation of the RAD2 gene of Saccharomyces cerevisiae.* Mol Microbiol, 1989. **3**(12): p. 1697-707.

233. Goh, P.Y. and U. Surana, *Cdc4, a protein required for the onset of S phase, serves an essential function during G(2)/M transition in Saccharomyces cerevisiae.* Mol Cell Biol, 1999. **19**(8): p. 5512-22.

234. Dohrmann, P.R. and R.A. Sclafani, *Novel role for checkpoint Rad53 protein kinase in the initiation of chromosomal DNA replication in Saccharomyces cerevisiae.* Genetics, 2006. **174**(1): p. 87-99.

235. Hartwell, L.H. and D. Smith, *Altered fidelity of mitotic chromosome transmission in cell cycle mutants of S. cerevisiae.* Genetics, 1985. **110**(3): p. 381-95.

236. Palmer, R.E., E. Hogan, and D. Koshland, *Mitotic transmission of artificial chromosomes in cdc mutants of the yeast, Saccharomyces cerevisiae.* Genetics, 1990. **125**(4): p. 763-74.

237. Maine, G.T., P. Sinha, and B.K. Tye, *Mutants of S. cerevisiae defective in the maintenance of minichromosomes.* Genetics, 1984. **106**(3): p. 365-85.

238. Nakai, K. and P. Horton, *PSORT: a program for detecting sorting signals in proteins and predicting their subcellular localization.* Trends Biochem Sci, 1999. **24**(1): p. 34-6.

239. Benson, D.A., et al., *GenBank.* Nucleic Acids Res, 2006. **34**(Database issue): p. D16-20.

240. Hopwood, B. and S. Dalton, *Cdc45p assembles into a complex with Cdc46p/Mcm5p, is required for minichromosome maintenance, and is essential for chromosomal DNA replication.* Proc Natl Acad Sci U S A, 1996. **93**(22): p. 12309-14.

241. Moir, D., et al., *Cold-sensitive cell-division-cycle mutants of yeast: isolation, properties, and pseudoreversion studies.* Genetics, 1982. **100**(4): p. 547-63.

242. Ricke, R.M. and A.K. Bielinsky, *Mcm10 regulates the stability and chromatin association of DNA polymerase-alpha.* Mol Cell, 2004. **16**(2): p. 173-85.

243. Zhu, W., et al., *Mcm10 and And-1/CTF4 recruit DNA polymerase alpha to chromatin for initiation of DNA replication.* Genes Dev, 2007. **21**(18): p. 2288-99.

244. Burich, R. and M. Lei, *Two bipartite NLSs mediate constitutive nuclear localization of Mcm10.* Curr Genet, 2003. **44**(4): p. 195-201.

245. Pramila, T., et al., *Conserved homeodomain proteins interact with MADS box protein Mcm1 to restrict ECB-dependent transcription to the M/G1 phase of the cell cycle.* Genes Dev, 2002. **16**(23): p. 3034-45.

246. Braun, K.A. and L.L. Breeden, *Nascent transcription of MCM2-7 is important for nuclear localization of the minichromosome maintenance complex in G1.* Mol Biol Cell, 2007. **18**(4): p. 1447-56.

247. Stewart, M., *Molecular mechanism of the nuclear protein import cycle.* Nat Rev Mol Cell Biol, 2007. **8**(3): p. 195-208.

248. Jones, A.L., et al., *SAC3 may link nuclear protein export to cell cycle progression.* Proc Natl Acad Sci U S A, 2000. **97**(7): p. 3224-9.

249. Kahana, J.A., B.J. Schnapp, and P.A. Silver, *Kinetics of spindle pole body separation in budding yeast.* Proc Natl Acad Sci U S A, 1995. **92**(21): p. 9707-11.

250. Hodel, A.E., et al., *Nuclear localization signal receptor affinity correlates with in vivo localization in Saccharomyces cerevisiae.* J Biol Chem, 2006. **281**(33): p. 23545-56.

251. Straight, A.F. and A.W. Murray, *The spindle assembly checkpoint in budding yeast.* Methods Enzymol, 1997. **283**: p. 425-40.

252. Riddick, G. and I.G. Macara, *The adapter importin-alpha provides flexible control of nuclear import at the expense of efficiency.* Mol Syst Biol, 2007. **3**: p. 118.

253. Dasso, M., et al., *RCC1, a regulator of mitosis, is essential for DNA replication.* Mol Cell Biol, 1992. **12**(8): p. 3337-45.

254. Carazo-Salas, R.E., et al., *Ran-GTP coordinates regulation of microtubule nucleation and dynamics during mitotic-spindle assembly.* Nat Cell Biol, 2001. **3**(3): p. 228-34.

255. Quimby, B.B., C.A. Wilson, and A.H. Corbett, *The interaction between Ran and NTF2 is required for cell cycle progression.* Mol Biol Cell, 2000. **11**(8): p. 2617-29.

256. Schatz, C.A., et al., *Importin alpha-regulated nucleation of microtubules by TPX2.* Embo J, 2003. **22**(9): p. 2060-70.

257. Cosgrove, A.J., C.A. Nieduszynski, and A.D. Donaldson, *Ku complex controls the replication time of DNA in telomere regions.* Genes Dev, 2002. **16**(19): p. 2485-90.

258. Ferguson, B.M. and W.L. Fangman, *A position effect on the time of replication origin activation in yeast.* Cell, 1992. **68**(2): p. 333-9.

259. Raghuraman, M.K., B.J. Brewer, and W.L. Fangman, *Cell cycle-dependent establishment of a late replication program.* Science, 1997. **276**(5313): p. 806-9.

260. Koike, M., et al., *The nuclear localization signal of the human Ku70 is a variant bipartite type recognized by the two components of nuclear pore-targeting complex.* Exp Cell Res, 1999. **250**(2): p. 401-13.

261. Dazy, S., et al., *Broadening of DNA replication origin usage during metazoan cell differentiation.* EMBO Rep, 2006. **7**(8): p. 806-11.

262. Gregoire, D., K. Brodolin, and M. Mechali, *HoxB domain induction silences DNA replication origins in the locus and specifies a single origin at its boundary.* EMBO Rep, 2006. **7**(8): p. 812-6.

263. Sclafani, R.A. and T.M. Holzen, *Cell cycle regulation of DNA replication.* Annu Rev Genet, 2007. **41**: p. 237-80.

264. Piatti, S., C. Lengauer, and K. Nasmyth, *Cdc6 is an unstable protein whose de novo synthesis in G1 is important for the onset of S phase and for preventing a 'reductional' anaphase in the budding yeast Saccharomyces cerevisiae.* Embo J, 1995. **14**(15): p. 3788-99.

265. Hartwell, L.H., *Sequential function of gene products relative to DNA synthesis in the yeast cell cycle.* J Mol Biol, 1976. **104**(4): p. 803-17.

266. Bueno, A. and P. Russell, *Dual functions of CDC6: a yeast protein required for DNA replication also inhibits nuclear division.* Embo J, 1992. **11**(6): p. 2167-76.

267. Kohler, M., et al., *Evidence for distinct substrate specificities of importin alpha family members in nuclear protein import.* Mol Cell Biol, 1999. **19**(11): p. 7782-91.